

Oil & Natural Gas Technology

DOE Award No.: DE-NT0006555

Second Annual Report

October 1, 2009 to September 30, 2010

USE OF POLYMERS TO RECOVER VISCOUS OIL FROM UNCONVENTIONAL RESERVOIRS

Submitted by:

New Mexico Petroleum Recovery Research Center
New Mexico Tech, 801 Leroy, Socorro, NM 87801

Authored By: Randall Scott Seright (Principal Investigator)

Prepared for:

United States Department of Energy
National Energy Technology Laboratory

October 1, 2010



Office of Fossil Energy

DISCLAIMER

This report was prepared as an account of work sponsored by an agency of the United States Government. Neither the United States Government nor any agency thereof, nor any of their employees, makes any warranty, expressed or implied, or assumes any legal liability or responsibility for the accuracy, completeness, or usefulness of any information, apparatus, product, or process disclosed, or represents that its use would not infringe privately owned rights. Reference herein to any specific commercial product, process, or service by trade name, trademark, manufacturer, or otherwise does not necessarily constitute or imply its endorsement, recommendation, or favoring by the United States Government or any agency thereof. The views and opinions of authors expressed herein do not necessarily state or reflect those of the United States Government or any agency thereof.

DEDICATION

This report is dedicated to the memory of my great friend Robert Dunn Sydansk. Bob showed extraordinary dedication toward advancing the science, engineering, and application of conformance improvement in reservoirs using polymers and gels. Bob invented the Cr(III)-carboxylate-HPAM gel conformance improvement technology. Weekly (and often daily) technical discussions with him were among the best parts of my job. I miss his insights, vision, and friendship.

ABSTRACT

This technical progress report describes work performed from October 1, 2009, through September 30, 2010, for the second year of the project, "Use of Polymers to Recover Viscous Oil from Unconventional Reservoirs." For HPAM (partially hydrolyzed polyacrylamide) solutions with a sufficiently low salinity (i.e., tap water or distilled water) and/or sufficiently high polymer concentration, shear thinning can be observed in porous media at moderate to low fluxes. However, under practical conditions where HPAM is used for EOR, the degree of shear thinning is slight or non-existent, especially compared to the level of shear thickening that occurs at high fluxes. Xanthan solutions are well known to exhibit shear thinning both in viscometers and in porous media. Contrary to recent suggestions in the literature, shear thinning by polymer solutions is shown not to be a significant liability for vertical sweep efficiency. The overall viscosity (resistance factor) of the polymer solution is of far greater relevance than the rheology. Contrary to earlier claims, permeability reduction associated with polymers is shown not to benefit vertical sweep efficiency during polymer flooding.

In our previous work, we used fractional flow calculations to examine the potential of polymer flooding when the polymer flood was initiated immediately after primary recovery—i.e., with no intermediate waterflood. We extended the fractional flow calculations to examine the effectiveness of polymer flooding when a waterflood (with 1-cp water) was implemented prior to the polymer flood. We showed that polymer flooding can be effective in viscous (1,000-cp) oil reservoirs even if waterflooding has been underway for some time (up to 5 pore volumes). Fractional flow analysis reveals that if polymers can reduce the S_{or} , this phenomenon will be an important factor during recovery of viscous oils. As expected, the magnitude of the oil recovery increases as the S_{or} is reduced. For one example examined, if the polymer reduces S_{or} from 0.3 to 0.25, a 10% increase in oil recovery can be expected. Also, for a given S_{or} , the magnitude of the oil recovery increases as the viscosity of the injected polymer solution increases.

We examined two new biopolymers for possible use in enhanced oil recovery. The first was CP Kelco's EX9719 xanthan. This polymer is a very effective viscosifier, providing 25-100% higher viscosities than other xanthans, depending on the polymer concentration. EX9719 also shows good filterability. The second polymer was CP Kelco's gellan gum, KELCOGEL HT, which is probably not a serious candidate for polymer flooding since it only dissolves in distilled water.

A study of the SNF associative polymers, C1205 and B192, revealed low-flux resistance factors (for fresh polymer solutions) that were greater than expectations from viscosity measurements. We are examining whether this effect can be made to materialize deep within the porous rock of a reservoir. Fresh C1205 solutions provided about the same viscosity as fresh 3830S solutions (a conventional HPAM). However, in a 10-darcy core, fresh C1205 solutions provided low-flux resistance factors that were about twice those for fresh 3830S solutions. Both polymers showed modest (0-8%) viscosity losses (at 7.3 s^{-1}) after exposure to a 235 psi/ft pressure gradient in a core. However, C1205 solutions experienced 31-45% loss in low-flux resistance factor, whereas 3830S solutions experienced only 0-15% loss. After 235 psi/ft, low-flux resistance factors for C1205 solutions were often similar to those for fresh 3830S solutions. After exposure to a 2,500 psi/ft pressure gradient, C1205 solutions experienced 19-35% viscosity loss, whereas 3830S solutions experienced 5-17% viscosity loss. After 2,500 psi/ft, low-flux resistance factors for C1205 solutions were the same or less than those for 3830S solutions.

TABLE OF CONTENTS

Disclaimer	ii
Dedication	ii
Abstract	iii
List of Tables	v
Table of Figures	v
Acknowledgements.....	viii
Executive Summary	ix
1. INTRODUCTION.....	1
Project Objectives	1
Report Content	1
2. CAN HPAM SOLUTIONS SHOW SHEAR THINNING IN POROUS MEDIA?	2
HPAM in Very Low Salinity Water	3
Relation between the Onset of Shear Thinning in a Viscometer versus the Onset of Shear Thickening in Porous Media	3
Significance of Observations	5
Conclusions.....	5
3. IS PERMEABILITY REDUCTION BY POLYMERS A GOOD THING?	6
Linear Flow, No Crossflow.....	6
Radial Flow, No Crossflow.....	7
Comparison with Laboratory Data.....	8
Cases with Crossflow.....	8
Effect of Differential Retention	9
Conclusions.....	10
4. DOES RHEOLOGY SIGNIFICANTLY AFFECT SWEEP EFFICIENCY?	11
Cases with Crossflow.....	11
Radial Flow, No Crossflow.....	11
Linear Flow, No Crossflow.....	11
Conclusion	12
5. IS POLYMER FLOODING OF VISCOUS OIL HURT BY A PRIOR WATERFLOOD?... 13	13
One Homogeneous Layer	13
Two Layers, Free Crossflow.....	15
Simple Benefit Analysis	16
Conclusion	17
6. EXAMINATION OF TWO BIOPOLYMERS	18
EX9719 Xanthan.....	18
Gellan Gum.....	21
Conclusions.....	22
7. EXAMINATION OF C1205 HYDROPHOBIC ASSOCIATIVE POLYMER.....	23
Viscosity	23
Filter Test Results	25
Cores	26
Resistance Factors and Face Plugging.....	26
Resistance Factor versus Flux and Concentration	27
Residual Resistance Factors.....	31

Repeat Set in a Longer Polyethylene Core	31
Mechanical Degradation	33
Length Dependence of Resistance Factors	41
Discussion of Results	42
Conclusions	45
8. EXAMINATION OF B192 HYDROPHOBIC ASSOCIATIVE POLYMER.....	46
First Test	46
Second Test.....	47
Third Test.....	50
Conclusion	51
9. DOES IT MATTER IF POLYMER REDUCES S_{OR} FOR VISCOUS OILS?	52
The Issue	52
Fractional Flow Calculations for One Layer	52
Future Work	54
Conclusions.....	55
 NOMENCLATURE	 56
REFERENCES	57
APPENDIX A—C1205 Resistance Factors versus Core Section, Flux, and Concentration.....	60

LIST OF TABLES

Table 1—Distance of polymer penetration.....	12
Table 2—Injection parameters for C1205 in a polyethylene core.....	27
Table 3—Injection parameters for C1205 in a Berea core	27
Table 4—Losses after being forced through a Berea core at given pressure gradient	41

TABLE OF FIGURES

Fig. 1—Rheology of 2,500-ppm SNF 3830S HPAM in porous media	2
Fig. 2—Shear thinning by HPAM solutions in porous media	4
Fig. 3—Onset of shear thickening versus HPAM concentration in a 5,120-md core	5
Fig. 4—Maximum allowable F_{r2}/F_{r1} for linear flow, no crossflow.....	7
Fig. 5—Maximum allowable F_{r2}/F_{r1} for radial flow, no crossflow.....	7
Fig. 6—Literature data compared with maximum allowable F_{r2}/F_{r1} values	8
Fig. 7—Understanding front movements for linear flow with crossflow, moderate F_r values	9
Fig. 8—Injection of 10-cp polymer initiated after waterflooding for specified PV, 1 layer.	14
Fig. 9—Injection of 100-cp polymer initiated after waterflooding for specified PV, 1 layer.	14
Fig. 10—Injection of 1,000-cp polymer initiated after waterflooding for specified PV, 1 layer.	14
Fig. 11—Injection of 10-cp polymer initiated after waterflooding for specified PV, 2 layers....	15
Fig. 12—Injection of 100-cp polymer initiated after waterflooding for specified PV, 2 layers..	15
Fig. 13—Injection of 1,000-cp polymer initiated after waterflooding for specified PV, 2 layers	16
Fig. 14—Simple benefit analysis for delayed polymer flooding	17
Fig. 15—Viscosity versus polymer concentration for EX9719 xanthan	18
Fig. 16—Viscosity versus polymer concentration for several polymers.....	18
Fig. 17—Viscosity versus shear rate for EX9719 xanthan.....	19
Fig. 18—Filterability for EX9719 xanthan and various polymers	19
Fig. 19—700-ppm EX9719 xanthan with (versus without) 35-ppm Cr (as $CrCl_3$)	20

Fig. 20—EX9719 xanthan with Cr (as CrCl ₃).....	20
Fig. 21—Viscosity versus shear rate for KELCOGEL HT gellan gum	21
Fig. 22—Gellan in distilled water with Cr (as CrCl ₃)	21
Fig. 23—Solutions of 3830S versus C1205.....	23
Fig. 24—Viscosity versus polymer concentration.....	24
Fig. 25—Viscosity versus shear rate, PaarPhysica.....	24
Fig. 26—Viscosity versus shear rate, Brookfield.	25
Fig. 27— Filter Test Results: 3830S versus C1205.....	26
Fig. 28—500-ppm C1205 viscosity and resistance factor in Berea.....	28
Fig. 29—C1205 resistance factor versus flux in 12,313-md polyethylene.....	28
Fig. 30—C1205 resistance factor versus flux in 363-md Berea.....	28
Fig. 31—3830S HPAM resistance factor versus flux in 5,120-md polyethylene	29
Fig. 32—C1205 resistance factors versus viscosities	30
Fig. 33—C1205 resistance factor versus capillary bundle parameter	30
Fig. 34—Resistance factors in polyethylene: C1205 versus 3830S	31
Fig. 35—C1205 resistance factors versus concentration in 10,144-md polyethylene.....	32
Fig. 36—C1205 residual resistance factors in 10,144-md polyethylene	32
Fig. 37—500-ppm C1205 resistance factors at beginning versus end of the experiment	33
Fig. 38—Resistance factors for mechanically degraded 500-ppm C1205 (after 2,500 psi/ft)	34
Fig. 39—Resistance factors for mechanically degraded 900-ppm C1205 (after 2,500 psi/ft)	34
Fig. 40—Resistance factors for mechanically degraded 1,500-ppm C1205 (after 2,500 psi/ft) .	35
Fig. 41—Resistance factors for mechanically degraded 2,500-ppm C1205 (after 2,500 psi/ft) .	35
Fig. 42—Resistance factors for mechanically degraded 500-ppm C1205 (after 235 psi/ft)	36
Fig. 43—Resistance factors for mechanically degraded 900-ppm C1205 (after 235 psi/ft)	36
Fig. 44—Resistance factors for mechanically degraded 1,500-ppm C1205 (after 235 psi/ft)	36
Fig. 45—Resistance factors for mechanically degraded 2,500-ppm C1205 (after 235 psi/ft)	37
Fig. 46—Resistance factors for mechanically degraded 500-ppm 3830S (after 2,500 psi/ft).....	38
Fig. 47—Resistance factors for mechanically degraded 900-ppm 3830S (after 2,500 psi/ft).....	38
Fig. 48—Resistance factors for mechanically degraded 1,500-ppm 3830S (after 2,500 psi/ft)..	38
Fig. 49—Resistance factors for mechanically degraded 2,500-ppm 3830S (after 2,500 psi/ft)..	39
Fig. 50—Resistance factors for mechanically degraded 500-ppm 3830S (after 235 psi/ft).....	39
Fig. 51—Resistance factors for mechanically degraded 900-ppm 3830S (after 235 psi/ft).....	39
Fig. 52—Resistance factors for mechanically degraded 1,500-ppm 3830S (after 235 psi/ft).....	40
Fig. 53—Resistance factors for mechanically degraded 2,500-ppm 3830S (after 235 psi/ft).....	40
Fig. 54—Low-flux resistance factors relative to low-shear-rate viscosities.....	40
Fig. 55—Resistance factors for fresh 2,500-ppm 3830S	42
Fig. 56—Resistance factors for 500-ppm polymer: C1205 versus 3830S.....	43
Fig. 57—Resistance factors for 900-ppm polymer: C1205 versus 3830S.....	44
Fig. 58—Resistance factors for 1,500-ppm polymer: C1205 versus 3830S.....	44
Fig. 59—Resistance factors for 2,500-ppm polymer: C1205 versus 3830S.....	44
Fig. 60—B192 resistance factors in 5-darcy polyethylene	47
Fig. 61—1,300-ppm B192 pressure gradients in 5-darcy polyethylene	47
Fig. 62—500-ppm B192 pressure gradients in 12.3-darcy polyethylene	48
Fig. 63—300-ppm B192 pressure gradients in polyethylene. Rates: high to low	49
Fig. 64—300-ppm B192 pressure gradients in polyethylene. Rates: low to high	49
Fig. 65—300-ppm B192 pressure gradients in polyethylene. Flow direction reversed	49

Fig. 66—300-ppm B192 pressure gradients in polyethylene. Second core section	50
Fig. 67—300-ppm B192 pressure gradients in Berea. Rates: high to low	50
Fig. 68—300-ppm B192 pressure gradients in Berea. Rates: low to high	51
Fig. 69—Effect of S_{or} on recovery for 1-cp water, 1,000-cp oil.....	52
Fig. 70—Effect of S_{or} on recovery for 1-cp water, 1-cp oil.....	53
Fig. 71—Effect of S_{or} on recovery for 10-cp polymer, 1,000-cp oil	54
Fig. 72—Effect of S_{or} on recovery for 100-cp polymer, 1,000-cp oil	54

ACKNOWLEDGMENTS

Financial support for this work is gratefully acknowledged from the United States Department of Energy (NETL/National Petroleum Technology Office), the State of New Mexico, CP Kelco, SNF Floerger, and Statoil. ConocoPhillips was kind in providing information on relevant North Slope viscous oil reservoirs. I greatly appreciate the efforts of those individuals who contributed to this project. Tian Fan performed most of the corefloods. Professor Rosangela Balaban (U Federal Rio Grande Do Norte, Brazil) performed some of the corefloods in Chapter 7. Kate Wavrik performed most of the viscosity measurements. I also appreciate useful discussions with Nicolas Gaillard of SNF for Chapters 7 and 8. Hao Wan helped with considerations in Chapter 7. Karthik Kamaraj, Guoyin Zhang, and Yi Lui helped with considerations in Chapter 9. I especially appreciate the thorough review of this manuscript by Julie Ruff. This material is based upon work supported by the Department of Energy under Award Number DE- NT0006555.

EXECUTIVE SUMMARY

This technical progress report describes work performed from October 1, 2009, through September 30, 2010, for the project, "Use of Polymers to Recover Viscous Oil from Unconventional Reservoirs." The objective of this three-year research project is to develop methods using water soluble polymers to recover viscous oil from unconventional reservoirs (i.e., on Alaska's North Slope). The project has three technical tasks. First, limits will be re-examined and redefined for where polymer flooding technology can be applied with respect to unfavorable displacements. Second, we will test existing and new polymers for effective polymer flooding of viscous oil, and we will test newly proposed mechanisms for oil displacement by polymer solutions. Third, we will develop novel methods of using polymer gels to improve sweep efficiency during recovery of unconventional viscous oil.

Can HPAM Solutions Show Shear Thinning in Porous Media Deep within a Formation?

Previous work demonstrated that HPAM resistance factors increase with increased flux at moderate to high flux values. This behavior was attributed to the viscoelastic character of HPAM and the elongational flow field in porous rock. At moderate to low fluxes, HPAM resistance factors usually show Newtonian (flow-rate-independent) or near-Newtonian behavior under practical conditions experienced during polymer floods. From previous work, we also know that experimental artifacts can make shear thinning appear to occur for HPAM in short cores. We made a concerted effort to establish whether some level of shear thinning can be seen for HPAM solutions in porous media at low flux. For HPAM solutions with a sufficiently low salinity and/or sufficiently high polymer concentration, we show that shear thinning can be observed in porous media at moderate to low fluxes. However, under practical conditions where HPAM is used for EOR, the degree of shear thinning is slight or non-existent, especially compared to the level of shear thickening that occurs at high fluxes. The shear rate for the transition from Newtonian to shear-thinning behavior in a viscometer decreases quite strongly with increasing HPAM concentration. In contrast, the flux at the onset of shear-thickening behavior in porous media decreases modestly with increasing HPAM concentration.

Is Permeability Reduction by Polymers Beneficial to a Polymer Flood? Contrary to earlier claims, permeability reduction associated with polymers is shown not to benefit vertical sweep efficiency during polymer flooding. Resistance factors (effective polymer solution viscosities in porous media) and residual resistance factors (permeability reduction values) tend to increase with decreased permeability. We considered various cases (linear flow, radial flow, with crossflow, without crossflow) where vertical sweep efficiency was evaluated when the resistance factor (F_{r2}) in a low-permeability layer (of permeability, k_2) was greater than in an adjacent high-permeability layer (with resistance factor F_{r1} and permeability, k_1). For applications with linear flow (e.g., fractured wells) with no crossflow, the maximum allowable ratio of F_{r2}/F_{r1} (so that polymer injection does not harm vertical sweep) is about the same as the permeability ratio, k_1/k_2 . Thus, linear flow applications can be reasonably forgiving if the permeability contrast and the polymer solution resistance factors are sufficiently large. Radial flow (with no crossflow) is much less forgiving to high F_{r2}/F_{r1} values. Even for high permeability contrasts (e.g., $k_1/k_2 = 20$), the maximum allowable F_{r2}/F_{r1} values were less than 1.4. In most cases when crossflow can occur (either linear or radial flow), the F_{r2}/F_{r1} ratio has little effect on the relative distance of polymer penetration into the various zones.

Does Rheology Significantly Affect Vertical Sweep Efficiency? Xanthan solutions are well known to exhibit shear thinning both in viscometers and in porous media. Contrary to recent suggestions in the literature, shear thinning by polymer solutions is shown not to be a significant liability for vertical sweep efficiency. The overall viscosity (resistance factor) of the polymer solution is of far greater relevance than the rheology. These observations were demonstrated for both radial and linear flow and both with and without crossflow.

Is Polymer Flooding of Viscous Oil Hurt by a Prior Waterflood? In our previous work, we used fractional flow calculations to examine the potential of polymer flooding when the polymer flood was initiated immediately after primary recovery—i.e., with no intermediate waterflood. We extended the fractional flow calculations to examine the effectiveness of polymer flooding when a waterflood (with 1-cp water) was implemented prior to the polymer flood. We showed that polymer flooding can be effective in viscous (1,000-cp) oil reservoirs even if waterflooding has been underway for some time. Certainly, the EOR target will be diminished as the throughput increases for the pre-polymer waterflood. However, fractional flow analysis indicates that a significant oil bank can develop and be recovered from a polymer flood, even if a significant waterflood precedes the polymer project. This point was demonstrated both with a homogeneous 1-layer reservoir and in a 2-layer reservoir with free crossflow.

Examination of Two Biopolymers: EX9719 and Gellan Gum. We examined two new biopolymers for possible use in EOR. The first was CP Kelco's EX9719 xanthan. EX9719 is a very effective viscosifier, providing 25-100% higher viscosities than other xanthans, depending on the polymer concentration. EX9719 also shows good filterability. The polymer can be crosslinked with CrCl_3 , but it is not clear that these Cr-xanthan gels have any advantages over existing Cr(III)-acetate-HPAM gels. The second polymer was CP Kelco's gellan gum, KELCOGEL HT. This polymer is probably not a serious candidate for polymer flooding since it only dissolves in distilled water. Solutions with 700- to 5,000-ppm gellan (in distilled water) all formed solid gels within 1 day when mixed with CrCl_3 at room temperature.

Examination of Associative Polymer, C1205. An important concept from our previous studies of HPAM and xanthan was that low-flux resistance factors in porous media should match reasonably closely with expectations from low-shear-rate viscosity measurements. Our work with the SNF polymer, C1205, indicates low-flux resistance factors (for fresh polymer solutions) that were much greater than expectations from viscosity measurements. C1205 is a new anionic-polyacrylamide-based tetra-polymer that has associative properties. Typically, the hydrophobic monomer content ranges from 0.025 to 0.25 mol%. Molecular weights range from 12-17 million for C1205. Total anionic content is between 15 and 25 mol%. Less than 8 mol% sulfonic monomer is present in C1205.

Many similarities were noted between C1205 and 3830S. Viscosity versus concentration and shear rate for C1205 (in a 2.52% TDS brine at 25°C) was quite similar to that for SNF Flopaam 3830S (a conventional HPAM). The molecular weight of C1205 was given as 12-17 million g/mol, while 3830S was 18-20 million g/mol. Both 3830S and C1205 show excellent filterability at lower concentrations (1,000 ppm or lower), but plugged within 200 cm^3/cm^2 throughput at higher concentrations (1,500 ppm).

Important differences exist between the behavior of the two polymers. C1205 solutions were noticeably more turbid than those of 3830S. In Berea sandstone and porous polyethylene cores, low-flux resistance factors for fresh C1205 were at least twice those for 3830S. In cores with multiple sections, we saw no evidence of face plugging. This was true in both 347-md Berea sandstone and 10-12 darcy porous polyethylene. Also, plots of resistance factor versus flux (after normalization for permeability using the capillary bundle correlation) were the same for both 347-md Berea sandstone and 12-darcy porous polyethylene. These observations argue against the importance of microgels, since microgels should cause higher resistance factors in less-permeable rock. The observations also argue against polymer retention effects since polymer adsorption/retention should be greater in 347-md Berea sandstone (which is hydrophilic) than in 12-darcy polyethylene (which is hydrophobic). Also, plots of resistance factor versus flux in 10-darcy polyethylene were the same after injecting 17.6 *PV* of C1205 solution as when only 1-3.4 *PV* had been injected. If throughput-dependent microgel propagation or polymer retention were important, we might have expected later resistance factors to be greater than earlier resistance factors.

Fresh C1205 solutions provided about the same viscosity as fresh 3830S solutions. However, in 10-darcy polyethylene, fresh C1205 solutions provided low-flux resistance factors that were about twice those for fresh 3830S solutions. Both polymers showed modest (0-8%) viscosity losses (at 7.3 s⁻¹) after exposure to a 235 psi/ft pressure gradient in a core. However, C1205 solutions experienced 31-45% loss in low-flux resistance factor, whereas 3830S solutions experienced only 0-15% loss. After 235 psi/ft, low-flux resistance factors for C1205 solutions were often similar to those for fresh 3830S solutions. After exposure to 2,500 psi/ft pressure gradient, C1205 solutions experienced 19-35% viscosity loss, whereas 3830S solutions experienced 5-17% viscosity loss. After 2,500 psi/ft, low-flux resistance factors for C1205 solutions were the same or less than those for 3830S solutions.

In short (13-14 cm) Berea sandstone or porous polyethylene cores, we also saw no length dependence of resistance factors for C1205. However, in a 78-cm long 10-darcy polyethylene core, we saw a length dependence of C1205 resistance factors for the higher polymer concentrations. If the observed length trend can be extrapolated, it suggests that resistance factors might not be any higher than expectations from viscosity after 8 ft. Consequently, more work is needed in longer cores to establish whether the higher-than expected resistance factors will propagate deep into a formation.

Examination of Associative Polymer, B192. We received a second new hydrophobic associative polymer from SNF: Superpusher B 192 (hereafter called B192). B192 is an anionic-polyacrylamide-based ter-polymer. Typically, the hydrophobic monomer content ranges from 0.025 to 0.25 mol%. B192 contains 4 times more hydrophobic monomer than C1205. Molecular weights range from 3 to 7 million for B192. Total anionic content is between 15 and 25 mol%. Our coreflood results using B192 were intriguing, in that (1) resistance factors are much higher than expected from viscosity measurements, (2) pressure gradients can be independent of flux over a wide range, and (3) regions of constant pressure gradient were observed in high-permeability polyethylene cores but not in less-permeable Berea sandstone cores. More work will be needed to understand the behavior of this polymer.

Does It Matter If Polymer Reduces S_{or} for a Viscous Oil? Fractional flow analysis reveals that if polymers can reduce the S_{or} , this phenomenon will be an important factor during recovery of viscous oils. As expected, the magnitude of the oil recovery increases as the S_{or} is reduced. For one example examined, if the polymer reduces S_{or} from 0.3 to 0.25, a 10% increase in oil recovery can be expected. Also, for a given S_{or} , the magnitude of the oil recovery increases as the viscosity of the injected polymer solution increases.

1. INTRODUCTION

A tremendous resource of viscous oil exists in the United States and throughout the world. Usually, thermal methods (e.g., steam flooding) are considered first for recovering this oil. However, circumstances often exist that preclude application of thermal methods. Consequently, we are exploring where polymer flooding can be viable for recovering viscous oil. This report describes research performed during the second year of the project, "Use of Polymers to Recover Viscous Oil from Unconventional Reservoirs."

Project Objectives

The objective of this three-year research project is to develop methods using water soluble polymers to recover viscous oil from unconventional reservoirs (i.e., on Alaska's North Slope). The project has three technical tasks. First, limits will be re-examined and redefined for where polymer flooding technology can be applied with respect to unfavorable displacements. Second, we will test existing and new polymers for effective polymer flooding of viscous oil, and we will test newly proposed mechanisms for oil displacement by polymer solutions. Third, we will develop novel methods of using polymer gels to improve sweep efficiency during recovery of unconventional viscous oil.

Report Content

In Chapter 2, we experimentally demonstrate that very low salinities (i.e., tap water or distilled water) and/or high polymer concentrations are needed in order for partially hydrolyzed polyacrylamides (HPAM) to show shear-thinning behavior in porous media. Chapter 3 reports an analytical study of when the permeability dependence of polymer resistance factors is detrimental to vertical sweep efficiency. Chapter 4 analytically considers whether shear-thinning or shear-thickening polymer rheology has a significant effect on vertical sweep efficiency. In Chapter 5, we use fractional flow calculations to examine how much waterfloods of various sizes reduce the potential for subsequent polymer floods in reservoirs with viscous oils. Chapter 6 experimentally examines the rheology, filterability, and gelation characteristics of a new xanthan (EX9719) and gellan gum. Chapter 7 extensively investigates the rheology in porous media for a new hydrophobic associative polymer, C1205. Chapter 8 reports an examination of another new hydrophobic associative polymer, B192. In Chapter 9, we consider whether a polymer's ability to reduce the residual oil saturation is important during a polymer flood in a reservoir with viscous oil.

Our latest research results, along with detailed documentation of our past work, can be found on our web site at <http://baervan.nmt.edu/randy/>.

2. CAN HPAM SOLUTIONS SHOW SHEAR THINNING IN POROUS MEDIA?

Resistance factors for solutions of partially hydrolyzed polyacrylamide (HPAM) increase substantially with increased flux at moderate to high flux values. This behavior was attributed to the viscoelastic character of HPAM and the elongational flow field in porous rock. At moderate to low fluxes, HPAM resistance factors usually show Newtonian or near-Newtonian behavior under practical conditions experienced during polymer floods (Seright et al. 2009a). Fig. 1 illustrates this behavior. (In Fig. 1, u is flux, ϕ is porosity, and k is permeability.)

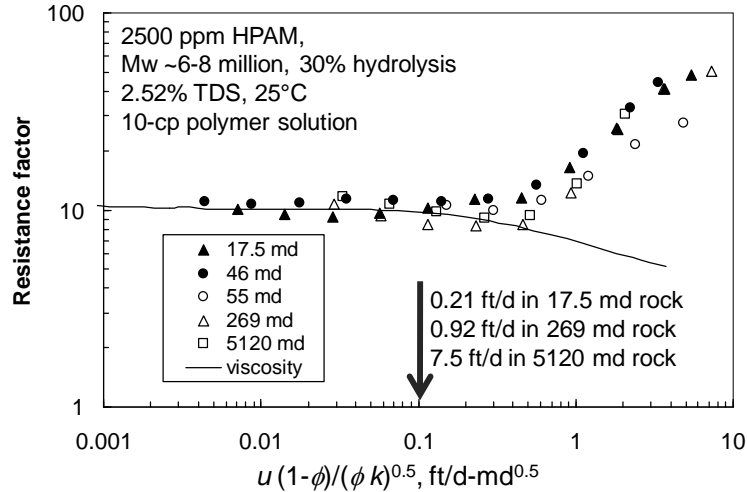


Fig. 1—Rheology of 2,500-ppm SNF 3830S HPAM in porous media.

Along with others, Chauveteau (1981) noted that HPAM solutions showed shear thickening at moderate to high velocities in porous media. However, he speculated that at moderate to low flux values in capillary constrictions or in porous media, HPAM resistance factors might show shear-thinning behavior, and ultimately, show Newtonian behavior at the very lowest velocities. Consequently, he suggested that resistance factors should exhibit a minimum value at intermediate fluxes. Data published by Heemskirk *et al.* (1984), Masuda *et al.* (1992), and Delshad *et al.* (2008) could be viewed as indicating that HPAM in porous media exhibits a subtle shear thinning at low fluxes and a shallow minimum in resistance factor at intermediate fluxes. The open squares in Fig. 2 may support this view for freshly prepared 900-ppm HPAM (SNF Flopaam 3830S) in 2.52% TDS brine, when flowing through 5,120-md porous polyethylene. However, the degree of shear thinning that was reported/observed was very mild, and the existence of the shallow minimum is debatable. An earlier publication (Seright *et al.* 2009a) proposed that the observed shear thinning for HPAM solutions at low flux values in porous media could be an experimental artifact due to (1) use of insufficiently accurate pressure transducers, (2) inadequate temperature control, and (3) the polymer molecular weight that is too high to propagate without forming an internal or external filter cake (i.e., if the polymer contains significant concentrations of “microgels” or high molecular weight species that are too large to flow efficiently through the pore structure). The latter point was demonstrated in our earlier work (Seright 2009b). Introduction of air into the core can also induce apparent shear thinning. If these experimental artifacts are avoided, can shear thinning occur during flow of polymer solutions in cores?

HPAM in Very Low Salinity Water

Our previous work was performed in brines with moderate to high salinity (at least 0.3% total dissolved solids, TDS). Gogarty (1967) reported a definitive shear thinning in cores for 1,200- to 1,800-ppm HPAM in water with less than 700-ppm (0.07%) TDS. Thus, it appears that shear thinning could materialize for HPAM solutions in porous rock if the salinity is sufficiently low. To confirm this possibility, we prepared HPAM solutions in distilled water, and injected them at various rates into a 5,120-md porous polyethylene core. Fig. 2 shows the results using SNF Flopaam 3830S HPAM (with M_w of 18-20 million G/mol and degree of hydrolysis of 40%). For 400-ppm HPAM in distilled water (solid diamonds in Fig. 2), shear-thinning behavior was noted for flux values between 0.06 and 4.3 ft/d. The slope was -0.56 for a plot of $\ln(\text{resistance factor})$ versus $\ln(\text{flux})$. A similar slope was noted for 1000-ppm HPAM in distilled water for flux values between 0.135 and 4.3 ft/d (solid squares in Fig. 2). However, for higher flux values, the resistance factors leveled off and began a gradual increase. This latter behavior may be due to the viscoelastic nature of the polymer. Interestingly, the slope of plots of $\ln(\text{viscosity})$ versus $\ln(\text{shear rate})$ were -0.85 for 400-ppm HPAM and -0.94 for 1000-ppm HPAM. Thus, the very strong shear-thinning character of these solutions was moderated considerably during flow through porous media.

As mentioned earlier, the open squares in Fig. 2 show the behavior of 900-ppm HPAM in 2.52% TDS brine. Consistent with Fig. 1, this curve shows a strong shear-thickening behavior at moderate to high flux values and near-Newtonian behavior at low flux values. (Although one could argue the existence of a shallow minimum between 1 and 7 ft/d.) Thus, two key points may be taken from Fig. 2, along with our other results. First, HPAM solutions can show a definitive shear-thinning behavior at low flux values in porous media if the solvent is distilled water (or a solvent with *very* low salinity). Second, for HPAM solutions in more practical brines (i.e., >0.3% TDS), Newtonian or near-Newtonian behavior is expected at low flux values deep within a reservoir.

Relation between the Onset of Shear Thinning in a Viscometer versus the Onset of Shear Thickening in Porous Media

As shear rate is increased for a polymer solution in a viscometer, a shear rate is encountered that marks the transition from Newtonian behavior to shear thinning. This transition shear rate is associated with the “longest relaxation time in the linear viscoelastic spectrum” (Graessley 1974). Some think of this point as the shear rate where polymer conformations experience their first departure from a random coil configuration. The onset of shear thickening by HPAM solutions in porous media is also associated with a change in polymer conformation—specifically where the polymers undergo a coil-stretch transition, resulting in highly extended polymer conformations and large extensional stresses (Durst *et al.* 1982, Southwick and Manke 1988). A comparison of the solid curve and the data points in Fig. 1 implies that these two transition points (i.e., the transition from Newtonian behavior to shear thinning in a viscometer and the onset of shear thickening in porous media) might coincide. To explore this idea, we performed experiments using various concentrations (25 ppm to 1,600 ppm) of SNF Flopaam 3830S in 2.52% TDS brine. For this polymer under these conditions, we determined C^* (the concentration at which polymer behavior transitions from dilute to semi-dilute behavior) to be 200 ppm.

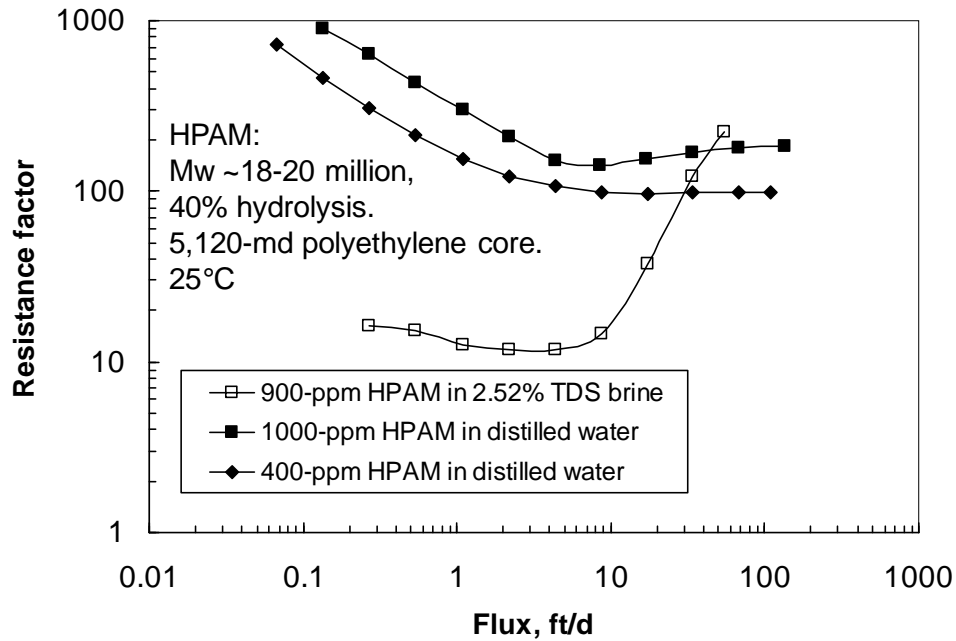


Fig. 2—Shear thinning by HPAM solutions in porous media.

Fig. 3 plots resistance factor versus flux during injection of many polymer solutions into a 5,120-md porous polyethylene core. For polymer concentrations even as low as 25 ppm (one-eighth the value of C^*), shear thickening was evident. In contrast, viscosity versus shear rate showed Newtonian behavior, with a value very close to 1 cp. As described in the literature (Durst *et al.* 1982), the elongational flow field associated with porous media can accentuate viscoelastic behavior that is not apparent from a pure shear field. This observation provides our first reason to doubt that the transition from Newtonian behavior to shear-thinning in a viscometer correlates directly with the onset of shear thickening in porous media.

In Fig. 3, as polymer concentration increased from C^* (200 ppm) to 1,600 ppm, the onset of shear thickening decreased by a factor of two. For comparison, from viscosity-versus-shear-rate data, the shear rate at the transition from Newtonian behavior to shear thinning decreased by a factor of 10 (from 10 to 1 s^{-1}) over the same range of polymer concentration. Since the variation in transition shear rate (10, from the viscosity data) was much greater than the variation in onset of shear thickening (2, from resistance-factor data), the apparent correlation between the two transitions seen in Fig. 1 must be coincidental.

At low flux values in Fig. 3, the curves for the highest three polymer concentrations show slight shear thinning. The slopes of these curves were -0.236 for 1,600-ppm HPAM and -0.114 for 480-ppm HPAM. For comparison, the slopes of the shear-thinning portions of $\ln(\text{viscosity})$ -versus- $\ln(\text{shear rate})$ curves were -0.218 and -0.127 for the two concentrations, respectively. The similarity of the shear-thinning slopes from viscosity and core data suggests that shear thinning might occur in porous media, even in saline brines. This information also indicates that the apparent correlation between the two transitions seen in Fig. 1 was coincidental.

Significance of Observations

For HPAM solutions with a sufficiently low salinity and/or sufficiently high polymer concentration, shear thinning can be observed in porous media at moderate to low fluxes. However, the degree of shear thinning is quite mild, especially compared to the level of shear thickening at higher fluxes.

Our earlier work (Seright *et al.* 2009a, 2009b) indicate that under practical conditions for chemical flooding field applications, HPAM solutions show Newtonian or near-Newtonian behavior at low flux values, if ultra-high M_w polymer species are not present. Why is this point worth arguing? The reason is that most chemical flooding simulators have incorrectly assumed that the shear-thinning behavior observed by HPAM solutions in a viscometer will be directly applicable in porous rock—ignoring the importance of shear thickening. This incorrect assumption leads to (1) an overly optimistic prediction of polymer injectivity if wells are not fractured, (2) often, an incorrect prediction that fractures will not be open during polymer injection, (3) an overly complex calculation of polymer resistance factors, and (4) prediction of resistance factors that are too high deep in a formation.

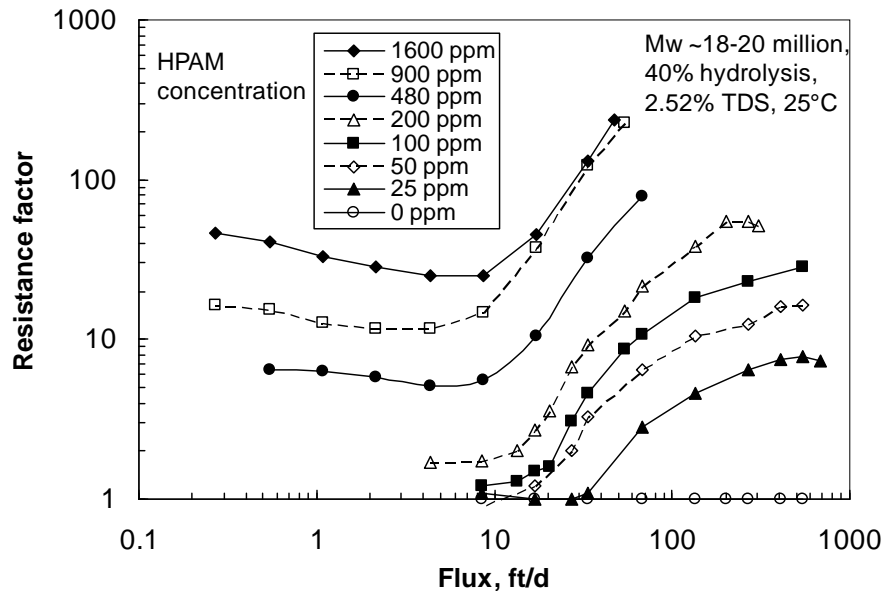


Fig. 3—Onset of shear thickening versus HPAM concentration in a 5,120-md core.

Conclusions

1. For HPAM solutions with a sufficiently low salinity and/or sufficiently high polymer concentration, shear thinning can be observed in porous media at moderate to low fluxes. However, under practical conditions where HPAM is used for EOR, the degree of shear thinning is slight or non-existent, especially compared to the level of shear thickening that occurs at high fluxes.
2. The shear rate for the transition from Newtonian to shear-thinning behavior in a viscometer decreased quite strongly with increased HPAM concentration. In contrast, the flux at the onset of shear-thickening behavior in porous media decreased modestly with increased HPAM concentration.

3. IS PERMEABILITY REDUCTION BY POLYMERS A GOOD THING?

Early work (Jennings *et al.* 1971, Hirasaki and Pope 1974) recognized that high molecular weight HPAM sometimes reduced the mobility (λ or k/μ) of aqueous solutions in porous media by a greater factor than can be rationalized based on the viscosity (μ) of the solution. The incremental reduction in mobility was attributed to reduction in permeability (k), caused by adsorption or mechanical entrapment of the high molecular weight polymers—especially from the largest polymers in the molecular weight distribution for a given polymer. In the 1960s and 1970s, this effect was touted to be of great benefit (Jennings *et al.* 1971) for polymer floods (simply because the polymer appeared to provide significantly more apparent viscosity in porous media than expected from normal viscosity measurements). However, these benefits were often not achievable in field applications because normal field handling and flow through an injection sand face at high velocities mechanically degraded the large molecules that were responsible for the permeability reduction (Seright *et al.* 1981, Seright 1983). Also, the largest molecules were expected to be preferentially retained (i.e., by mechanical entrapment in pores) and stripped from the polymer solution before penetrating deep into the formation.

Even if high permeability reductions could be achieved, would this effect actually be of benefit? More specifically, the concern focuses on how the mobility reduction varies with permeability of porous media. For adsorbed polymers, resistance factors (F_r , apparent viscosities in porous media relative to brine) and residual resistance factors (F_{rr} , permeability reduction values) increase with decreasing permeability (Pye 1964, Jennings *et al.* 1971, Hirasaki and Pope 1974, Vela *et al.* 1976, Jewett and Schurz 1979, Zaitoun and Kohler 1987, Rousseau *et al.* 2005). In other words, these polymers can reduce the flow capacity of low permeability rock by a greater factor than high permeability rock. Depending on the magnitude of this effect, these polymers and gels can harm injection or production flow profiles in wells, even though the polymer penetrates significantly farther into the high permeability rock (Seright 1988, Seright 1991, Liang *et al.* 1993, Zhang and Seright 2007).

Linear Flow, No Crossflow

For the cases discussed earlier, the resistance factors (effective viscosities) in all layers were assumed to be equal. Spreadsheets in Seright 2009a are capable of performing calculations with different resistance factors in different zones (although only single-phase flow is considered). We used these spreadsheets to generate Fig. 4 for linear flow with no crossflow. The x -axis plots the resistance factor in Zone 1 (F_{r1}). We are interested in how high the resistance factor can be in Zone 2 (F_{r2}) without impairing the vertical sweep efficiency. The y -axis plots the maximum allowable ratio, F_{r2}/F_{r1} , that meets this criterion. These calculations were made for several permeability ratios, k_1/k_2 , between 2 and 20. Fig. 4 shows that for F_{r1} values greater than 10, the maximum allowable ratio of F_{r2}/F_{r1} was about the same as the permeability ratio, k_1/k_2 . Thus, linear flow applications can be reasonably forgiving if the permeability contrast and the polymer solution resistance factors are sufficiently large.

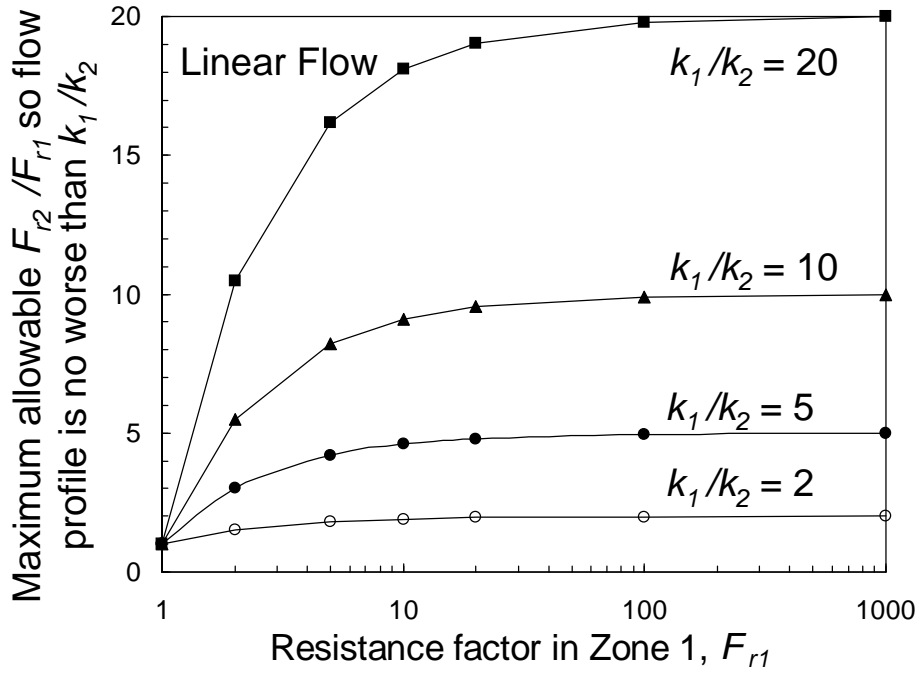


Fig. 4—Maximum allowable F_{r2}/F_{r1} for linear flow, no crossflow.

Radial Flow, No Crossflow

Similar calculations were performed for radial flow (with no crossflow), and the results are shown in Fig. 5. These calculations reveal that radial flow is much less forgiving to high values of F_{r2}/F_{r1} . Even for high permeability contrasts (e.g., $k_1/k_2 = 20$), the maximum allowable F_{r2}/F_{r1} values were less than 1.4.

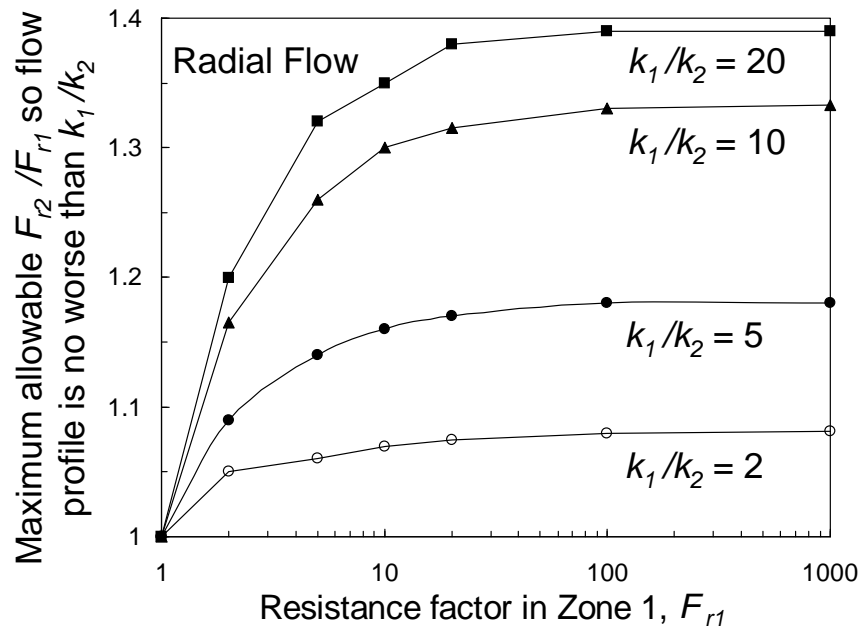
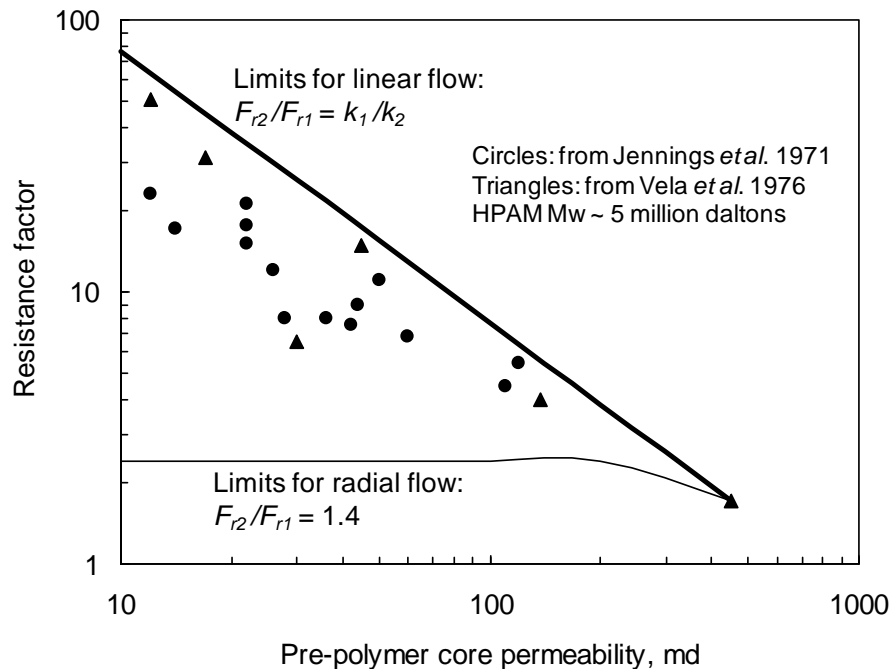


Fig. 5—Maximum allowable F_{r2}/F_{r1} for radial flow, no crossflow.

Comparison with Laboratory Data

Jennings *et al.* 1971 and Vela *et al.* 1976 reported resistance factors obtained in cores with a wide range of permeability, using HPAM that had a molecular weight of $\sim 5 \times 10^6$ g/mol (symbols in Fig. 6). The thick line in Fig. 6 plots the maximum acceptable behavior of resistance factors for linear flow cases, while the thin line plots the maximum acceptable behavior of resistance factors for radial flow cases. In these plots, F_{r1} refers to the measured resistance factor in the 453-md rock, while F_{r2} refers to the maximum acceptable resistance factor in a given less permeable rock or zone. For the data provided, the measured behavior of resistance factors was barely acceptable for linear flow, and definitely unacceptable for radial flow. A logical remedy for this situation would be to choose a polymer with a lower molecular weight, so resistance factors do not increase so much with decreasing permeability (Wang *et al.* 2008, 2009). Whether or not a given polymer will be acceptable in a given reservoir may depend on a number of factors, including polymer molecular weight, rock permeability, water salinity, presence of residual oil, reservoir temperature, and possibly other factors (such as clay content, pore structure, and degree of mechanical degradation before entering the rock).



Zapata and Lake 1981, Sorbie and Seright 1992). For vertical equilibrium, the pressure gradients in two adjacent zones (with no flow barriers) are the same for any given horizontal position. Put another way, for a given distance from the wellbore (if gravity can be neglected), the pressure is the same in both zones.

Consider a polymer solution flowing through two adjacent zones where crossflow can occur (Fig. 7). Zone 1 (the high-permeability layer) has a permeability of k_1 , a porosity of ϕ_1 , and exhibits a polymer resistance factor of F_{r1} . Zone 2 (the low-permeability layer) has a permeability of k_2 , a porosity of ϕ_2 , and exhibits a polymer resistance factor of F_{r2} . The average movement rates for polymer fronts in the two zones are v_1 and v_2 . Of course, crossflow may make the polymer front uneven (i.e., not vertical) in Zone 2. So in the simple analysis here, we consider the average front positions. If vertical equilibrium exists, the pressure difference between the polymer fronts will be the same in the two zones. Darcy's law can then be applied to estimate the average front movement rates. For Zone 2, this rate, v_2 , is

$$v_2 \cong \Delta p k_2 / (\mu \phi_2 L) \dots\dots\dots(1)$$

For Zone 1, this rate, v_1 , is

$$v_1 \cong \Delta p k_1 / (\mu F_{r1} \phi_1 L) \dots\dots\dots(2)$$

The ratio of average front rates is

$$v_2/v_1 \cong F_{r1} k_2 \phi_1 / (k_1 \phi_2) \dots\dots\dots(3)$$

Consequently, the relative rate of polymer front movement is not sensitive to the resistance factor in Zone 2. Eq. 3 is the same expression that is derived when resistance factors are equal for the two zones (Sorbie and Seright 1992).

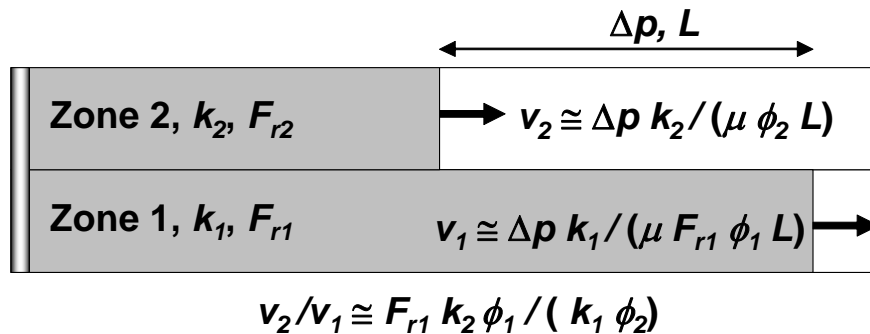


Fig. 7—Understanding front movements for linear flow with crossflow, moderate F_r values.

Effect of Differential Retention

For many years, people have recognized that polymer resistance factors, residual resistance factors, and chemical retention values in porous media increase with decreasing permeability (Jennings et al. 1971, Vela et al. 1976, Zaitoun and Kohler 1987). These trends impede polymer propagation into the less permeable zones, and therefore do not aid vertical sweep (Seright 1988, Seright 1991).

Conclusions

Contrary to earlier claims, permeability reduction associated with polymers does not benefit vertical sweep efficiency during polymer flooding. For applications with linear flow (e.g., fractured wells) with no crossflow, the maximum allowable ratio of F_{r2}/F_{r1} (so that polymer injection does not harm vertical sweep) is about the same as the permeability ratio, k_1/k_2 . Thus, linear flow applications can be reasonably forgiving if the permeability contrast and the polymer solution resistance factors are sufficiently large. Radial flow (with no crossflow) is much less forgiving to high F_{r2}/F_{r1} values. Even for high permeability contrasts (e.g., $k_1/k_2 = 20$), the maximum allowable F_{r2}/F_{r1} values were less than 1.4. In most cases when crossflow can occur (either linear or radial flow), the F_{r2}/F_{r1} ratio has little effect on the relative distance of polymer penetration into the various zones.

4. DOES RHEOLOGY SIGNIFICANTLY AFFECT SWEEP EFFICIENCY?

Recently, some authors claimed that shear thinning exhibited by polymer solutions is detrimental to sweep efficiency (Deshad et al. 2008, AlSofi and Blunt 2009). They cited Jones (1980) to support their position. Jones argued that if two non-communicating layers of different permeability were completely filled with a shear-thinning fluid, the vertical flow profile would be worse than for a Newtonian fluid. Although correct (and verified by Table 2 of Seright 1991), the argument is not relevant to polymer floods. In a polymer flood, a viscous polymer solution displaces oil and/or water. For this circumstance, the overall viscosity (resistance factor) of the polymer solution is of far greater relevance than the rheology (Seright 1991). This point can be appreciated by considering several cases.

Cases with Crossflow

First, consider adjacent layers that have substantially different permeabilities, but free crossflow (vertical equilibrium) occurs between the layers. The vertical sweep efficiency is insensitive to the rheology of the injection fluid (within reasonable limits that are really achievable by xanthan or HPAM) if a sufficiently stable displacement is maintained (Sorbie and Seright 1992, Zhang and Seright 2007). For a specific example, consider a 600-ppm xanthan solution that exhibits a power-law exponent of 0.5 in Berea sandstone. For an applied pressure gradient of 2.4 psi/ft, the solution resistance factors were measured as 13.3 in 55-md Berea and 8.1 in 269-md Berea. If this information is input into Eq. 3, an efficient vertical sweep is predicted, even though a 5-fold permeability contrast exists between the layers. Consideration of Eq. 3 reveals that vertical sweep efficiency would be no different for a Newtonian or shear-thickening fluid. Experimental verification of this point can be found at <http://baervan.nmt.edu/randy/> (more specifically, the link to Videos of Polymer Flooding and Crossflow Concepts). Consequently, for cases with crossflow, a fear of using shear-thinning fluids is not warranted.

Radial Flow, No Crossflow

Next, consider layers or pathways that are distinctly separated (i.e., no crossflow between layers). For two non-communicating layers with a 10-fold permeability contrast, the central part of Table 1 (data taken from Seright 1991) shows the relative differences for the displacement (polymer) fronts with radial flow of various rheologies and for factors up to a 100-fold difference in applied pressure drop between two wells. Table 1 indicates that the shear-thickening fluid (HPAM) consistently provided a better vertical flow profile than a 100-cp Newtonian fluid, which in turn, gave a better flow profile than the shear-thinning fluid (xanthan). However, the differences were generally small—i.e., maximum of 12% difference between the shear-thickening fluid (0.384) and the shear-thinning fluid (0.339). Consequently, for radial flow with no crossflow, a fear of using shear-thinning fluids is not warranted.

Linear Flow, No Crossflow

Most polymer floods to date may have had open fractures intersecting the injection wells (Seright et al. 2009a). Therefore, linear flow cases may be the most relevant. In the right part of Table 1 (the cases for linear flow with no vertical communication between layers), there are large percentage differences in the vertical flow profiles for different rheologies. For some cases at high pressure gradients, the shear-thinning fluid gave a noticeably less efficient displacement than for the Newtonian or shear-thickening fluids. However, the differences were most

pronounced at high pressure gradients that are unlikely to be achieved in real field applications (>10 psi/ft). For relatively low pressure gradients, the shear-thinning fluid gave a vertical sweep no worse than the Newtonian or shear-thickening fluids. In the fourth and fifth columns of Table 1, the vertical sweeps for the shear-thickening fluid were less than for the shear-thinning fluid. This situation occurred because the low-flux (low-pressure-gradient) resistance factors were less for the shear-thickening fluid than for the shear-thinning fluid. In summary, for all practical cases, a fear of using shear-thinning fluids is not warranted. The overall viscosity (resistance factor) of the polymer solution is of far greater relevance than the rheology.

Table 1—Distance of polymer penetration into a 100-md layer relative to that in a 1,000-md layer (no crossflow)

Data from Seright 1991	Radial flow			Linear flow			
	$(r_{p2}-r_w)/(r_{p1}-r_w)$			L_{p2}/L_{p1}			
Pressure drop (psi over 50 ft for radial flow) or pressure gradient (psi/ft, for linear flow):	50	500	5000	1	10	100	1000
Assumed rheology:							
Newtonian, $F_r=1$	0.309	0.309	0.309	0.100	0.100	0.100	0.100
Newtonian, $F_r=10$	0.352	0.352	0.352	0.256	0.256	0.256	0.256
Newtonian, $F_r=100$	0.357	0.357	0.357	0.309	0.309	0.309	0.309
Newtonian, $F_r=1,000$	0.358	0.358	0.358	0.316	0.316	0.316	0.316
Shear-thinning, Xanthan, Carreau model,	0.339	0.326	0.325	0.316	0.297	0.174	0.132
Shear-thickening, HPAM, Durst-Bird model	0.384	0.360	0.356	0.253	0.278	0.283	0.284

Conclusion

Contrary to recent suggestions, shear thinning by polymer solutions is not a significant liability. The overall viscosity (resistance factor) of the polymer solution is of far greater relevance than the rheology.

5. IS POLYMER FLOODING OF VISCOUS OIL HURT BY A PRIOR WATERFLOOD?

One Homogeneous Layer

In our previous work (Seright 2010), we used fractional flow calculations to examine the potential of polymer flooding when the polymer flood was initiated immediately after primary recovery—i.e., with no intermediate water flood. In this chapter, we extend the fractional flow calculations to examine the effectiveness of polymer flooding when a waterflood (with 1-cp water) was implemented prior to the polymer flood. The bottom thin solid curves in Figs. 8-10 show oil recovery projections for continuous water injection, while the top thick solid curves show projections for continuous polymer solution injection. In these figures, flow was linear, one homogeneous layer was present, porosity was 0.3, the reservoir contained 1,000-cp oil at connate water saturation ($S_{wr}=0.3$) and our “base-case” parameters were used:

$$k_{rw} = k_{rwo} [(S_w - S_{wr}) / (1 - S_{or} - S_{wr})]^{nw} \dots\dots\dots (4)$$

$$k_{ro} = k_{roo} [(1 - S_{or} - S_w) / (1 - S_{or} - S_{wr})]^{no} \dots\dots\dots (5)$$

$$k_{rwo} = 0.1, k_{roo} = 1, S_{or} = 0.3, S_{wr} = 0.3, nw = 2, no = 2 \dots\dots\dots (6)$$

Fig. 8 applies to injection of 10-cp (Newtonian) polymer solution (where polymer adsorption exactly balances inaccessible pore volume). Fig. 9 applies to injection of 100-cp polymer, and Fig. 10 applies to injection of 1,000-cp polymer. The near-vertical line segments that connect the continuous-water-injection to the continuous-polymer-injection curves show cases where polymer flooding was initiated after injecting the specified volumes of water (from 0.2 to 10 pore volumes, PV). To explain these curves, consider the case of injecting a 10-cp polymer solution after first injecting 0.5 PV of water into a one-layer reservoir. In Fig. 8, oil recovery follows the bottom, waterflooding curve for 1.15 PV (i.e., 0.5 PV associated with water injection plus 0.65 PV delay associated with polymer propagating through the reservoir). After that point, a 0.337-PV oil bank arrives at the production well, the oil recovery rate increases significantly, and the recovery curve jumps to join the continuous-polymer-injection curve. The curves associated with the other cases follow a similar behavior (Figs. 8-10). The key message from Figs. 8-10 is that polymer flooding can be effective in viscous oil reservoirs even if waterflooding has been underway for some time. Certainly, the EOR target will be diminished as the throughput increases for the pre-polymer waterflood. However, fractional flow analysis indicates that a significant oil bank can develop and be recovered from a polymer flood, even if a significant waterflood precedes the polymer project.

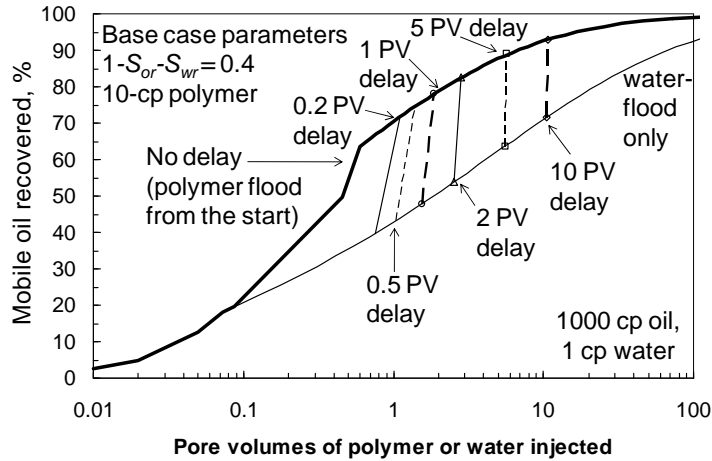


Fig. 8—Injection of 10-cp polymer initiated after waterflooding for specified PV, 1 layer.

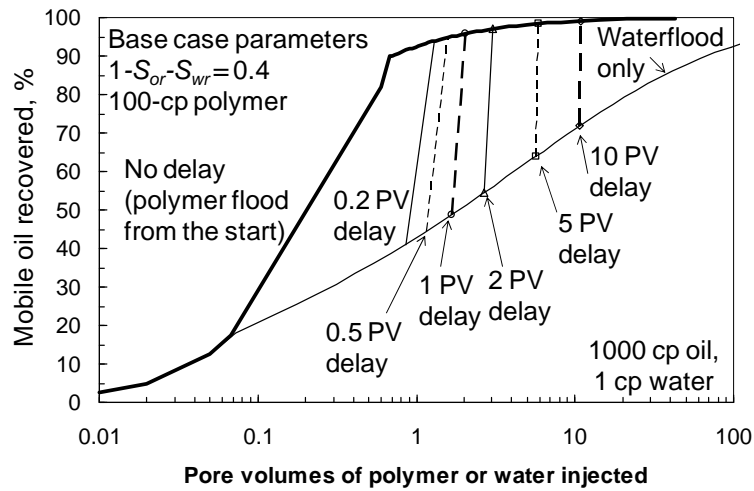


Fig. 9—Injection of 100-cp polymer initiated after waterflooding for specified PV, 1 layer.

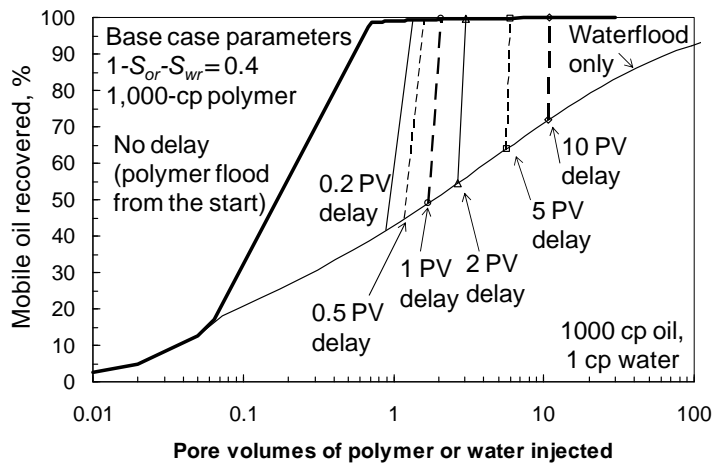


Fig. 10—Injection of 1,000-cp polymer initiated after waterflooding for specified PV, 1 layer.

Two Layers, Free Crossflow. Figs. 11-13 provide similar results for fractional flow calculations where two layers were present. For these cases, the two layers had the same height ($h_1=h_2$), but one layer was 10 times more permeable than the other ($k_1=10k_2$). Free crossflow was allowed between the layers (i.e., vertical equilibrium). A comparison of Figs. 8 and 11 reveals that the waterflood delay values are different. For example, the first delay factor was 0.2 PV in Fig. 8 but 0.1 PV in Fig. 11. This situation occurred because in the two-layer system, a throughput of 0.2 PV in the high-permeability layer corresponds to a throughput of 0.1 PV in the combined two-layer system. So in Fig. 11, total (pre-polymer) water throughputs of 0.1, 0.26, 0.53, 1.06, 2.7, and 5.3 PV correspond to throughputs in the high-permeability layer of 0.2, 0.5, 1, 2, 5, and 10 PV, respectively. The trends in Figs. 11-13 are qualitatively similar to those in Figs. 8-10.

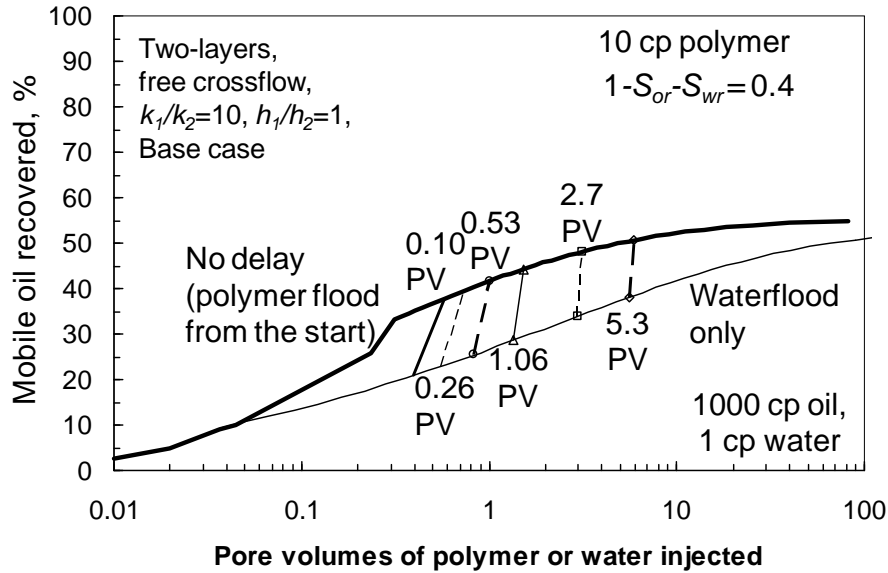


Fig. 11—Injection of 10-cp polymer initiated after waterflooding for specified PV, 2 layers.

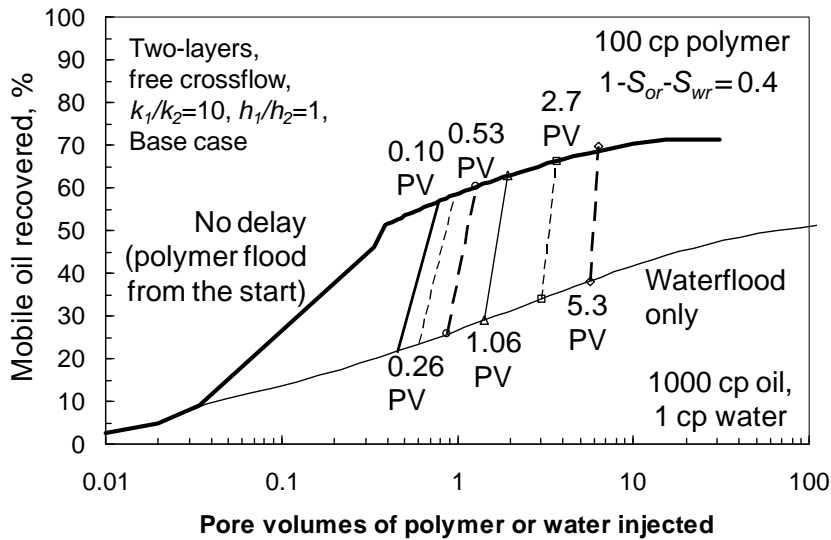


Fig. 12—Injection of 100-cp polymer initiated after waterflooding for specified PV, 2 layers.

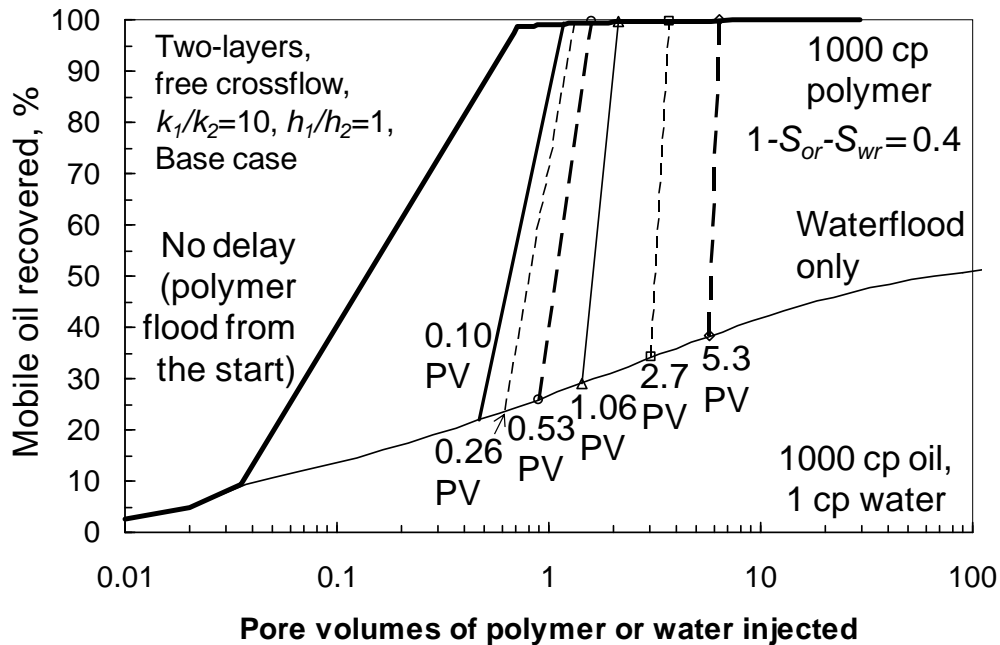


Fig. 13—Injection of 1,000-cp polymer initiated after waterflooding for specified PV, 2 layers.

Simple Benefit Analysis. A simple benefit analysis was performed to evaluate the impact of delaying the start of polymer flooding (i.e., implementing a polymer flood after commencing a waterflood). In this analysis, for a given case in Figs. 8-13, we considered injection of just enough polymer solution for the oil bank to be produced (i.e., the points where the delayed polymer curves joined the continuous-polymer-injection curves). To determine the benefit, the value of the oil in the oil bank (i.e., difference between the continuous-polymer curve and the waterflood-only curve, along a give delayed-polymer line) was divided by the cost of the polymer bank injected. Oil was assumed to be valued at \$20/bbl, and polymer solution viscosities were based on SNF Flopaam 3830S in 2.52% TDS brine at 25°C. A 10-cp polymer solution required 900 ppm polymer at a cost of \$0.72 per barrel; a 100-cp polymer solution required 3,077 ppm polymer at a cost of \$1.87 per barrel; and a 1,000-cp polymer solution required 10,542 ppm polymer at a cost of \$5.78 per barrel.

Fig. 14 shows the results of the simple benefit analysis. For a given polymer solution and layering, the benefit was relatively insensitive to the size of the pre-polymer waterflood (although the benefit decreased modestly for larger waterfloods). Interestingly, with either 1 or 2 layers, this method of analysis favored using 10-cp polymer solutions over more viscous solutions. Other types of comparison can favor using more viscous solutions in some circumstances (Seright 2010).

This work will provide a basis for comparison for our future efforts, which will contrast using the “Bright Water” technology versus normal polymer flooding.

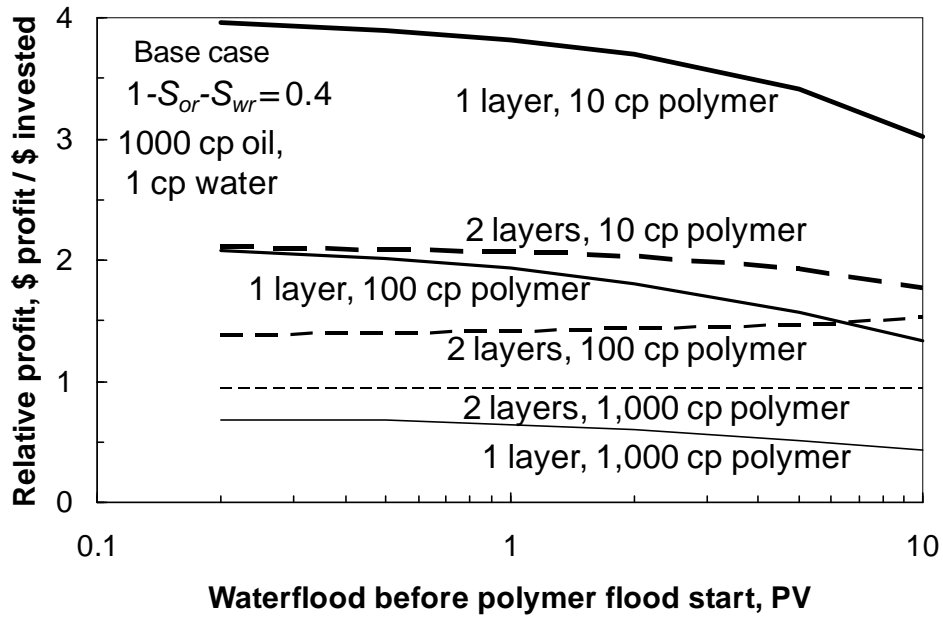


Fig. 14—Simple benefit analysis for delayed polymer flooding.

Conclusion

We extended the fractional flow calculations to examine the effectiveness of polymer flooding when a waterflood (with 1-cp water) was implemented prior to the polymer flood. We showed that polymer flooding can be effective in viscous (1,000-cp) oil reservoirs even if waterflooding has been underway for some time. Certainly, the EOR target will be diminished as the throughput increases for the pre-polymer waterflood. However, fractional flow analysis indicates that a significant oil bank can develop and be recovered from a polymer flood, even if a significant waterflood precedes the polymer project. This point was demonstrated both with a homogeneous 1-layer reservoir and in a 2-layer reservoir with free crossflow.

6. EXAMINATION OF TWO BIOPOLYMERS

EX9719 Xanthan

CP Kelco provided two new biopolymers for consideration in EOR. The first was the xanthan, EX9719. The anticipated benefit of this polymer was that it should provide a greater viscosity than normal xanthans, and therefore be more cost effective. Fig. 15 plots \log (viscosity) (at 7.3 s⁻¹, 25°C) versus \log (polymer concentration). This plot forms a line with a slope of 1.62 (Fig. 15).

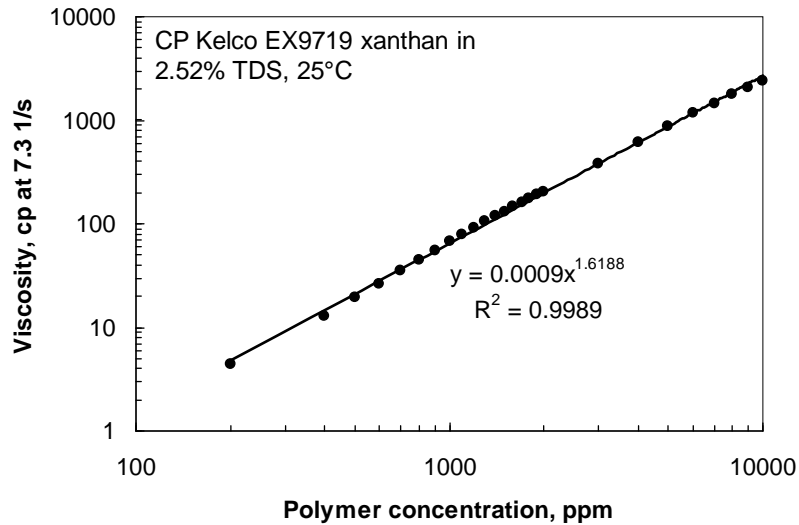


Fig. 15—Viscosity versus polymer concentration for EX9719 xanthan.

Fig. 16 compares viscosity versus concentration for several polymers. In this figure, 3830S and KYPAM 5 are HPAMs, while the other polymers are xanthans. Fig. 16 reveals that EX9719 is a more effective viscosifier (in this brine) than the other polymers, providing 25-100% higher viscosities than other xanthans, depending on the polymer concentration. Fig. 17 plots viscosity versus shear rate for EX9719 at many polymer concentrations.

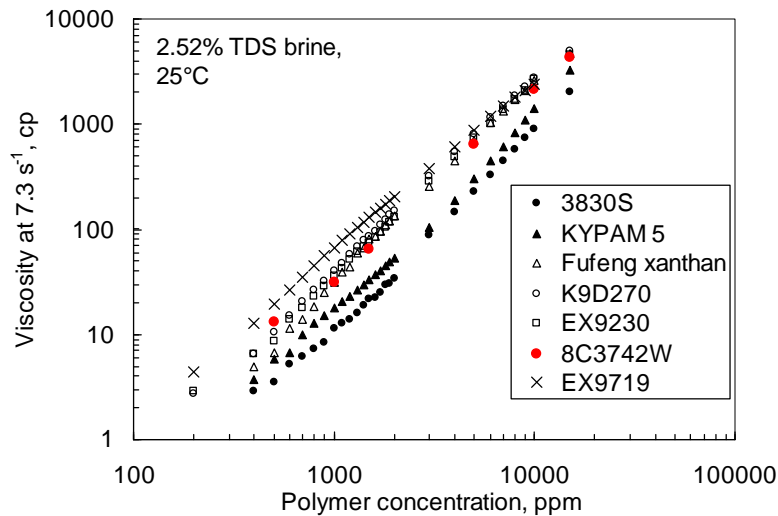


Fig. 16—Viscosity versus polymer concentration for several polymers.

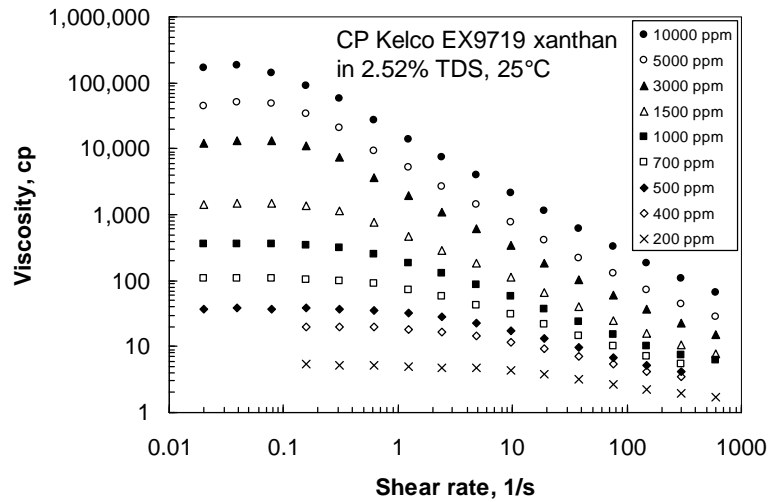


Fig. 17—Viscosity versus shear rate for EX9719 xanthan.

Fig. 18 compares filterability of EX9719 versus other polymers. Our filter test uses a Millipore AP10™ filter pad upstream of a 10 μm polycarbonate (Sterlitech Track Etch™) membrane filter (both 13 mm in diameter) (see Seright *et al.* 2009). The *x*-axis in Fig. 18 plots the volume (actually throughput) of polymer solution that has passed through the filters (i.e., volume per area of filter), while the *y*-axis plots the filter cake resistance (which is directly proportional to the pressure drop across the filter divided by the flow rate). In this figure, better filterability occurs if the filter cake resistance remains small until high throughput values. Fig. 18 shows that EX9719 shows filterability that is similar to that for K9D270, Kelzan, and Kelzan HV xanthans.

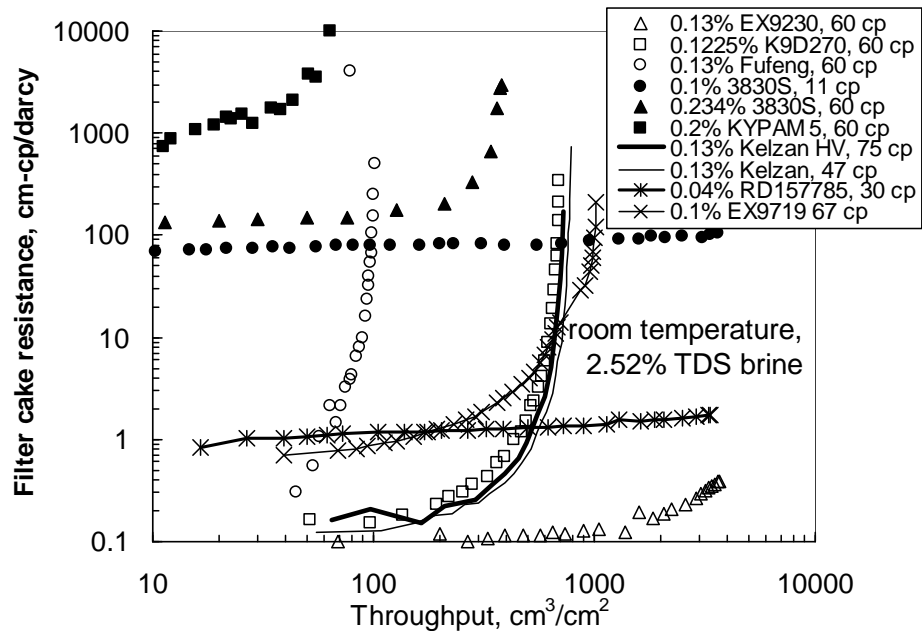


Fig. 18—Filterability for EX9719 xanthan and various polymers.

We also examined whether EX9719 xanthan could form gels with either CrCl_3 or Cr(III)-acetate . In 2.52% TDS brine at room temperature, we examined solutions containing between 700- and 5,000-ppm xanthan, with a polymer/Cr ratio of 20:1 (by weight). Within 1 day of adding the CrCl_3 crosslinker, all xanthan solutions turned from clear to milky (as in Fig. 19). However, only the formulation with 5,000-ppm xanthan formed a solid gel (Fig. 20). Solutions with Cr(III)-acetate turned from clear to milky, but never form any solid gels. (Although we suspect that the milky formulations probably would have plugged a core face if injection was attempted.) It is not yet clear that these xanthan gels have any advantages over other (i.e., HPAM) gels.

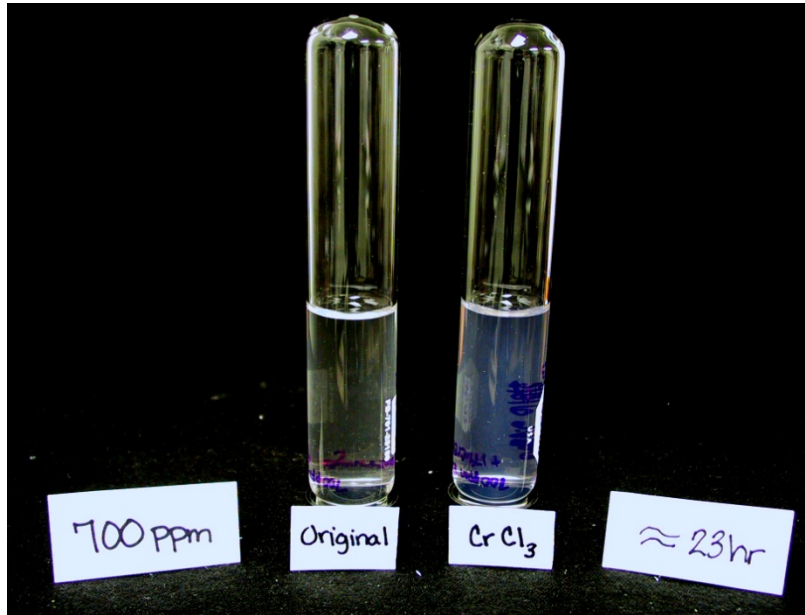


Fig. 19—700-ppm EX9719 xanthan with (versus without) 35-ppm Cr (as CrCl_3).

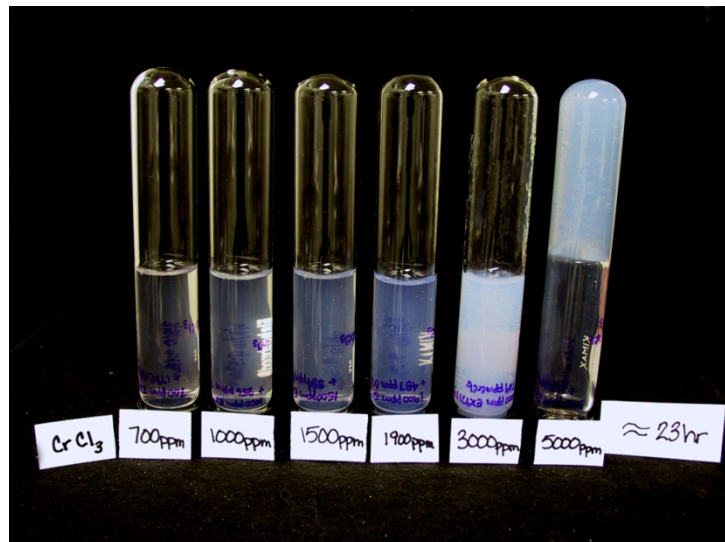


Fig. 20—EX9719 xanthan with Cr (as CrCl_3). (ppm values in this figure refer to polymer concentrations. Cr concentrations are 1/20 X polymer concentration).

Gellan Gum

CP Kelco also provided a gellan gum, KELCOGEL HT, lot 6L8092A. This gel is probably not a serious candidate for polymer flooding since it only dissolves in distilled water. Fig. 21 shows viscosity versus shear rate for this polymer in distilled water. In brines, the polymer forms a gel. These solutions showed very high viscosities, even with only 400-ppm polymer. However, the utility of these solutions as viscosifiers is unclear since distilled water would never be used in field applications. We also added CrCl_3 (20:1 polymer-to-Cr ratio, as with the xanthan cases) to these solutions to test their ability to gel. As shown in Fig. 22, solutions with 700- to 5,000-ppm gellan all formed solid gels within 1 day when mixed with CrCl_3 at room temperature.

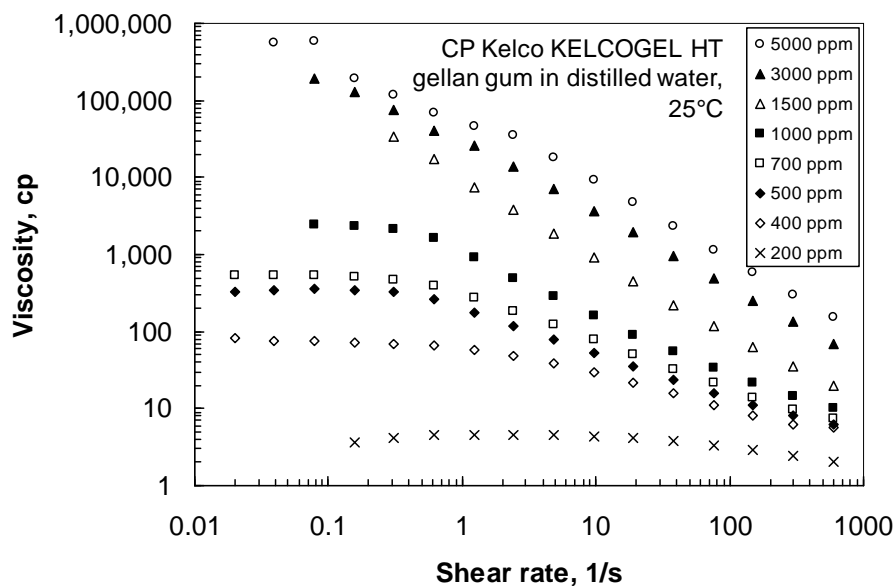


Fig. 21—Viscosity versus shear rate for KELCOGEL HT gellan gum.



Fig. 22—Gellan in distilled water with Cr (as CrCl_3). (ppm values in this figure refer to polymer concentrations. Cr concentrations are 1/20 X polymer concentration).

Conclusions

We examined two new biopolymers for possible use in EOR. The first was CP Kelco's EX9719 xanthan. EX9719 is a very effective viscosifier, providing 25-100% higher viscosities than other xanthans, depending on the polymer concentration. EX9719 also shows good filterability. The polymer can be crosslinked with CrCl_3 , but it is not clear that these Cr-xanthan gels have any advantages over existing Cr(III)-acetate-HPAM gels. The second polymer was CP Kelco's gellan gum, KELCOGEL HT. This polymer is probably not a serious candidate for polymer flooding since it only dissolves in distilled water. Solutions with 700- to 5,000-ppm gellan all formed solid gels within 1 day when mixed with CrCl_3 at room temperature.

7. EXAMINATION OF C1205 HYDROPHOBIC ASSOCIATIVE POLYMER

We received a new hydrophobic associative polymer from SNF: Superpusher DP/C1205, Lot GC 2882/6 (hereafter called C1205). We examined this polymer in hopes that it may provide improved performance and/or cost-effectiveness over conventional polymers. For hydrophobic associated polymers, incorporation of a small fraction of hydrophobic monomer into an HPAM polymer is intended to promote intermolecular associations and thereby enhance viscosities and resistance factors. C1205 is an anionic-polyacrylamide-based tetra-polymer that has associative properties as described in patent WO2005100423. Typically, the hydrophobic monomer content ranges from 0.025 to 0.25 mol%. Molecular weights range from 12-17 million for C1205. Total anionic content is between 15 and 25 mol%. Less than 8 mol% sulfonic monomer is present in C1205. During our studies, the brine contained 2.52% total dissolved solids (TDS), specifically with 2.3% NaCl and 0.22% NaHCO₃. The studies were performed at 25°C.

Comparisons will be made with the performance of a conventional HPAM, SNF Flopaam 3830S (Lot X 1899). This polymer has a molecular weight of 18-20 million and a degree of hydrolysis of 40%. Fig. 23 compares the appearance of 1,500-ppm 3830S and C1205 solutions. The C1205 polymer took longer to dissolve and resulted in more turbid solutions (see Fig. 23).



Fig. 23—Solutions of 3830S versus C1205.

Viscosity

Viscosity (at 7.3 s⁻¹, 25°C) versus polymer concentration for C1205 is compared with several other polymers in Fig. 24. The viscosity behavior of C1205 (solid squares) was quite similar to that for SNF Flopaam 3830S (an HPAM with Mw of 18-20 million and 40% degree of hydrolysis). Viscosity versus shear rate and polymer concentration is plotted in Fig. 25 using an

Anton Paar Physica MCR 301 viscometer and in Fig. 26 using a Brookfield viscometer with UL adapter. For polymer concentrations of 500 ppm, 900 ppm, 1500 ppm and 2,500 ppm in Fig. 25, viscosity versus shear rate was quite similar for Flopaam 3830S and C1205.

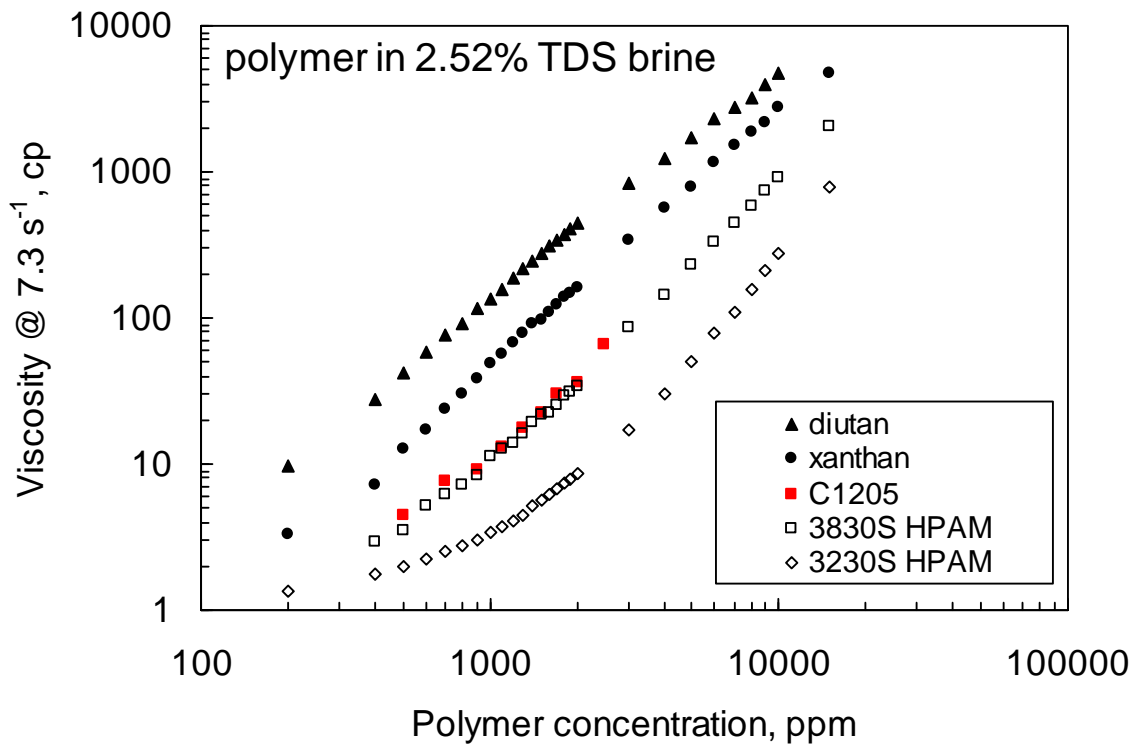


Fig. 24—Viscosity versus polymer concentration.

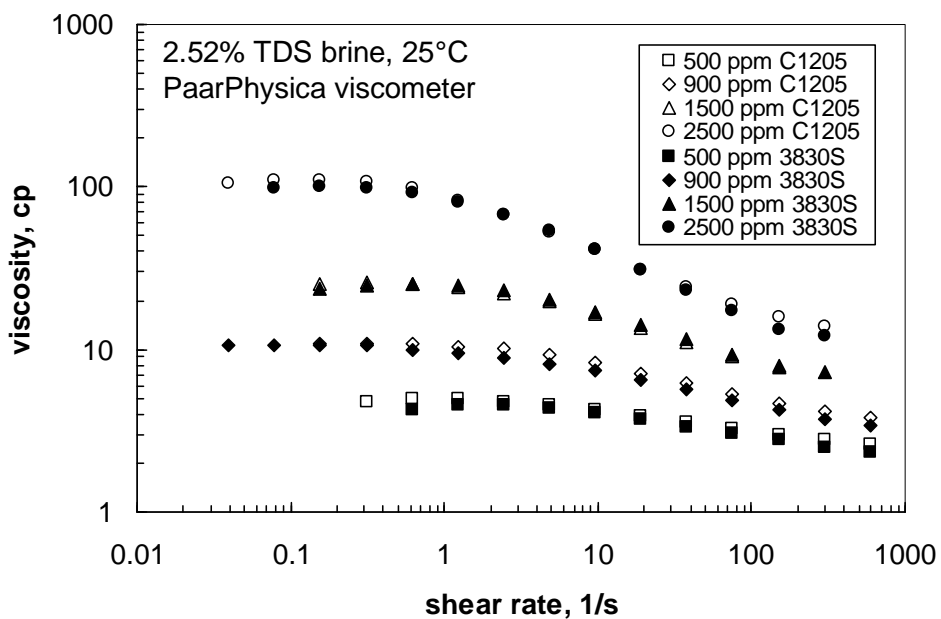


Fig. 25—Viscosity versus shear rate, PaarPhysica.

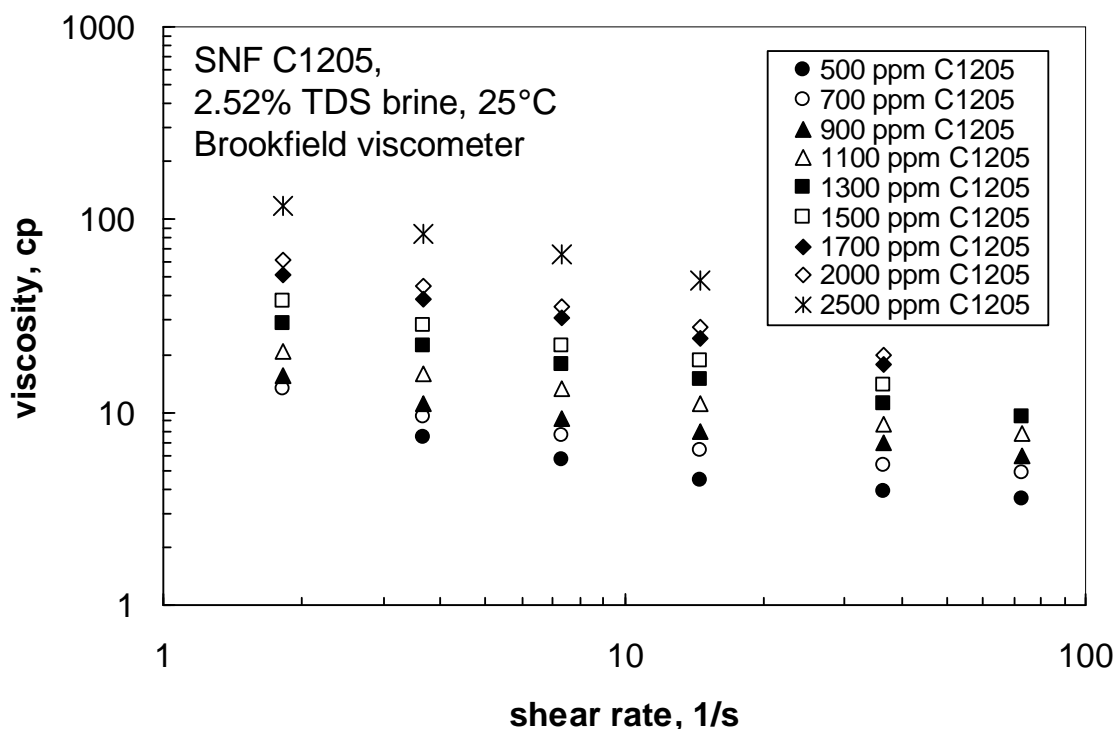


Fig. 26—Viscosity versus shear rate, Brookfield.

Filter Test Results

Our previous work (Seright *et al.* 2009a) identified a filter test that allows comparison of the face-plugging characteristics of polymers. In this test, a Millipore AP10™ filter pad is placed in a filter holder upstream of a 10 μm polycarbonate (Sterlitech Track Etch™) membrane filter (both 13 mm in diameter). Using a fixed pressure drop across the filter holder, we record filter cake resistance (calculated using the Darcy equation, with units of cm-cp/darcy) versus throughput (volume of fluid injection per filter area, in cm³/cm².) Fig. 27 compares filtration results for Flopaam 3830S HPAM (solid symbols) and C1205 (open symbols). Notice that both 3830S and C1205 show excellent filterability at lower concentrations (1,000 ppm or lower), but plugged within 70 cm³/cm² throughput at higher concentrations (1,500 ppm). Thus, the higher turbidity associated with C1205 (see Fig. 23) did not impair its filterability, relative to 3830S.

The results in Fig. 27 raise an interesting question: If 1,500-ppm solutions plug within 70 cm³/cm² throughput and if microgels or particulate debris caused the plugging, one might expect a 1,000-ppm solution to plug within 105 cm³/cm² throughput (i.e., 70x1,500/1,000). Instead, no plugging was evident for 1,000-ppm of either C1205 or 3830S after 3,000 cm³/cm² throughput. One might argue that increased hydrophobic associations caused the plugging for the 1,500-ppm C1205 solution. However, that explanation loses credibility upon viewing the results for 1,500-ppm 3830S. Whatever plugging entity that develops in 1,500-ppm C1205 also appears to develop in 1,500-ppm 3830S.

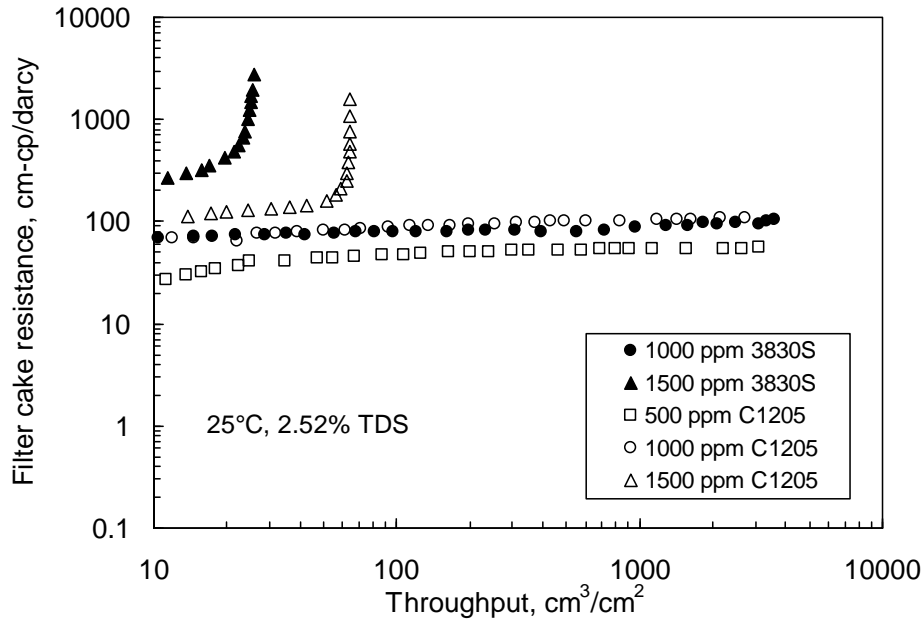


Fig. 27—Filter Test Results: 3830S versus C1205.

Cores

Two cores were used in our first work. The cores were saturated with the 2.52% TDS brine (2.3% NaCl, 0.22% NaHCO₃) before use. The first core was porous polyethylene, 14.05 cm long with a porosity of 0.435, a pore volume of 71.2 cm³, core cross-section of 11.64 cm², and an average permeability of 7,914 md. This core had two internal pressure taps, one located 2.46 cm from the inlet face and one located 2.36 cm from the outlet face. Thus, the middle section of this core was 9.23 cm long. Permeabilities of the three core sections were 4,338, 12,313, and 5,147 md, respectively.

The second core was Berea sandstone, 12.96 cm long with a porosity of 0.229, a pore volume of 34.3 cm³, core cross-section of 11.58 cm², and an average permeability of 347 md. This core had two internal pressure taps, one located 1.56 cm from the inlet face and one located 2.32 cm from the outlet face. Thus, the middle section of this core was 9.08 cm long. Permeabilities of the three core sections were 373, 363, and 284 md, respectively.

Resistance Factors and Face Plugging

Resistance factor is defined as brine mobility (before polymer injection) divided by polymer solution mobility. (Mobility is permeability divided by viscosity.) In both cores, we first injected 10.4 pore volumes (PV) of 500-ppm C1205 (in 2.52% TDS brine) at a high rate. After measuring stabilized resistance factors in the three core sections, the injection rate was reduced (typically cut in half), and stabilized resistance factors were measured again. This process was repeated in stages to low rates, until the Honeywell quartz transducers could no longer accurately measure pressures. Then, a more concentrated polymer solution was injected. Tables 2 and 3 list the sequence of polymer concentrations injected into each core. The second data column in each table lists the number of pore volumes that were injected before the first resistance factor was measured at a given concentration. The third data column lists the total number of pore volumes injected at the specified concentration. The fourth data column lists the cumulative pore volumes

injected, and the final column lists the cumulative polymer solution throughput (total volume of polymer solution injected divided by the cross-sectional area of the core) to a given point.

Table 2—Injection parameters for C1205 in a polyethylene core.

Polymer, ppm	Flush PV	Final PV	Cumulative PV	Total throughput, cm^3/cm^2
500	10.4	18.4	18.4	112.5
700	6.9	12.3	30.7	187.9
900	6.4	10.5	41.2	252.3
1,100	6.9	11.0	52.2	319.7
1,300	6.6	10.3	62.5	382.2
1,500	6.8	10.6	73.1	447.4
2,000	9.8	13.1	84.2	527.4
2,500	7.3	10.6	96.8	580.1

Table 3—Injection parameters for C1205 in a Berea core.

Polymer, ppm	Flush PV	Final PV	Cumulative PV	Total throughput, cm^3/cm^2
500	10.4	14.4	14.4	42.7
900	11.0	13.8	28.2	83.7
1,500	9.2	12.9	31.1	121.0
1,700	9.3	11.2	32.3	154.2
2,000	10.4	12.3	34.6	190.7
2,500	6.1	20.3	50.9	247.7

Fig. 28 plots stabilized resistance factor as a function of flux in each of the three core sections for injection of 500-ppm C1205 in the Berea sandstone core. At a given flux, the resistance factors were reasonably consistent in the three core sections. The resistance factors were generally higher in the third core section, which argues against plugging of the inlet face. Appendix A provides similar plots for different C1205 concentrations injected into the Berea and polyethylene cores. Close examination of these figures also argues against any definitive face plugging. In Fig. 28, consistent with normal HPAM behavior (Seright *et al.* 2010), a strong shear thickening was seen at moderate-to-high flux values and Newtonian or a slight shear-thinning behavior was seen at low flux values.

Resistance Factor versus Flux and Concentration

Resistance factors (in the second and longest core section) versus flux and C1205 concentration are plotted in Fig. 29 (for 12,313-md polyethylene) and Fig. 30 (for 363-md Berea sandstone). For comparison, Fig. 30 provides an analogous plot for Flopaam 3830S in 5,120-md polyethylene. Interestingly, for C1205 in both polyethylene and Berea, shear thickening at high flux values became less pronounced as polymer concentration increased (Figs. 29 and 30), while shear thinning at low flux values became more pronounced. In contrast, for Flopaam 3830S, shear thickening at high flux remained important at all polymer concentrations (Fig. 31).

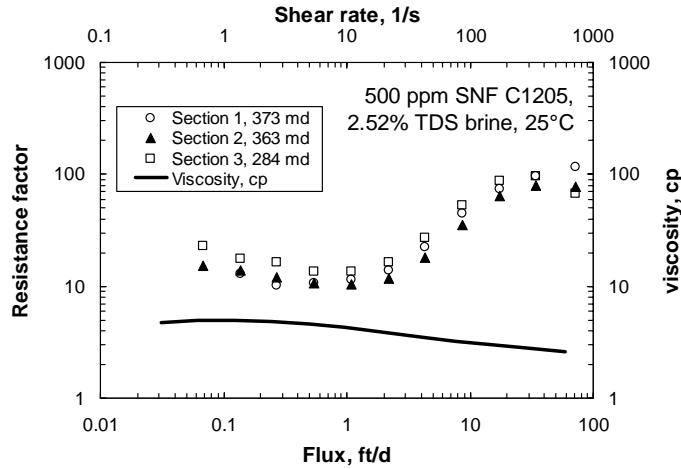


Fig. 28—500-ppm C1205 viscosity and resistance factor in Berea.

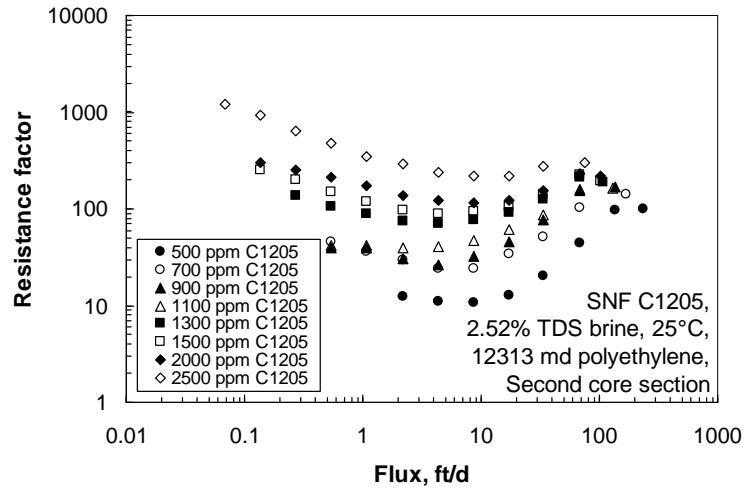


Fig. 29—C1205 resistance factor versus flux in 12,313-md polyethylene.

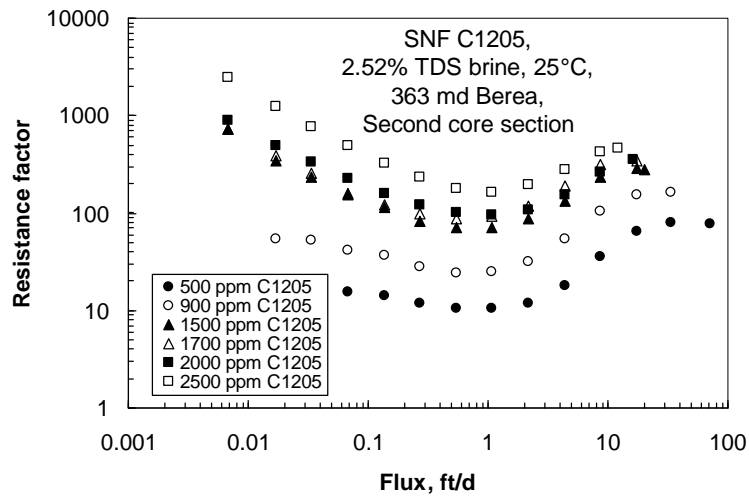


Fig. 30—C1205 resistance factor versus flux in 363-md Berea.

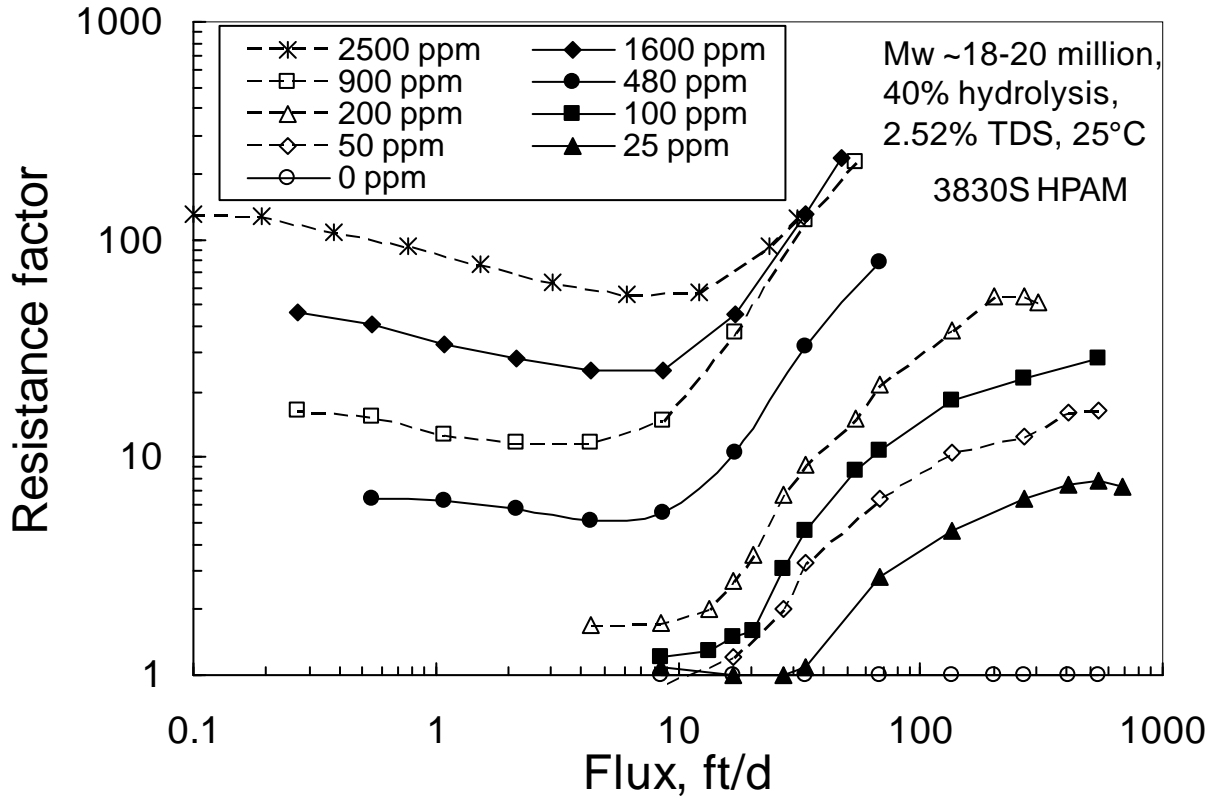


Fig. 31—3830S HPAM resistance factor versus flux in 5,120-md polyethylene.

Fig. 28 also plots viscosity versus shear rate for 500-ppm C1205 (solid curve). Note that at all flux values, resistance factors were considerably greater than expectations from viscosity measurements. This behavior was noted in both Berea and porous polyethylene for all (fresh) C1205 concentrations tested. Interesting, for conventional HPAM and xanthan polymers, resistance factors at low fluxes were reasonably consistent with expectations from viscosity measurements unless a pore-plugging effect occurred (Seright *et al.* 2010)—e.g., if the permeability was too low to accommodate the size of the highest molecular weight species within the polymer.

Fig. 32 confirms that for the other C1205 concentrations in 363-md Berea and 12,313-md polyethylene, the lowest resistance factors were noticeably greater than (roughly twice) the highest measured viscosity (i.e., Brookfield viscosity at 1.8 s^{-1}). If this result was caused by pore plugging or by large polymer adsorption or retention, we might have expected higher resistance factors in the 363-md Berea than in 12,313-md polyethylene. Fig. 33 also supports the idea that the higher than expected resistance factors may not be due to pore plugging. In Fig. 33, resistance factors for selected concentrations (500, 900, 1,500, and 2,500 ppm) are plotted against the capillary bundle parameter, $u(1-\phi)/(\phi k)^{0.5}$. For all four C1205 concentrations, the behavior in 363-md Berea correlated well with that seen in 12,313-md polyethylene. For a given x -axis value, resistance factors should have been greater in 363-md Berea than in 12,313-md polyethylene if pore plugging was important.

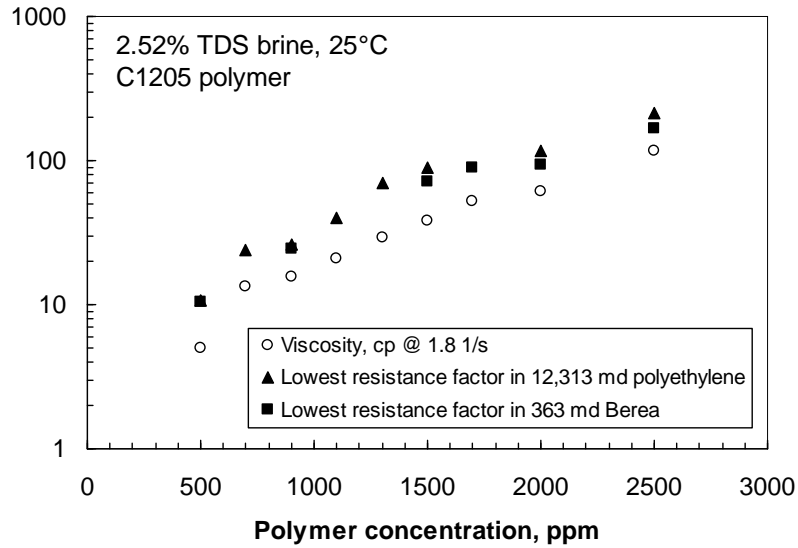


Fig. 32—C1205 resistance factors versus viscosities.

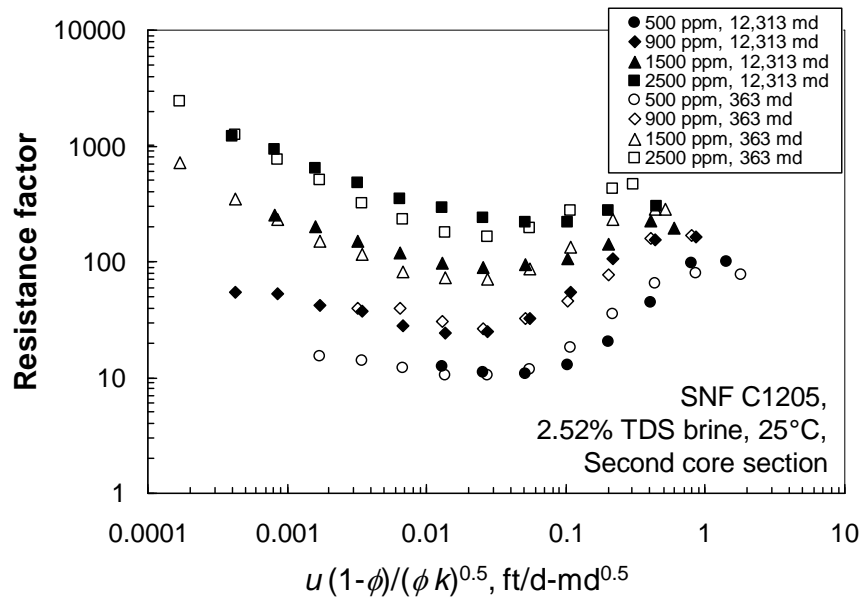


Fig. 33—C1205 resistance factor versus capillary bundle parameter.

Fig. 34 compares resistance factors in porous polyethylene for C1205 versus 3830S HPAM. For all three concentration levels examined (~500 ppm, 900 ppm, and ~1,500 ppm), resistance factors (at a given flux) were substantially greater for C1205 than for 3830S. Specifically, 500-ppm C1205 (solid circles) acts similar to 900-ppm 3830S (open triangles), and 900-ppm C1205 (solid triangles) acts similar to 1,600-ppm 3830S (open squares). Considering that these two polymers show the same viscosity behavior (Figs. 24 and 25), an important unanswered question is, Why does C1205 provide substantially higher resistance factors in porous media? As mentioned earlier in this section, the reason does not appear to be that C1205 causes a much greater pore-plugging effect.

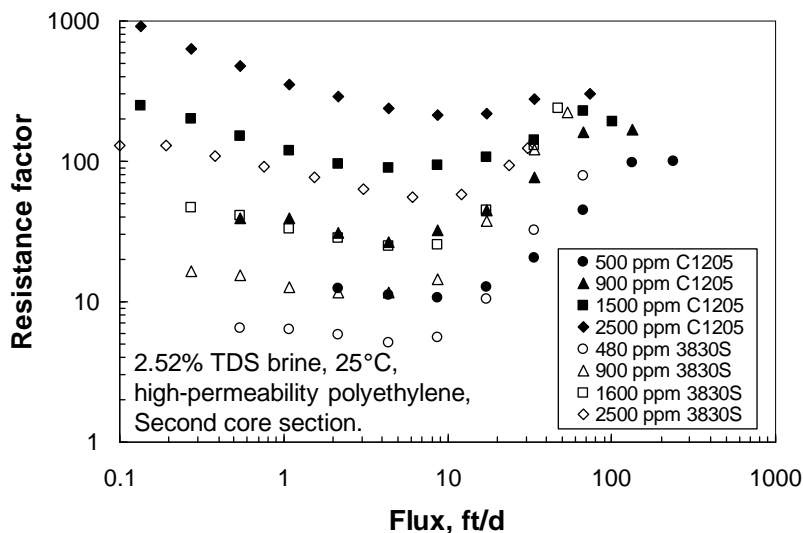


Fig. 34—Resistance factors in polyethylene: C1205 versus 3830S.

Residual Resistance Factors

At the end of C1205 polymer injection, many pore volumes of brine were injected to determine residual resistance factors in the Berea and polyethylene cores. After injecting 109 *PV* of brine into the polyethylene core, residual resistance factors were 1.9, 2.1, and 1.3 in the first, second, and third sections, respectively. This result is consistent with a suggestion of little to no significant pore plugging in the 12,313-md polyethylene core. However, after injecting 170 *PV* of brine into the Berea core, residual resistance factors were 13.0, 19.3, and 15.3 in the first, second, and third sections, respectively. This result suggests that some pore plugging or higher polymer retention may have occurred in the 363-md Berea core. In both cores, residual resistance factors were not sensitive to flow rate.

Repeat Set in a Longer Polyethylene Core

A repeat set of experiments was performed in a longer porous polyethylene core. In this case, the total core length was 78.09 cm, the porosity was 0.377, and the pore volume was 343 cm³. The core had two internal pressure drops that divided the core into three sections of equal length (i.e., 26.03 cm each). The section permeabilities were 7,295, 10,144, and 8,717 md, respectively. After saturating with brine, we injected 1 *PV* of 500-ppm C1205 at 108 ft/d. Then over the next 3.4 *PV*, we determined resistance factor for progressively lower flux values. These results (specifically for the second, 10,144-md core section) are plotted as the open circles in Fig. 35. Next, over the course of an additional 3.4 *PV*, the rates were increased, and the results are plotted as the solid triangles in Fig. 35. The open circles and solid triangles in Fig. 35 are sufficiently similar that the resistance factor behavior for 500-ppm C1205 was well-established between 3.4 and 6.8 *PV*.

Additional floods were performed in this same core using higher C1205 concentrations, as indicated in Fig. 35. At the end of injecting the most concentrated polymer solution (2,500-ppm C1205), a total of 17.6 *PV* of polymer solution had been injected (i.e., 6.8 *PV* at 500 ppm, 3.8 *PV* at 900 ppm, 3.7 *PV* at 1,500 ppm, and 3.3 *PV* at 2,500 ppm). Subsequently, we injected 24.7 *PV* of brine to determine residual resistance factors versus flux in the three core sections, as

indicated in Fig. 36. In this figure, it is evident that residual resistance factors strongly depend on flux, especially showing shear thickening at higher flux values. It is possible that 24.7 *PV* was not enough brine to flush all the 2,500-ppm C1205 from the core.

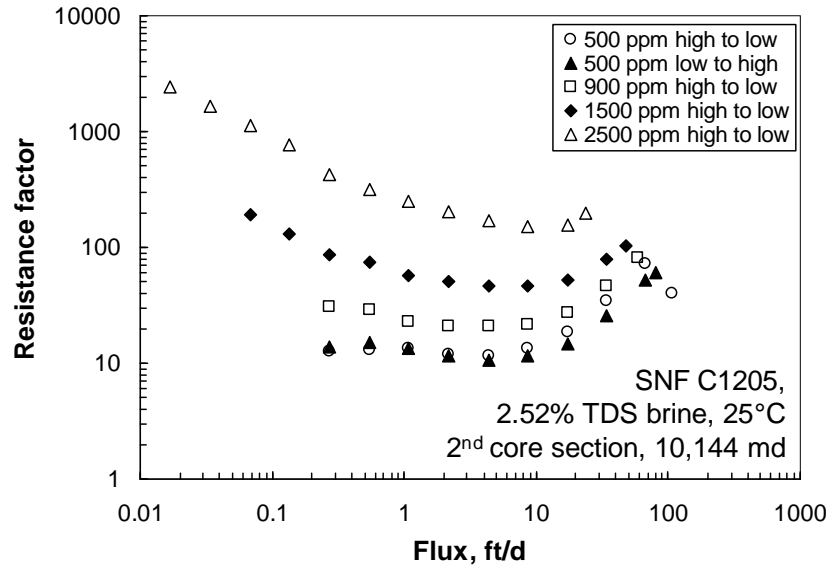


Fig. 35—C1205 resistance factors versus concentration in 10,144-md polyethylene.

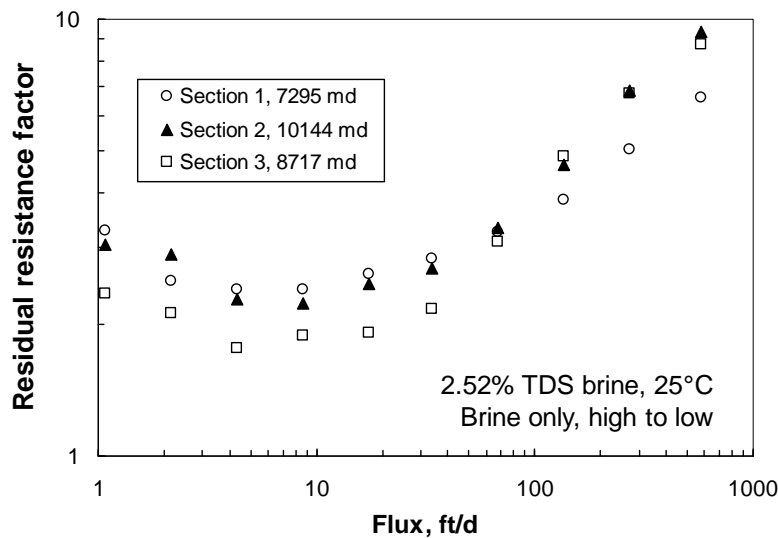


Fig. 36—C1205 residual resistance factors in 10,144-md polyethylene.

Finally, we injected 2 *PV* of 500-ppm C1205 at 81 ft/d, followed by 0.7 *PV* at various lower fluxes, to record the resistance factors associated with the solid triangles in Fig. 37. A comparison of these values with those from the first injection of 500-ppm C1205 (i.e., the open circles in Figs. 35 and 37) indicate that the 500-ppm C1205 showed the same behavior for the entire course of this experiment. So whatever phenomenon that caused the resistance factors to

be 2-3 times the value expected from viscosity measurements (see Figs. 28 and 37), it did not seem to change over the course of injecting many pore volumes of polymer solution. The results to this point imply that large, slow-moving microgels or very high Mw polymer species were not the cause of the higher than expected resistance factors. (However, as will be seen shortly, additional observations will complicate the issue.)

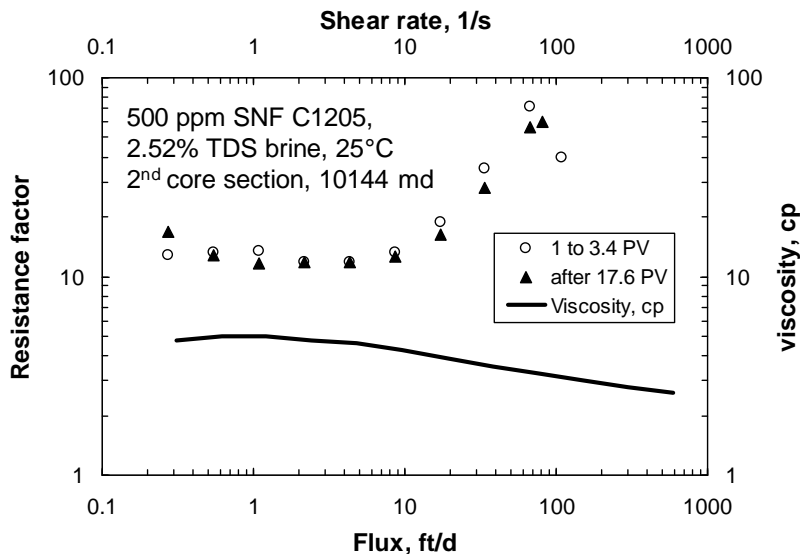


Fig. 37—500-ppm C1205 resistance factors at beginning versus end of the experiment.

Mechanical Degradation

In previous work (Seright *et al.* 2010) when xanthan or HPAM resistance factors were higher than expected at moderate to low flux values, the effect was shown to be due to a high Mw polymer species. For both xanthan and HPAM, this species was removed by flow through a few feet of porous rock. For HPAM, the species was readily destroyed by mechanical degradation. Either way, the species was not expected to propagate deep into a reservoir to provide low-flux resistance factors that were substantially higher than expectations from viscosity measurements. During a study of a hydrophobic associative polymer, Dupuis *et al.* (2010) concluded that it contained a high Mw species that propagated significantly slower than other components of the polymer sample. Because our studies to date involved injection of large volumes (throughputs) of polymer solution, we wondered whether the high resistance factors at moderate to low flux values might be due to a slow moving high-Mw polymer species. It is also possible that enhanced polymer adsorption/retention might be responsible for the effects that we are seeing. Specifically, we wondered whether mechanical degradation would mitigate the high resistance factors that we observed.

2,500 psi/ft. We examined the effects of mechanical degradation by first forcing 6.4 liters of a 500-ppm C1205 solution through a 13-cm long 347-md Berea core using a flux of 292 ft/d (resulting in a pressure gradient of 2,500 psi/ft). (We recognize that this may be a fairly extreme stress to put on the polymer.) The effluent from this experiment was then re-injected into a new 78.2-cm long polyethylene core that had four equally spaced internal pressure taps. The porosity of this core was 44% and the pore volume was 390.6 cm³. The permeabilities of the five 15.64-cm long core sections were 8,316, 11,554, 11,105, 11,222, and 10,370 md, respectively. Thus, the average permeability was 10,365 md.

Fig. 38 shows resistance factor versus flux for this mechanically degraded polymer. The solid curve in this figure shows viscosity versus shear rate. This figure reveals that the low-flux resistance factors for the mechanically degraded 500-ppm C1205 are consistent with expectations from low-shear-rate viscosity measurements.

We repeated this experiment using 900-ppm, 1,500-ppm, and 2,500-ppm C1205 solutions, where the pressure gradient was 2,500 psi/ft when forcing the solutions through the 347-md Berea core. The effluent from this core was then injected into the polyethylene core using a range of flow rates. Figs. 39-41 show the results. For these cases, the low-flux resistance factors were just slightly greater than the expectations from low-shear-rate viscosities. Thus for C1205 solutions with polymer concentrations between 500 and 2,500 ppm, mechanical degradation destroyed/removed the species that caused the unexpectedly high low-flux resistance factors seen in earlier figures. Incidentally, forcing the C1205 polymer solutions through the Berea core at 2,500 psi/ft resulted in low-shear viscosities (at 7.3 s^{-1}) dropping from 19% to 35%.

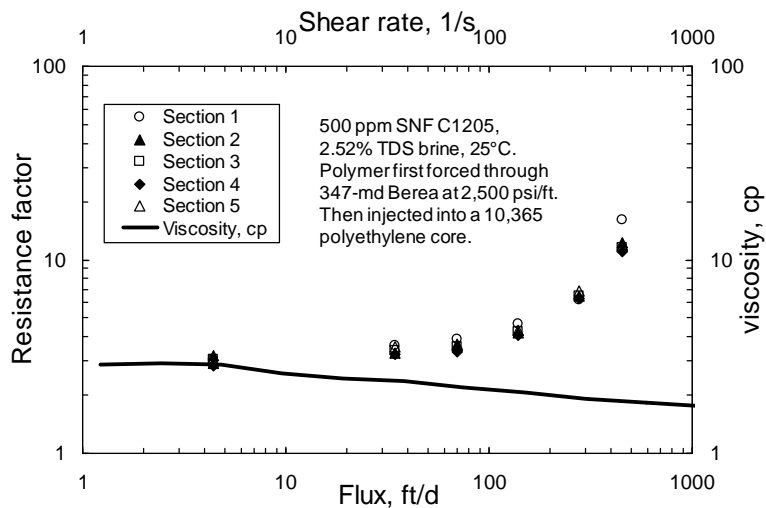


Fig. 38—Resistance factors for mechanically degraded 500-ppm C1205 (after 2,500 psi/ft).

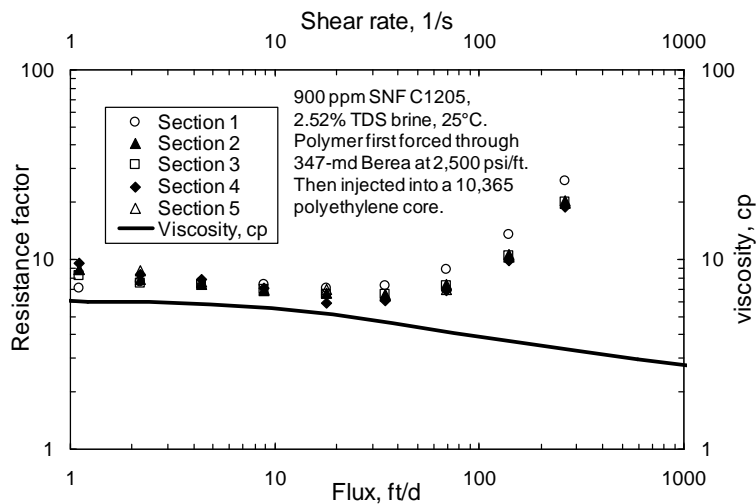


Fig. 39—Resistance factors for mechanically degraded 900-ppm C1205 (after 2,500 psi/ft).

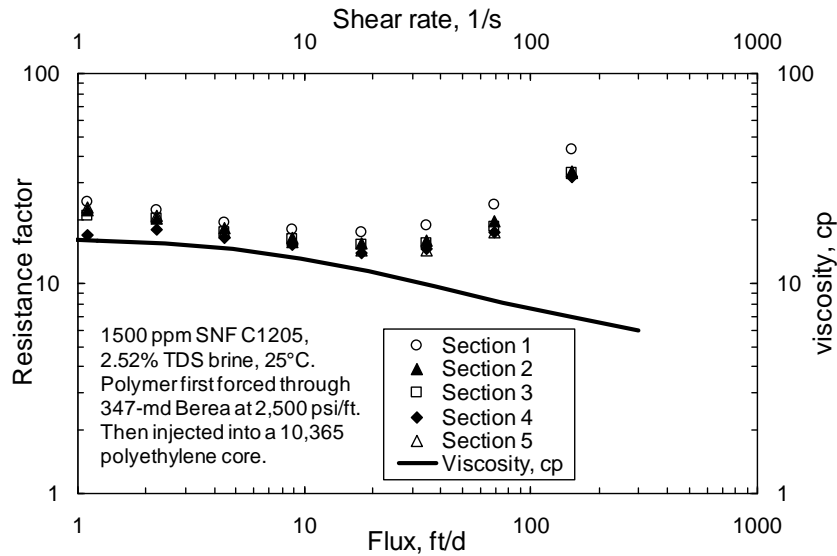


Fig. 40—Resistance factors for mechanically degraded 1,500-ppm C1205 (after 2,500 psi/ft).

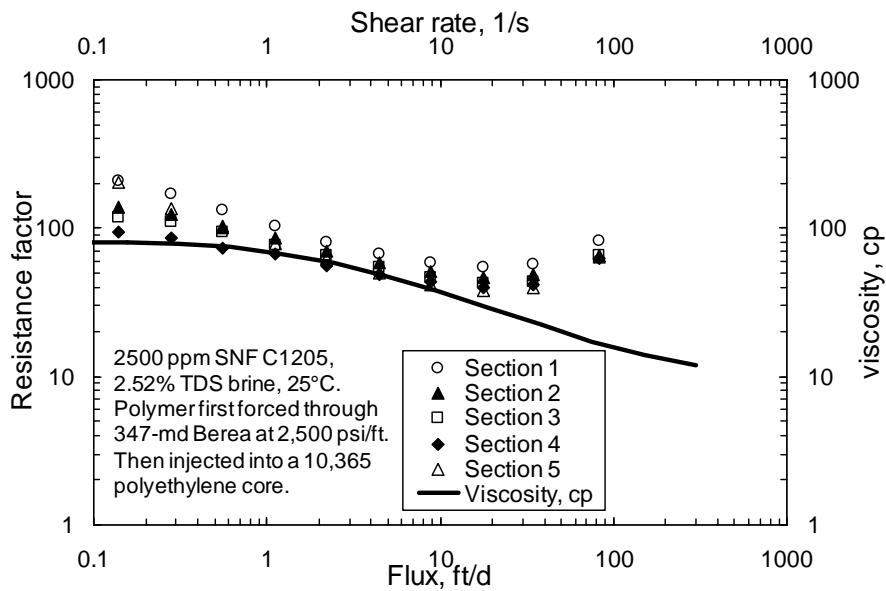


Fig. 41—Resistance factors for mechanically degraded 2,500-ppm C1205 (after 2,500 psi/ft).

235 psi/ft. Since the previously applied level of mechanical degradation (2,500 psi/ft pressure gradient) was fairly extreme, additional work with a lower level of mechanical degradation was performed. For these cases, the pressure gradient was 235 psi/ft when forcing the solutions through the 347-md Berea core. The effluent from this core was then injected into the polyethylene core using a range of flow rates. Forcing the C1205 polymer solutions through the Berea core at 235 psi/ft resulted in viscosities (at 7.3 s^{-1}) dropping 5-6%. Thus, this degradation process only resulted in mild viscosity losses. Figs. 42-45 show the resistance factor results. For these cases, the low-flux resistance factors were clearly greater (by roughly a factor of 2) than the low-shear rate viscosities. Thus, a moderate level of shear degradation did not eliminate the unexpectedly high resistance factors associated with C1205.

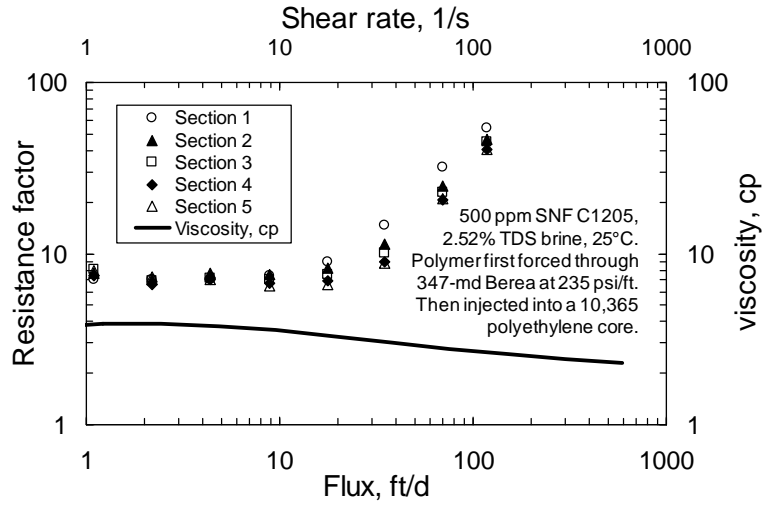


Fig. 42—Resistance factors for mechanically degraded 500-ppm C1205 (after 235 psi/ft).

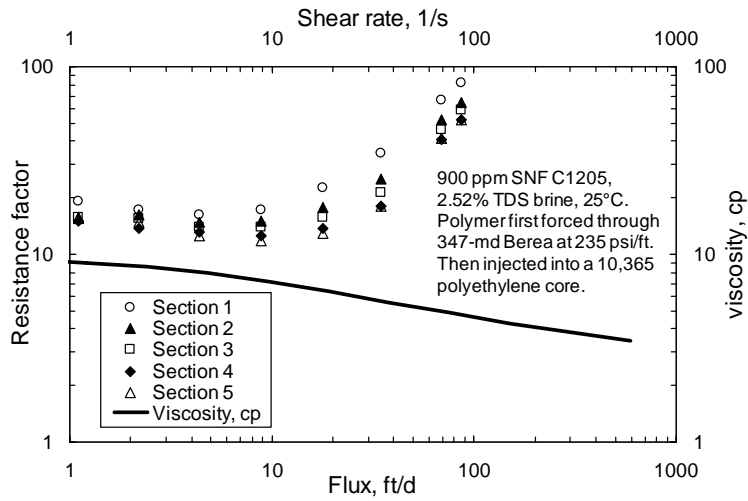


Fig. 43—Resistance factors for mechanically degraded 900-ppm C1205 (after 235 psi/ft).

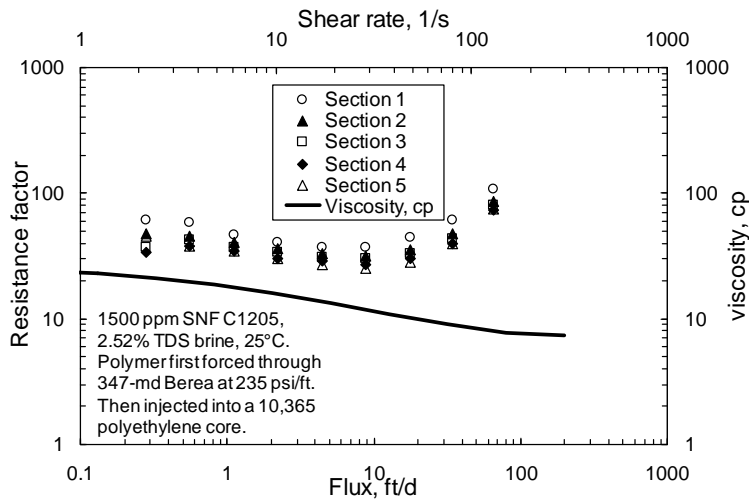


Fig. 44—Resistance factors for mechanically degraded 1,500-ppm C1205 (after 235 psi/ft).

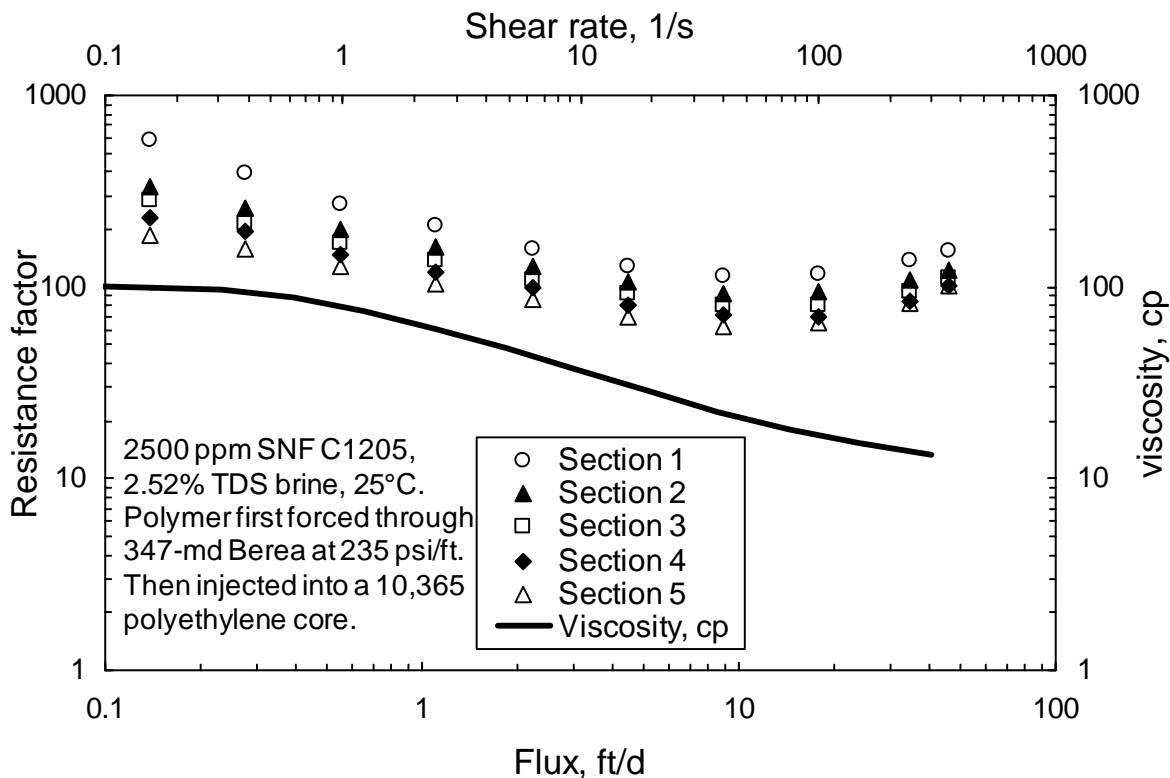


Fig. 45—Resistance factors for mechanically degraded 2,500-ppm C1205 (after 235 psi/ft).

Comparison with 3830S. Mechanical degradation experiments analogous to those shown in Figs. 37-44 for C1205 were performed using Flopaam 3830S, which is a conventional HPAM that has a molecular weight similar to that of C1205. The results are shown in Figs. 46-53. For the 3830S cases (fresh, 235 psi/ft, and 2,500 psi/ft), the low-flux resistance factors (in the middle core section) were usually the same or just slightly greater than expectations from the low-shear-rate viscosities. To quantify this point, Fig. 54 plots the ratio of (resistance factor at 1 ft/d flux in the middle core section) to (shear rate at 7.3 s^{-1}) for the two polymers, with different polymer concentrations and different levels of mechanical degradation. For all cases with 3830S HPAM concentrations up to 1,500 ppm, the low-flux resistance factor was only 0 to 33% greater than the low-shear-rate viscosity. For all cases (fresh, 235 psi/ft, and 2,500 psi/ft) with 2,500-ppm 3830S, the resistance factor at 1 ft/d was about twice the viscosity at 7.3 s^{-1} . However, a more detailed examination of the resistance-factor-versus-flux curves and the viscosity-versus-shear-rate curves (Figs. 49, 53, and 55) reveals that the low-flux resistance factors were actually just slightly above the low-shear-rate viscosities. Similarly, for cases with C1205 concentrations up to 1,500 ppm that had been exposed 2,500 psi/ft, the low-flux resistance factor was only 0 to 32% greater than the low-shear-rate viscosity. For C1205 solutions that were exposed to 235 psi/ft, the low-flux resistance factors were 1.6-3.3 times greater than the low-shear-rate viscosity. For fresh, undegraded C1205 solutions, the low-flux resistance factors were 2.5-5.6 times greater than the low-shear-rate viscosity.

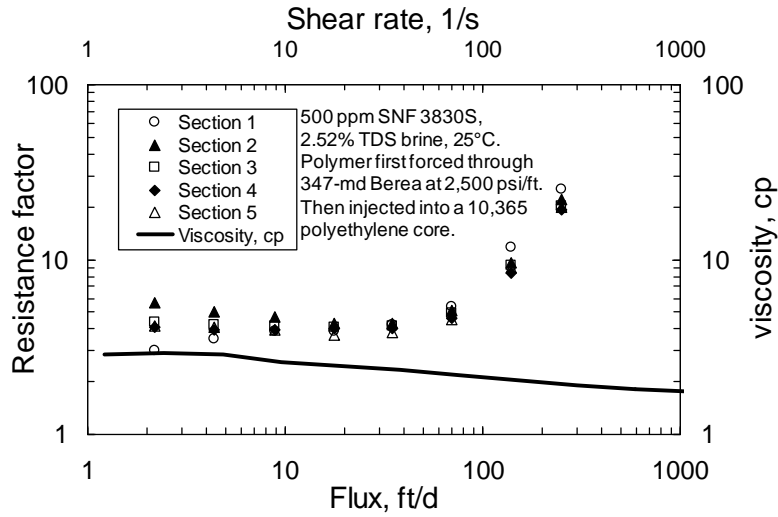


Fig. 46—Resistance factors for mechanically degraded 500-ppm 3830S (after 2,500 psi/ft).

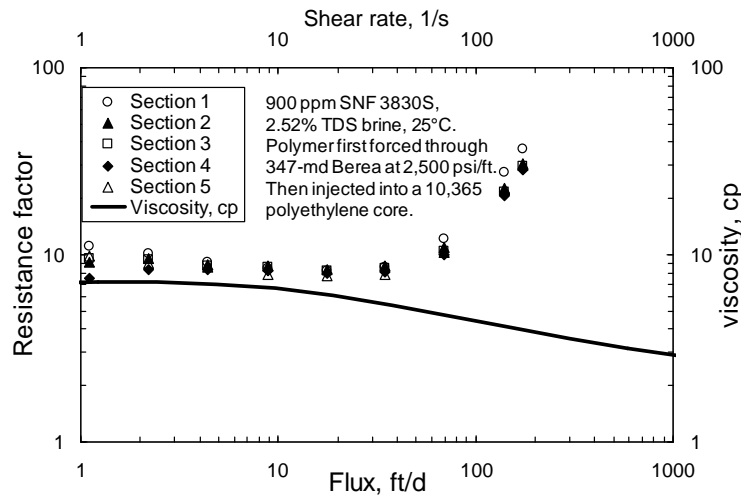


Fig. 47—Resistance factors for mechanically degraded 900-ppm 3830S (after 2,500 psi/ft).

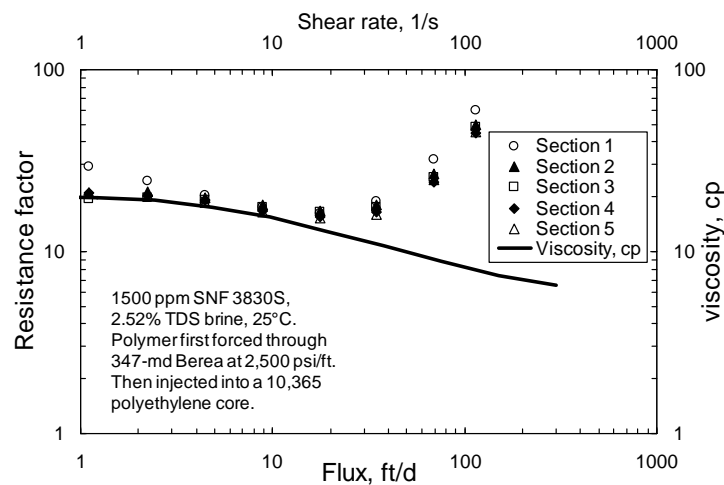


Fig. 48—Resistance factors for mechanically degraded 1,500-ppm 3830S (after 2,500 psi/ft).

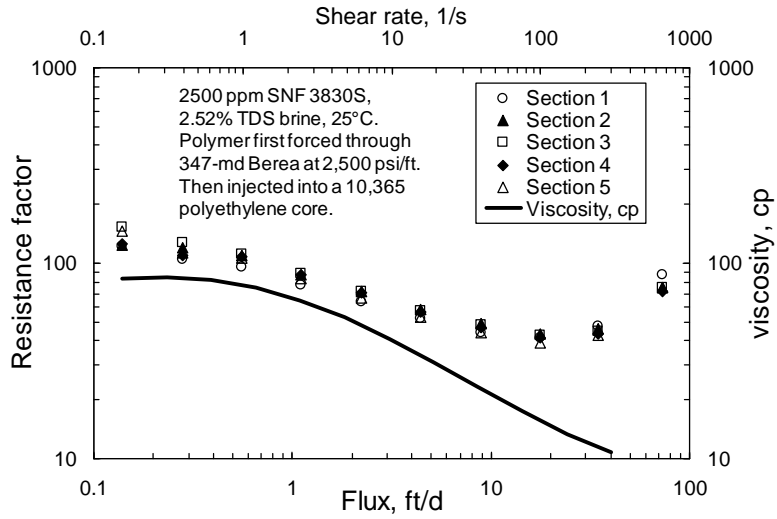


Fig. 49—Resistance factors for mechanically degraded 2,500-ppm 3830S (after 2,500 psi/ft).

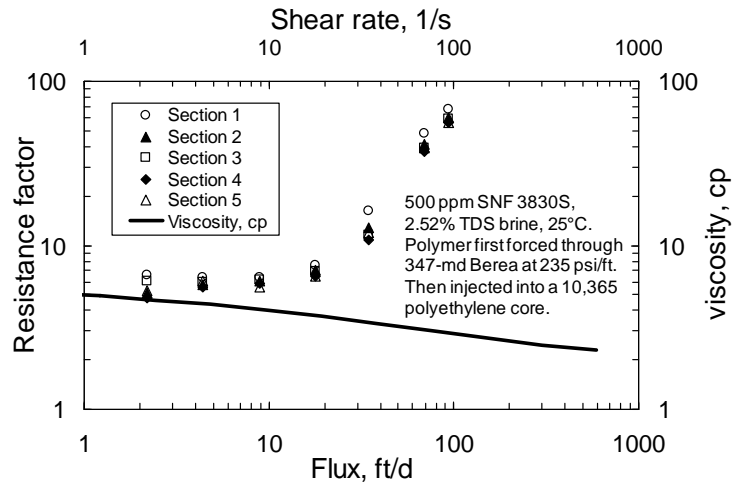


Fig. 50—Resistance factors for mechanically degraded 500-ppm 3830S (after 235 psi/ft).

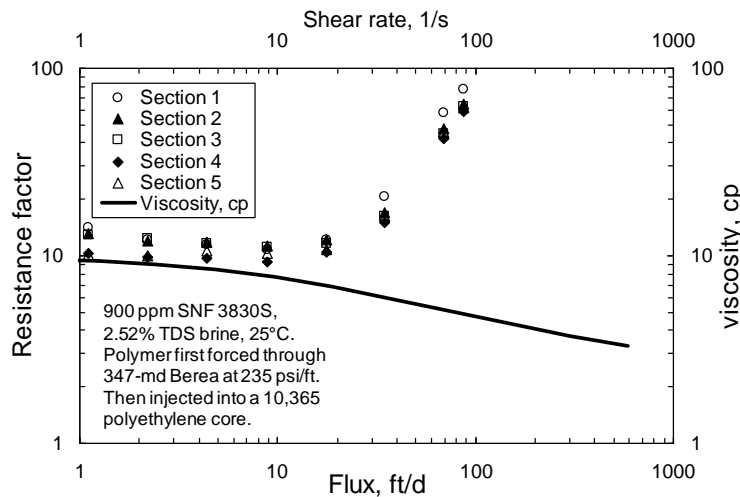


Fig. 51—Resistance factors for mechanically degraded 900-ppm 3830S (after 235 psi/ft).

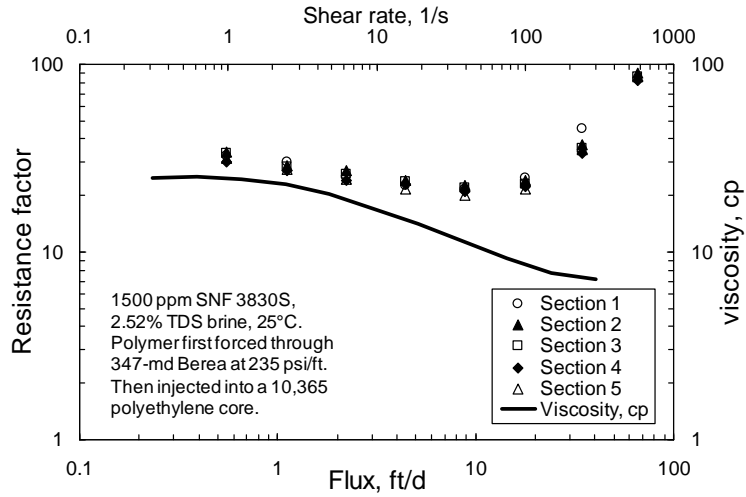


Fig. 52—Resistance factors for mechanically degraded 1,500-ppm 3830S (after 235 psi/ft).

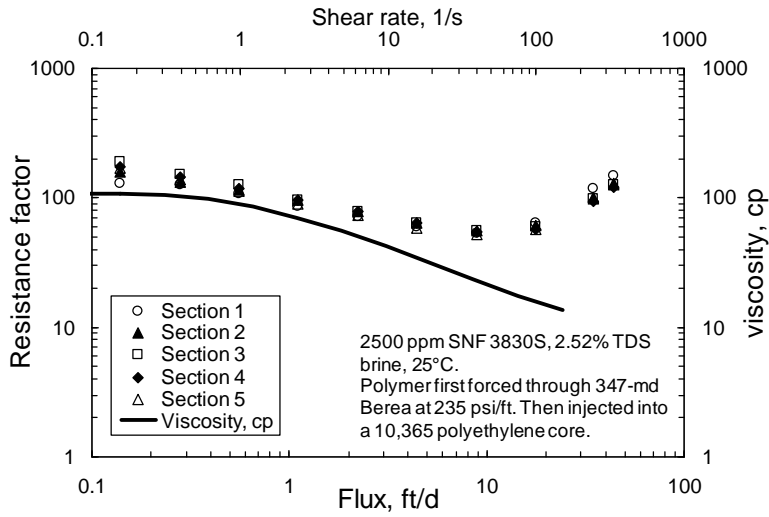


Fig. 53—Resistance factors for mechanically degraded 2,500-ppm 3830S (after 235 psi/ft).

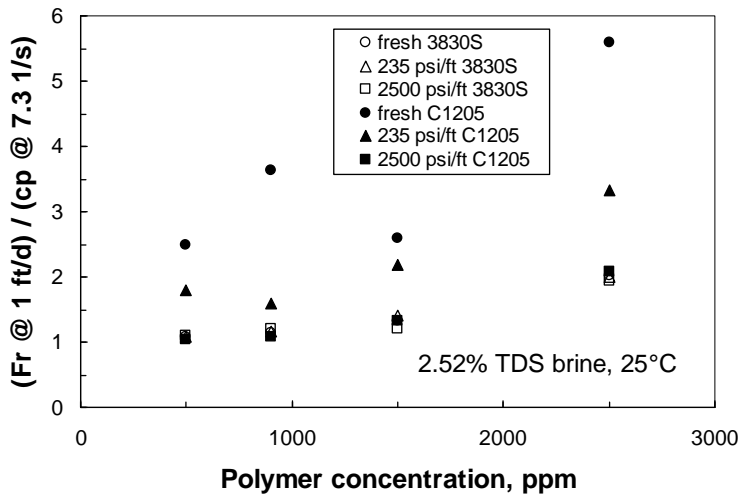


Fig. 54—Low-flux resistance factors relative to low-shear-rate viscosities.

Comparison of Viscosity and Resistance Factor Losses. Table 4 lists viscosity and resistance factor losses experienced by 3830S and C1205 solutions when forced through the 347-md Berea sandstone core at either 235 psi/ft or 2,500 psi/ft. The third and fourth columns in this table list the percent of the original viscosity that was lost, as measured at a shear rate of 7.3 s^{-1} and 25°C . The fifth and sixth columns in this table list the percent of the original resistance factor that was lost, as measured at a flux of 1 ft/d and 25°C . For both polymers at all concentrations, exposure to 235 psi/ft resulted in very little viscosity loss—from 0% to 8% of the original viscosity. Resistance factor losses for 3830S were modest (0-15%) after exposure to 235 psi/ft. However, resistance factor losses for C1205 were significant after exposure to 235 psi/ft—from 31-45%. For 3830S after exposure to 2,500 psi/ft, viscosity losses ranged from 5% to 17%. For C1205 after exposure to 2,500 psi/ft, viscosity losses were higher, ranging from 19% to 35%. Similarly, after exposure to 2,500 psi/ft, resistance factor losses were much greater for C1205 (53-71%) than for 3830S (9-41%).

Table 4—Losses after being forced through a Berea core at given pressure gradient.

Polymer	Concentration ppm	Viscosity loss, % of original @ 7.3 s^{-1}		Resistance factor loss, % of original @ 1 ft/d	
		235 psi/ft	2,500 psi/ft	235 psi/ft	2,500 psi/ft
3830S	500	1	11	4	31
C1205	500	6	35	39	53
3830S	900	2	17	0	24
C1205	900	5	19	31	64
3830S	1,500	0	10	15	41
C1205	1,500	3	27	36	64
3830S	2,500	1	5	0	9
C1205	2,500	8	23	45	71

Length Dependence of Resistance Factors

In previous work, no permeability dependence of resistance factors was noted for Flopaam 3830S in 13-15-cm long Berea sandstone cores with permeabilities of 269 md or above (Seright 2009b). In permeable polyethylene cores, we did not observe any length dependence of resistance factors for any concentration or level of mechanical degradation when using 3830S (see Figs. 46-53). This point is, perhaps, made most effectively in Fig. 55, which plots resistance factors for a fresh 2,500-ppm solution of 3830S in the five sections of the 78.2-cm long 10-darcy polyethylene core. In short (13-14 cm) Berea sandstone or porous polyethylene cores, we also saw no length dependence of resistance factors for C1205 (see Figs. 28, A-1, A-3 to A-13). However, in a 78-cm long 10-darcy polyethylene core, we saw a length dependence of C1205 resistance factors for the higher polymer concentrations (see Fig. 40, 41, 43, 44, and 45). If the length trend in Fig. 45 (for mechanically degraded 2,500-ppm C1205) can be extrapolated, it suggests that resistance factors might not be any higher than expectations from viscosity data after 8 ft. Consequently, more work is needed in longer cores to establish whether the higher-than-expected resistance factors will propagate deep into a formation.

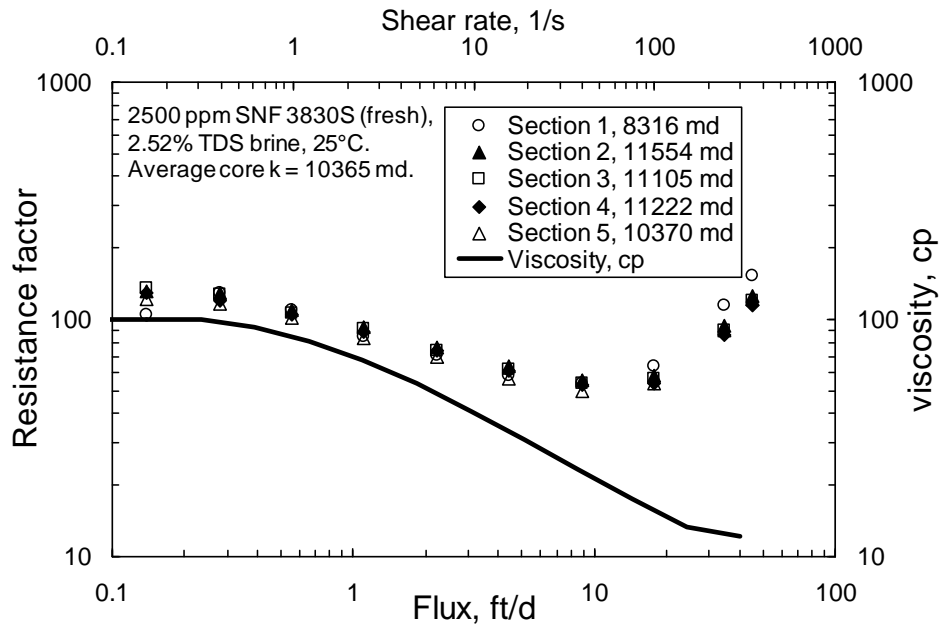


Fig. 55—Resistance factors for fresh 2,500-ppm 3830S.

Discussion of Results

An important concept from our previous studies (Seright *et al.* 2010) of HPAM and xanthan was that low-flux resistance factors in porous media should match reasonably closely with expectations from low-shear-rate viscosity measurements. Much of our work with the SNF hydrophobic associative polymer, C1205, indicates low-flux resistance factors that are noticeably greater than expectations from viscosity measurements in cores up to 78 cm in length. Our evidence to date is mixed regarding what is responsible for this effect. Possibilities include (1) microgels or a high molecular-weight polymer species, (2) relatively high polymer adsorption/retention, including multilayer adsorption and reversible flow-rate dependent retention, and (3) intermolecular polymer association that depends on polymer concentration and flow rate.

Many similarities were noted between C1205 and 3830S. Viscosity versus concentration and shear rate for C1205 (in a 2.52% TDS brine at 25°C) was quite similar to that for SNF Flopaam 3830S (a conventional HPAM). The molecular weight of C1205 was given as 12-17 million, while 3830S was 18-20 million. Both 3830S and C1205 show excellent filterability at lower concentrations (1,000 ppm or lower), but plugged within 200 cm³/cm² throughput at higher concentrations (1,500 ppm).

Important differences exist between the behavior of the two polymers. C1205 solutions were noticeably more turbid than those of 3830S. In Berea sandstone and porous polyethylene cores, low-flux resistance factors for fresh C1205 solutions were 2.5-5.6 times greater than those for 3830S. In cores with multiple sections, we saw no evidence of face plugging. We did not see a gradient of C1205 resistance factors through the core for core lengths of 13-15 cm. This was true in both 347-md Berea sandstone and 12,313-md porous polyethylene. Also, plots of resistance factor versus flux (after normalization for permeability using the capillary bundle correlation)

were the same for both 347-md Berea sandstone and 12,313-md porous polyethylene. These observations argue against the importance of microgels, since microgels should cause higher resistance factors in less-permeable rock. The observations also argue against polymer retention effects since polymer adsorption/retention should be greater in 347-md Berea sandstone (which is hydrophilic) than in 12,313-md polyethylene (which is hydrophobic). Also, plots of resistance factor versus flux in 10,144-md polyethylene were the same after injecting 17.6 *PV* of C1205 solution as when only 1-3.4 *PV* had been injected. If throughput-dependent microgel propagation or polymer retention were important, we might have expected later resistance factors to be greater than earlier resistance factors. On the other hand, the main observation that argues in favor of the importance of either microgels or polymer retention being responsible for the effects is that residual resistance factors (during brine injection after polymer flow) were much greater in 347-md Berea sandstone than in 12,313-md polyethylene.

Figs. 56-59 compare resistance factor (in the second core section) versus flux for C1205 and 3830S for various polymer concentrations and levels of mechanical degradation. In all four figures (i.e., at 500-, 900-, 1,500-, and 2,500-ppm polymer), the low-flux resistance factors for fresh C1205 (solid circles) were considerably greater (typically twice) than those for fresh 3830S (open circles). Second, for all but the highest concentration, low-flux resistance factors for C1205 that was degraded using 235 psi/ft (solid triangles) were about the same as those for fresh 3830S (open circles). Third, for all four concentrations, the low-flux resistance factors for C1205 that was degraded using 2,500 psi/ft (solid squares) were the same or less than those for 3830S that was degraded using 2,500 psi/ft (open squares). Fourth, the shear-thickening behavior (i.e., increase in resistance factors) at moderate to high flux values for fresh and 235-psi/ft-degraded 3830S was more pronounced than that for fresh and 235-psi/ft-degraded C1205.

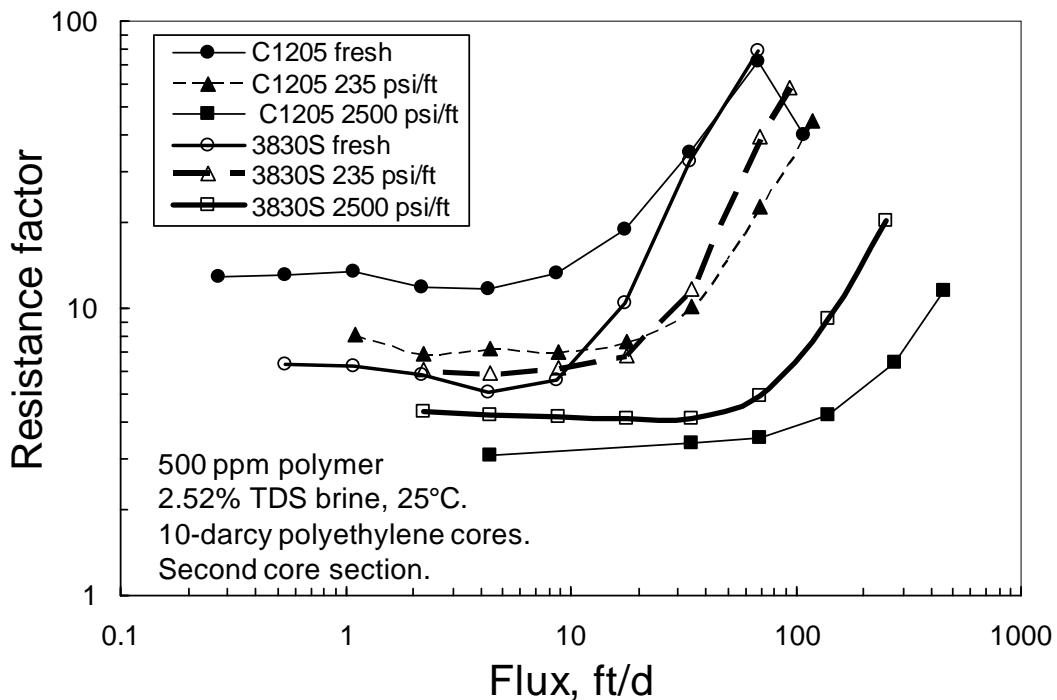


Fig. 56—Resistance factors for 500-ppm polymer: C1205 versus 3830S.

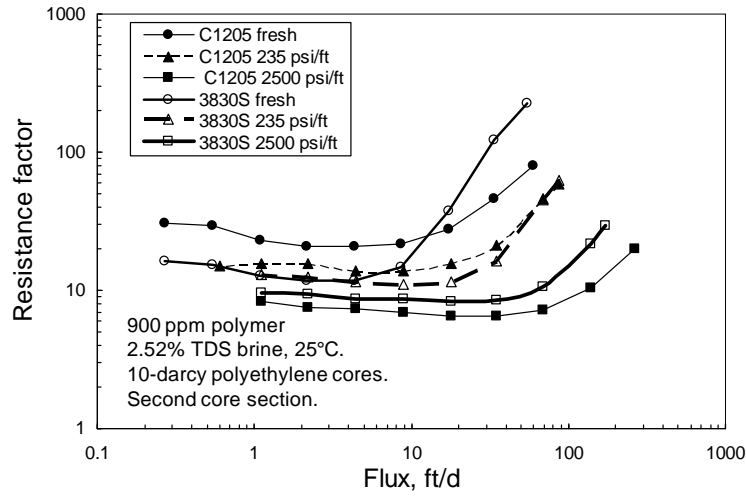


Fig. 57—Resistance factors for 900-ppm polymer: C1205 versus 3830S.

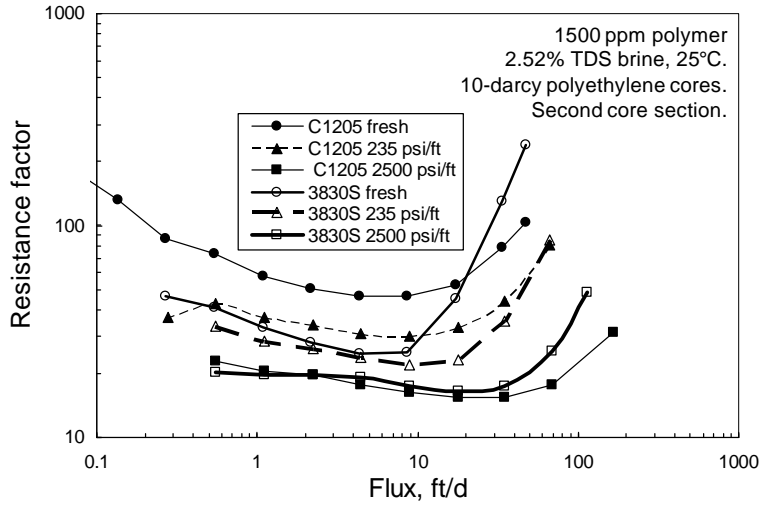


Fig. 58—Resistance factors for 1,500-ppm polymer: C1205 versus 3830S.

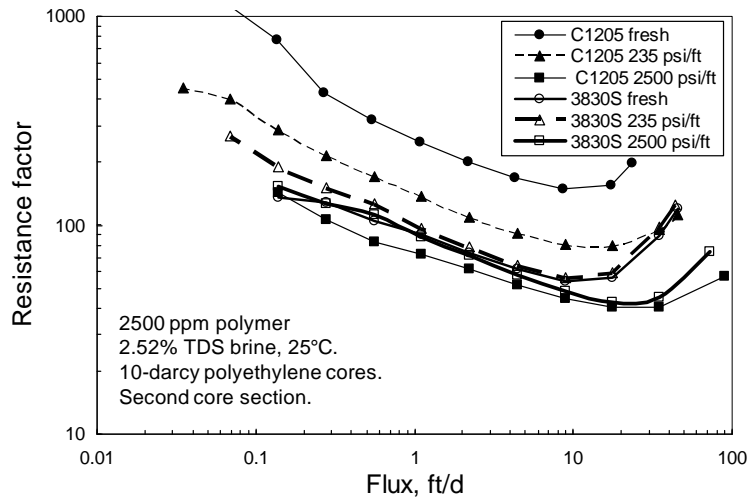


Fig. 59—Resistance factors for 2,500-ppm polymer: C1205 versus 3830S.

Conclusions

Many similarities were noted between C1205 and 3830S. Viscosity versus concentration and shear rate for C1205 (in a 2.52% TDS brine at 25°C) was quite similar to that for SNF Flopaam 3830S (a conventional HPAM). The molecular weight of C1205 was given as 12-17 million g/mol, while 3830S was 18-20 million g/mol. Both 3830S and C1205 show excellent filterability at lower concentrations (1,000 ppm or lower), but plugged within 200 cm³/cm² throughput at higher concentrations (1,500 ppm).

Important differences exist between the behavior of the two polymers. C1205 solutions were noticeably more turbid than those of 3830S. In Berea sandstone and porous polyethylene cores, low-flux resistance factors for fresh C1205 were at least twice those for 3830S. In cores with multiple sections, we saw no evidence of face plugging. This was true in both 347-md Berea sandstone and 10-12 darcy porous polyethylene. Also, plots of resistance factor versus flux (after normalization for permeability using the capillary bundle correlation) were the same for both 347-md Berea sandstone and 12-darcy porous polyethylene. These observations argue against the importance of microgels, since microgels should cause higher resistance factors in less-permeable rock. The observations also argue against polymer retention effects since polymer adsorption/retention should be greater in 347-md Berea sandstone (which is hydrophilic) than in 12-darcy polyethylene (which is hydrophobic). Also, plots of resistance factor versus flux in 10-darcy polyethylene were the same after injecting 17.6 *PV* of C1205 solution as when only 1-3.4 *PV* had been injected. If throughput-dependent microgel propagation or polymer retention were important, we might have expected later resistance factors to be greater than earlier resistance factors.

Fresh C1205 solutions provided about the same viscosity as fresh 3830S solutions. However, in 10-darcy polyethylene, fresh C1205 solutions provided low-flux resistance factors that were about twice those for fresh 3830S solutions. Both polymers showed modest (0-8%) viscosity losses (at 7.3 s⁻¹) after exposure to 235 psi/ft pressure gradient in a core. However, C1205 solutions experienced 31-45% loss in low-flux resistance factor, whereas 3830S solutions experienced only 0-15% loss. After 235 psi/ft, low-flux resistance factors for C1205 solutions were often similar to those for fresh 3830S solutions. After exposure to 2,500 psi/ft pressure gradient, C1205 solutions experienced 19-35% viscosity loss, whereas 3830S solutions experienced 5-17% viscosity loss. After 2,500 psi/ft, low-flux resistance factors for C1205 solutions were the same or less than those for 3830S solutions.

In short (13-14 cm) Berea sandstone or porous polyethylene cores, we also saw no length dependence of resistance factors for C1205. However, in a 78-cm long 10-darcy polyethylene core, we saw a length dependence of C1205 resistance factors for the higher polymer concentrations. If the observed length trend can be extrapolated, it suggests that resistance factors might not be any higher than expectations from viscosity data after 8 ft. Consequently, more work is needed in longer cores to establish whether the higher-than expected resistance factors will propagate deep into a formation.

8. EXAMINATION OF B192 HYDROPHOBIC ASSOCIATIVE POLYMER

We received a second new hydrophobic associative polymer from SNF: Superpusher B 192, Lot RG 2377.6 (hereafter called B192). B192 is an anionic-polyacrylamide-based ter-polymer that has associative properties as described in patent WO2005100423. Typically, the hydrophobic monomer content ranges from 0.025 to 0.25 mol%. B192 contains 4 times more hydrophobic monomer than C1205. Molecular weights range from 3 to 7 million for B192. Total anionic content is between 15 and 25 mol%. During our studies, the brine contained 2.52% total dissolved solids (TDS), specifically with 2.3% NaCl and 0.22% NaHCO₃. The studies were performed at 25°C.

First Test

Based on some initial work, we were intrigued by the behavior of SNF's B192 polymer. In particular, our initial work suggested conditions where the polymer could show a constant pressure gradient in a core over a wide range of flow rate. For this experiment, we used a porous polyethylene core that was 15.14 cm long, with a circular cross-section of 11.64 cm² and a diameter of 3.85 cm. The core porosity was 0.41, and the pore volume was 72.2 cm³. The core had two internal pressure taps, with one located 2.77 cm from the inlet face and the other located 2.43 cm from the outlet face. These taps divided the core into three sections, with the middle section having a length of 9.94 cm. After evacuation and saturation with the 2.52% TDS brine, the permeabilities of the first, second, and third core sections were 4,864 md, 5,489 md, and 4,091 md, respectively.

Figs. 60 and 61 plot resistance factor and pressure gradient versus flux for this first experiment using 1,300-ppm B192 in 2.52% TDS brine. In Fig. 60, note the very strong shear thinning shown by the resistance factors. Similar results were noted in all three core sections. For flux values between 0.03 and 30 ft/d, the slope of the log-log plot was -1, indicating a power-law exponent of 0. The high resistance factors in Fig. 60 are surprising, since viscosity-versus-shear-rate measurements revealed viscosities (Brookfield) of 14.6 cp at 3.65 s⁻¹, 10.6 cp at 7.3 s⁻¹, 8.9 cp at 14.6 s⁻¹, 7.5 cp at 36.5 s⁻¹, and 7.1 at 73 s⁻¹. This data indicates a power-law index of 0.77—a mild shear thinning. It is quite surprising that a polymer with less than 20-cp viscosity could provide a resistance factor up to 100,000 at low flux values.

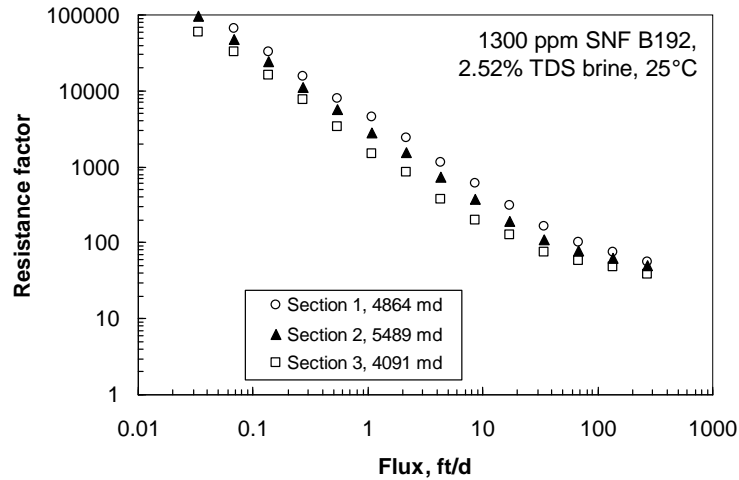


Fig. 60—B192 resistance factors in 5-darcy polyethylene.

Fig. 60 can be re-plotted to make Fig. 61. The surprising result from Fig. 61 is that the pressure gradient appears to be independent of flow rate for flux values between 0.03 and 30 ft/d. In the second core section, the pressure gradient was about 80 psi/ft. A caution should be mentioned regarding the above observations with B192. Specifically, the polymer was injected after flushing many pore volumes of other HPAM and hydrophobic associative polymers. Consequently, the unusual behavior mentioned above might, in part, be due to the previous treatment of the core.

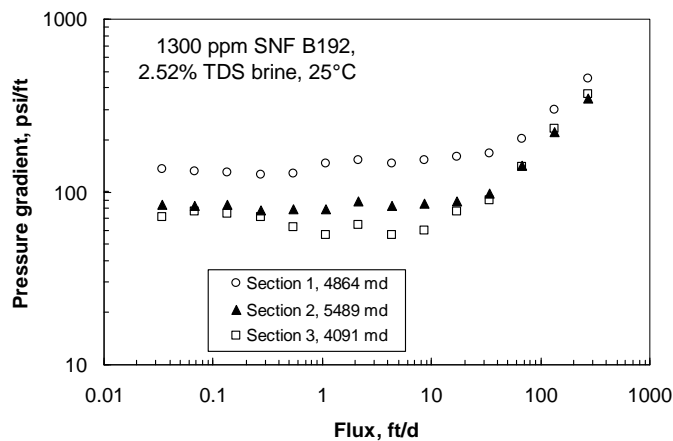


Fig. 61—1,300-ppm B192 pressure gradients in 5-darcy polyethylene.

Second Test

Because the cores that were used to examine a polymer called C1205 were available (as described in the next chapter), we decided to perform some additional tests with B192 (even though we recognized that previous exposure of the core to C1205 could influence the behavior that we see for B192). For the first test (Fig. 61 above, where 1,300-ppm B192 was injected), we were concerned that a pressure gradient of 80 psi/ft might be too high to be of practical value in a reservoir application. Therefore, we reduced the B192 concentration to 500 ppm for the first B192 polymer injected into the polyethylene core which had previously been exposed to the

polymer C1205. Fig. 62 plots pressure gradients versus flux in the three core sections. Just as for 1,300-ppm B192, pressure gradients were insensitive to flux over a wide range of rates. At moderate to low flux values, pressure gradient in the second core section (12,313 md) ranged from 35 to 56 psi/ft.

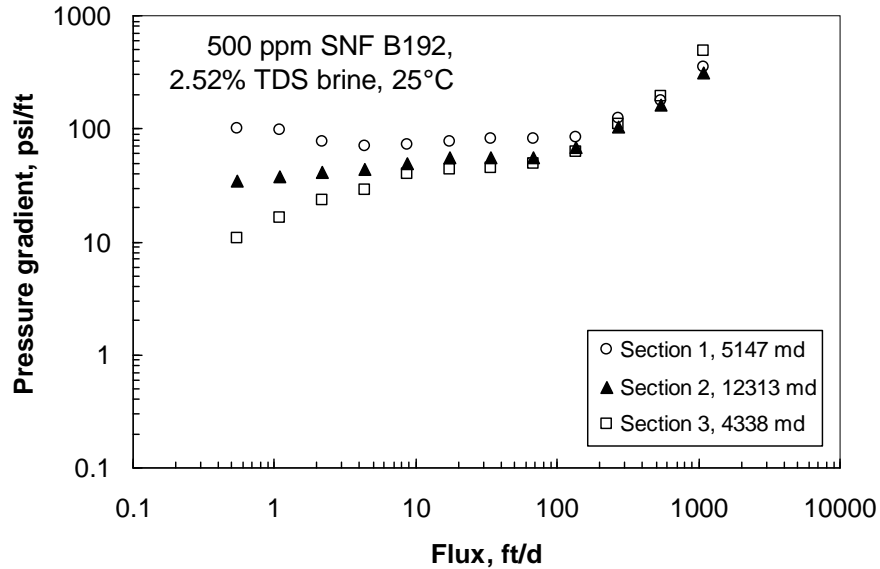


Fig. 62—500-ppm B192 pressure gradients in 12.3-darcy polyethylene.

We were concerned that 35-56 psi/ft might still be too high to be of practical interest. Therefore, we performed several experiments in the same core, injecting 300-ppm B192. Before injecting this polymer, we first injected 109 *PV* of brine to displace the previous polymer. Residual resistance factors were 1.9, 2.1, and 1.3 in the first, second, and third core sections, respectively. Then 15 *PV* of 300-ppm B192 were injected at a flux of 1,082 ft/d. After stabilization of pressures, the injection rate was reduced (typically halved), and stabilized pressures were again recorded. This procedure was repeated at a series of lower rates, as indicated in Fig. 63. (Varying rates from high to low flux values was our standard procedure.) Pressure gradients in the second core section averaged about 20 psi/ft over a wide range of flux (actually varying from 9 to 41 psi/ft over the flux range from 0.005 to 100 ft/d). However, pressure gradients diminished substantially from Core Section 1 to Core Section 3. After the lowest rate shown in Fig. 63, rates were increased in stages to produce Fig. 64. Then the orientation of the core was reversed (i.e., injecting into the face that was previously the outlet) and rates were varied from high values to low values to produce Fig. 65.

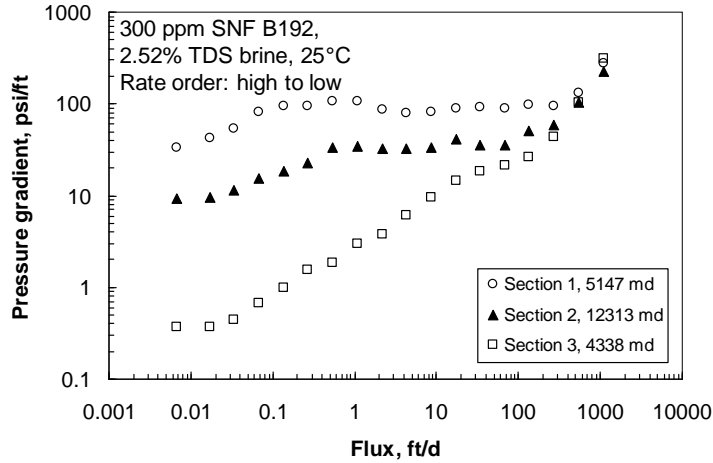


Fig. 63—300-ppm B192 pressure gradients in polyethylene. Rates: high to low.

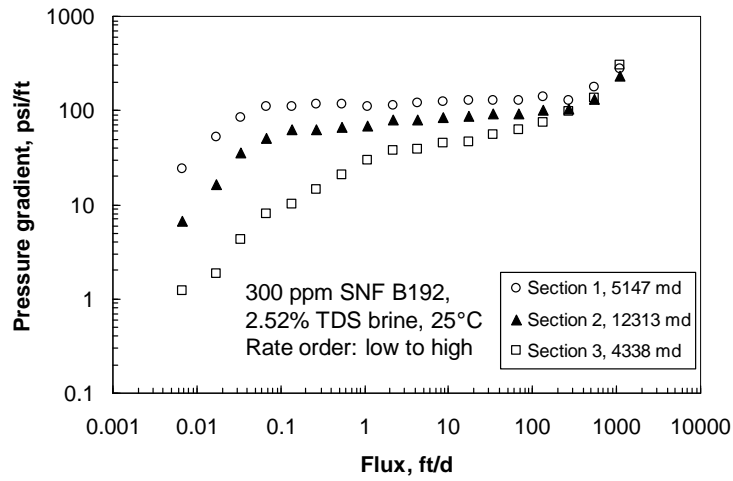


Fig. 64—300-ppm B192 pressure gradients in polyethylene. Rates: low to high.

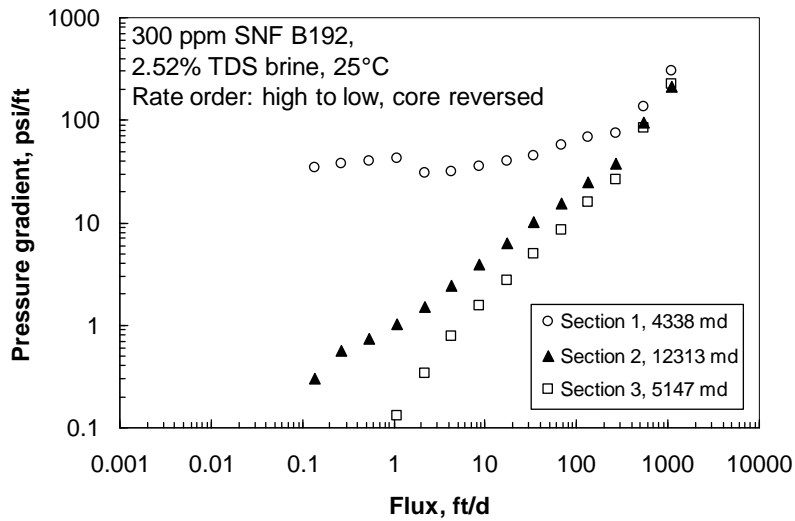


Fig. 65—300-ppm B192 pressure gradients in polyethylene. Flow direction reversed.

Fig. 66 compares the pressure gradients observed in the second core section for the floods associated with Figs. 61-63. A significant degree of hysteresis was observed.

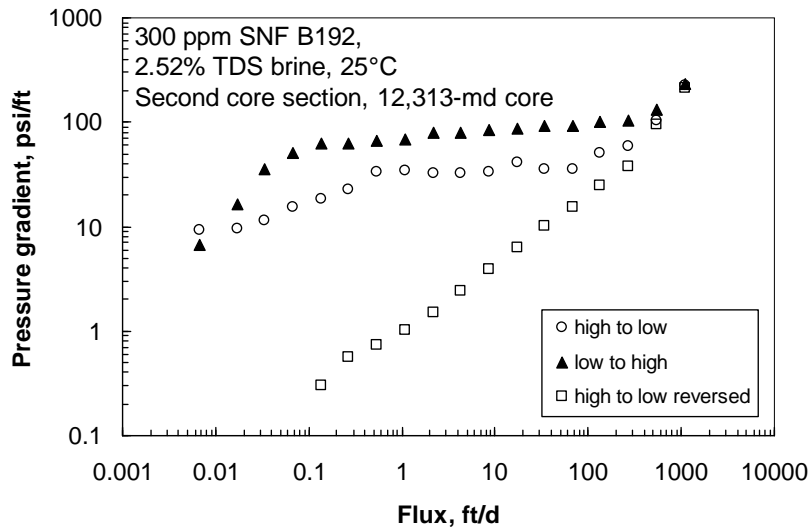


Fig. 66—300-ppm B192 pressure gradients in polyethylene. Second core section.

Third Test

Using the 363-md Berea sandstone core that was previously used to examine the polymer C1205 (see the previous chapter), we performed a similar set of experiments injecting 300-ppm B192. Figs. 64 and 65 plot pressure gradient versus flux when going from high rates to low rates (Fig. 67) and from low rates to high rates (Fig. 68). Interestingly, the regions of constant pressure gradient were not observed in the Berea core.

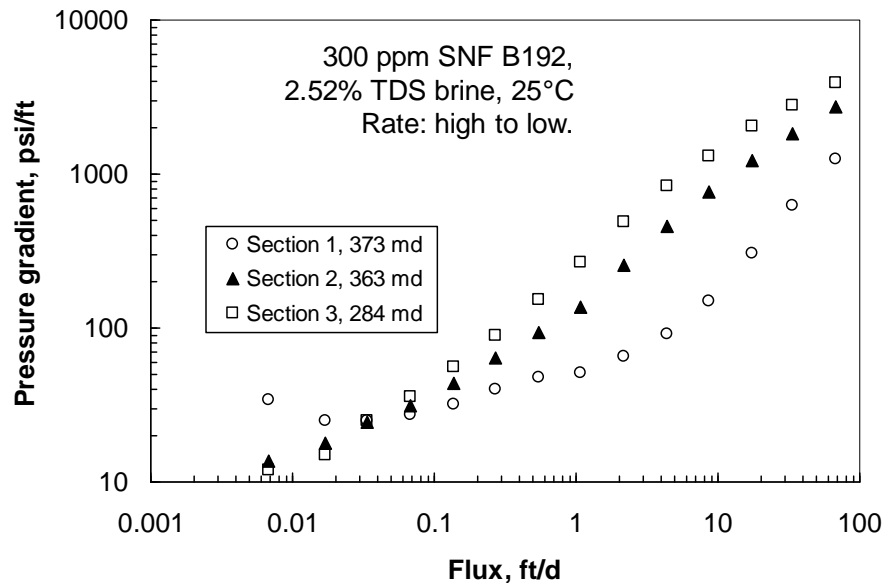


Fig. 67—300-ppm B192 pressure gradients in Berea. Rates: high to low.

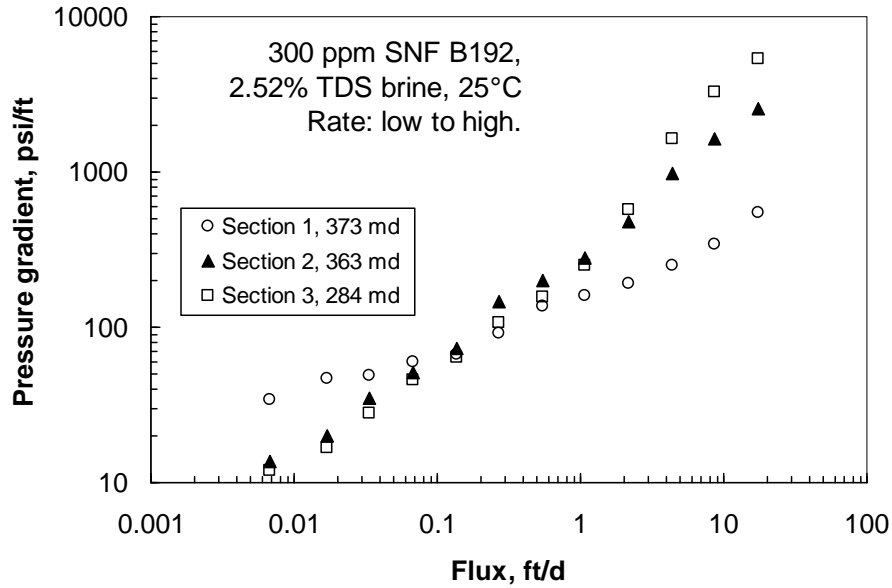


Fig. 68—300-ppm B192 pressure gradients in Berea. Rates: low to high.

Conclusion

The above coreflood results using B192 are intriguing, in that (1) resistance factors are much higher than expected from viscosity measurements, (2) pressure gradients can be independent of flux over a wide range, and (3) regions of constant pressure gradient were observed in high-permeability polyethylene cores but not in less-permeable Berea sandstone cores. Future tests using B192 solutions in virgin cores may be performed to investigate these issues.

9. DOES IT MATTER IF POLYMER REDUCES S_{OR} FOR VISCOUS OILS?

The Issue

Conventional wisdom argues that because EOR polymers do not significantly reduce oil/water interfacial tension, the ultimate residual oil saturation (after injecting many pore volumes) will be the same for a polymer flood as for an extended waterflood. However, Wu *et al.* (2007) observed that HPAM polymers reduced the residual oil saturation by up to 15 saturation percentage points (i.e., a S_{or} of 36.8% with waterflooding versus 21.75% for polymer flooding, using a constant capillary number of 5×10^{-5}) when displacing Daqing crude oil from cores. Part of our research project involves examining whether this effect could occur with North Slope viscous crude oils. However, during a recent visit to Calgary, Fred Wassmuth at the Alberta Innovates Technology Futures (formerly the Alberta Research Council) questioned whether a reduction in residual oil saturation was of practical relevance for waterfloods and polymer floods in reservoirs with viscous oils. In particular, if the displacement is inefficient, should improvements in the mobility ratio have a significantly greater impact on recovery efficiency than that associated with reducing the S_{or} ?

Fractional Flow Calculations for One Layer

To explore this question, we performed fractional flow calculations where the residual oil saturation was lower during polymer flooding than during waterflooding. For these calculations, we used the relative permeability characteristics listed in Eqs. 4-6 (also shown in Fig. 69) and assumed a single layer with connate (and initial) water saturation (S_{wr}) of 0.3. As with our previous calculations in earlier chapters, we assumed incompressible flow and neglected gravity and capillary forces. For the following figures, the y -axis plots the percent of the original oil in place (OOIP) that was recovered as a function of pore volumes (PV) of water injected. For Figs. 69-72, all cases had the same OOIP. For the first case considered (Fig. 69), we injected 1-cp water to displace 1,000-cp oil. For the base case (thick solid curve in Fig. 69), $S_{or}=0.3$. Three other cases, with $S_{or}=0.25$, 0.1, and 0 are also shown. For these cases, water breakthrough occurred very early—at 0.072 PV for $S_{or}=0.3$ and at 0.127 PV for $S_{or}=0$. Before 0.072 PV, no differences in oil recovery were seen. For larger PV throughput values, the four curves in Fig. 69 diverged, but in a moderate fashion. By 1 PV of water injection, the oil recovery was 24.4% for $S_{or}=0.3$, 26.6% for $S_{or}=0.25$, 33.1% for $S_{or}=0.1$, and 37% for $S_{or}=0$.

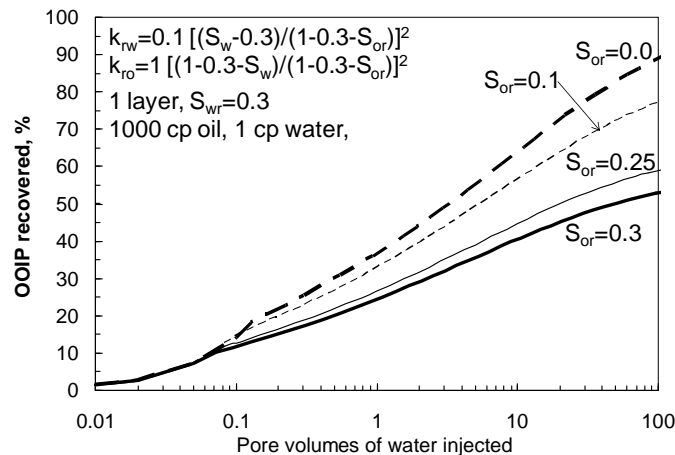


Fig. 69—Effect of S_{or} on recovery for 1-cp water, 1,000-cp oil.

For comparison, Fig. 70 provides a similar plot for 1-cp water displacing 1-cp oil. For these cases, water breakthrough occurred significantly later than those for the 1,000-cp oil—at 0.39 PV for $S_{or}=0.3$ and at 0.68 PV for $S_{or}=0$. Before 0.39 PV, no differences in oil recovery were seen. For larger PV throughput values, the four curves in Fig. 70 diverged abruptly. By 1 PV of water injection, the oil recovery was 56.6% for $S_{or}=0.3$, 63.6% for $S_{or}=0.25$, 84.5% for $S_{or}=0.1$, and 99.3% for $S_{or}=0$. In comparing Figs. 69 and 70, it is evident that decreasing the S_{or} significantly increases the breakthrough PV—by about 75% for both 1-cp oil and 1,000-cp oil. Also, it is evident that the magnitude of the increase in oil recovery (as the S_{or} is decreased) is substantially greater (when measured at 1 PV) for the 1-cp-oil case than for the 1,000-cp-oil case.

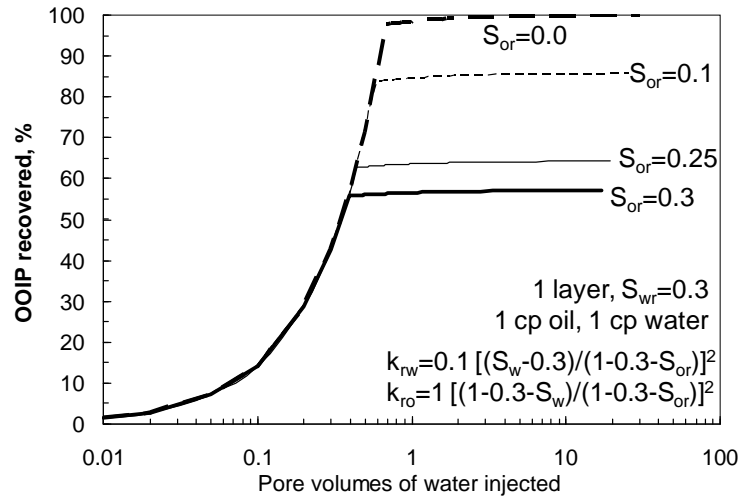


Fig. 70—Effect of S_{or} on recovery for 1-cp water, 1-cp oil.

For the next two cases, we consider injecting polymer solutions to displace 1,000-cp oil. Figs. 71 and 72 show cases where 10-cp polymer and 100-cp polymer were injected, respectively. In both figures, the lower solid thin curve shows the case for waterflooding for comparison. Both figures show that at 1 PV, there is a significant increase in recovery as S_{or} decreases. Examination of Figs. 69, 70, and 71 reveals that as the viscosity of the injected aqueous phase increases, the magnitude of the oil recovery increase (as S_{or} decreases) becomes greater. For example, at 1 PV with 1-cp water injected to displace 1,000-cp oil, the oil recovery increases from 24.4% for $S_{or}=0.3$, to 37% for $S_{or}=0$ —a 51.6% increase. With 10-cp polymer injected to displace 1,000-cp oil, the oil recovery increases from 40.2% for $S_{or}=0.3$, to 63% for $S_{or}=0$ —a 56.7% increase. With 100-cp polymer injected to displace 1,000-cp oil, the oil recovery increases from 52.8% for $S_{or}=0.3$, to 88.4% for $S_{or}=0$ —a 67.4% increase.

The above comparisons may seem optimistic since they assumed that polymer would decrease the residual oil saturation from 0.3 to 0. A more conservative comparison is generated by assuming that S_{or} is reduced from 0.3 to 0.25. At 1 PV with 1-cp water injected to displace 1,000-cp oil, the oil recovery increases from 24.4% for $S_{or}=0.3$, to 26.6% for $S_{or}=0.25$ —a 9% increase. With 10-cp polymer injected to displace 1,000-cp oil, the oil recovery increases from 40.2% for $S_{or}=0.3$, to 44.3% for $S_{or}=0.25$ —a 10.2% increase. With 100-cp polymer injected to displace 1,000-cp oil, the oil recovery increases from 52.8% for $S_{or}=0.3$, to 58.9% for $S_{or}=0.25$ —a 11.6% increase. Thus, a significant increase in oil recovery can be achieved if a polymer can reduce S_{or} , even

when displacing viscous oils. Of course, the magnitude of the oil recovery increases as the S_{or} is reduced. Also, for a given S_{or} , the magnitude of the oil recovery increases as the viscosity of the injected polymer solution increases.

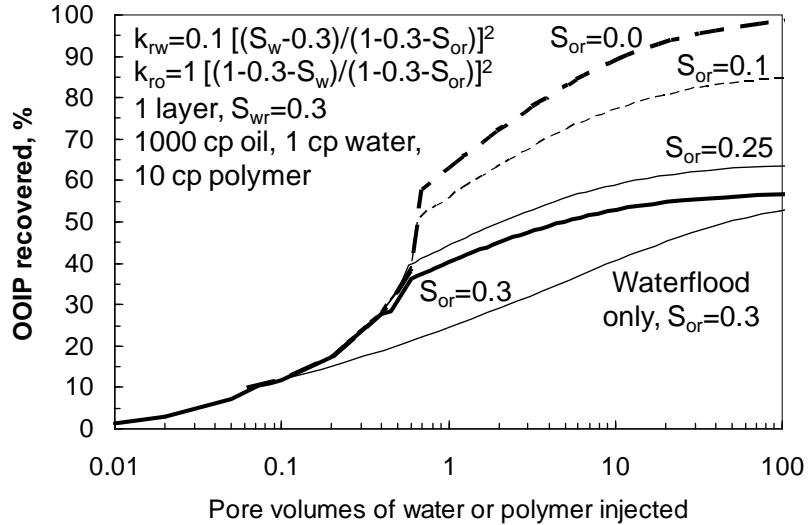


Fig. 71—Effect of S_{or} on recovery for 10-cp polymer, 1,000-cp oil.

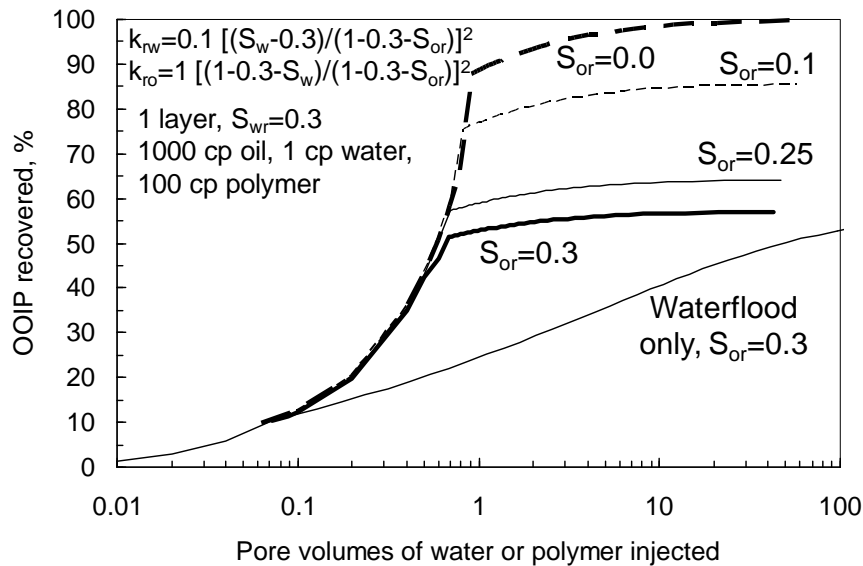


Fig. 72—Effect of S_{or} on recovery for 100-cp polymer, 1,000-cp oil.

Future Work

Future work will extend this analysis to cases with multiple layers, both with and without crossflow. We will also look at the impact of waterflooding before polymer flooding. Also, we will examine the results when a different set of relative permeability curves are used (North Slope case).

Conclusions

Fractional flow analysis reveals that if polymers can reduce the S_{or} , this phenomenon will be an important factor during recovery of viscous oils. As expected, the magnitude of the oil recovery increases as the S_{or} is reduced. For one example examined, if the polymer reduces S_{or} from 0.3 to 0.25, a 10% increase in oil recovery can be expected. Also, for a given S_{or} , the magnitude of the oil recovery increases as the viscosity of the injected polymer solution increases.

NOMENCLATURE

- F_r = resistance factor (water mobility/polymer solution mobility)
 F_{r1} = resistance factor in Layer 1 (high-permeability layer)
 F_{r2} = resistance factor in Layer 2 (low-permeability layer)
HPAM = partially hydrolyzed polyacrylamide
 h_1 = height of Zone 1, ft [m]
 h_2 = height of Zone 2, ft [m]
 k = permeability, darcys [μm^2]
 k_1 = permeability of Zone 1, darcys [μm^2]
 k_2 = permeability of Zone 2, darcys [μm^2]
 k_{ro} = relative permeability to oil
 k_{roo} = endpoint relative permeability to oil
 k_{rw} = relative permeability to water
 k_{rwo} = endpoint relative permeability to water
 L = linear distance, ft [m]
 L_{p1} = linear distance of polymer penetration into the high-permeability layer, ft [m]
 L_{p2} = linear distance of polymer penetration into the low-permeability layer, ft [m]
 M_w = molecular weight,
 no = oil saturation exponent in Eq. 5
 nw = water saturation exponent in Eq. 4
 PV = pore volumes of fluid injected
 Δp = pressure difference, psi [Pa]
 R = correlation coefficient
 r_{p1} = radius of polymer penetration into the high-permeability layer, ft [m]
 r_{p2} = radius of polymer penetration into the low-permeability layer, ft [m]
 r_w = wellbore radius, ft [m]
 S_{or} = residual oil saturation
 S_w = water saturation
 S_{wr} = residual water saturation
TDS = total dissolved solids
 u = flux, ft/d [m/d]
 v_1 = front velocity in Zone 1, ft/d [m/d]
 v_2 = front velocity in Zone 2, ft/d [m/d]
 λ = mobility, darcys/cp [$\mu\text{m}^2/\text{mPa}\cdot\text{s}$]
 μ = viscosity, cp [mPa-s]
 ϕ = porosity
 ϕ_1 = porosity in Zone 1
 ϕ_2 = porosity in Zone 2

REFERENCES

- AlSofi, A. M., and Blunt, M.J. 2009. Streamline-Based Simulation of Non-Newtonian Polymer Flooding. Paper SPE 123971 presented at the SPE Annual Technical Conference and Exhibition, New Orleans, Louisiana, 4–7 October.
- Chauveteau, G. 1981. Molecular Interpretation of Several Different Properties of Flow of Coiled Polymer Solutions Through Porous Media in Oil Recovery Conditions. Paper SPE 10060 presented at the SPE Annual Technical Conference and Exhibition, San Antonio, Texas, 5–7 October.
- Coats, K.H., Dempsey, J.R., and Henderson, J.H. 1971. The Use of Vertical Equilibrium in Two-Dimensional Simulation of Three-Dimensional Reservoir Performance. *SPEJ*, **11**(1): 63–71.
- Craig, F.F. 1971. *The Reservoir Engineering Aspects of Waterflooding*. Monograph Series, SPE, Richardson, Texas **3**: 45–75.
- Delshad, M., Kim, D.H., Magbagbeol, O.A., Huh, C., Pope, G.A., and Tarahhom, F. 2008. Mechanistic Interpretation and Utilization of Viscoelastic Behavior of Polymer Solutions for Improved Polymer-Flood Efficiency. Paper SPE 113620 presented at the SPE/DOE Improved Oil Recovery Symposium, Tulsa, Oklahoma, 19–23 April.
- Dupuis, G., Rousseau, D., Tabary, R., and Grassl, B. 2010. How to Get the Best Out of Hydrophobically Associative Polymers for IOR? New Experimental Insights. Paper SPE 129884 presented at the SPE Improved Oil Recovery Symposium, Tulsa, Oklahoma, 24–28 April.
- Durst, F., Haas, R., and Interthal, W. 1982. Laminar and Turbulent Flows of Dilute Polymer Solutions: A Physical Model. *Rheologica Acta* **21**(4-5): 572–577.
- Gogarty, W.B. 1967. Mobility Control with Polymer Solutions. *JPT* **19**(6): 161-173. SPE 1566B-PA.
- Graessley, W.W. 1974. The Entanglement Concept in Polymer Rheology. *Adv. Polymer Sci.* **16**: 126.
- Heemskerck, J., Rosmalen, R.J., Hotslag, R.J., and Teeuw, D. 1984. Quantification of Viscoelastic Effects of Polyacrylamide Solutions. Paper SPE 12652 presented at the SPE/DOE Symposium on Enhanced Oil Recovery Symposium, Tulsa, Oklahoma, 15–18 April.
- Hirasaki, G.J., and Pope, G.A. 1974. Analysis of Factors Influencing Mobility and Adsorption in the Flow of Polymer Solution Through Porous Media. *SPEJ* **14** (4): 337–346.
- Huh, C., and Pope, G.A. 2008. Residual Oil Saturation from Polymer Floods: Laboratory Measurements and Theoretical Interpretation. Paper SPE 113417 presented at the SPE/DOE Improved Oil Recovery Symposium, Tulsa, Oklahoma, 19–23 April.
- Jennings, R.R., Rogers, J.H., and West, T.J. 1971. Factors Influencing Mobility Control by Polymer Solutions. *JPT* **23**(3): 391–50, SPE 2867-PA.
- Jewett, R.L. and Schurz G.F. 1979 Polymer Flooding—A Current Appraisal. *JPT* **31**(6): 675–684.
- Jones, W.M. 1980. Polymer Additives for Reservoir Flooding for Oil Recovery: Shear Thinning or Shear Thickening? *J. Phy. D.: Appl. Phys.* **13**: L87-88.
- Masuda, Y., Tang, K-C., Mlyazawa, M., and Tanaka, S. 1992. 1D Simulation of Polymer Flooding Including the Viscoelastic Effect of Polymer Solution. *SPE* **7** (2): 247–252. SPE 9499-PA.

- Rousseau, D., Chauveteau, G. and Renard, M. 2005. Rheology and Transport in Porous Media of New Water Shutoff/Conformance Control Microgels. Paper SPE 93254 presented at the SPE International Symposium on Oilfield Chemistry, Houston, Texas, 2–4 February.
- Seright, R.S., Maerker, J.M., and Holzwarth G. 1981. Mechanical Degradation of Polyacrylamides Induced by Flow Through Porous Media. *American Chemical Society Polymer Preprints*, **22**: 30–33.
- Seright, R.S. 1983. The Effects of Mechanical Degradation and Viscoelastic Behavior on Injectivity of Polyacrylamide Solutions. *SPEJ* **23** (3): 475–485, SPE 9297-PA.
- Seright, R.S. 1988. Placement of Gels to Modify Injection Profiles. Paper SPE/DOE 17332 presented at the SPE/DOE Enhanced Oil Recovery Symposium, Tulsa, Oklahoma, 17–20 April.
- Seright, R.S. 1991. Effect of Rheology on Gel Placement. *SPEERE* **6** (2): 212–218; *Trans.*, AIME, **291**.
- Seright, R.S., Seheult, J.M., and Talashek, T.A. 2009a. Injectivity Characteristics of EOR Polymers. *SPEERE* **12** (5): 783–792.
- Seright, R.S. 2009b. Use of Polymers to Recover Viscous Oil from Unconventional Reservoirs. First Annual Report. Contract No.: DE-NT0006555, US DOE, Washington DC (October 2009).
- Seright, R.S., Fan, T., Wavrik, K., and Balaban, R.C. 2010. New Insights into Polymer Rheology in Porous Media. Paper SPE 129200 presented at the SPE Improved Oil Recovery Symposium, Tulsa, Oklahoma, 24–28 April.
- Seright, R.S. 2010. Potential for Polymer Flooding Reservoirs with Viscous Oils. *SPEERE* **13** (5): 783–792.
- Sorbie, K.S. and Seright, R.S. 1992. Gel Placement in Heterogeneous Systems with Crossflow. Paper SPE 24192 presented at the SPE/DOE Symposium on Enhanced Oil Recovery, Tulsa, Oklahoma, 22–24 April.
- Southwick, J.G., and Manke, C.W. 1988. Molecular Degradation, Injectivity, and Elastic Properties of Polymer Solutions. *SPEERE* **3** (4): 1193–1201.
- Vela, S., Peaceman, D.W. and Sandvik, E.I. 1976. Evaluation of Polymer Flooding in a Layered Reservoir with Crossflow, Retention, and Degradation. *SPEJ* **16**(2): 82–96.
- Wang, D.M., Seright, R.S., Shao, Z., and Wang, J. 2008. Key Aspects of Project Design for Polymer Flooding at the Daqing Oil Field. *SPEERE* **11** (6): 1117–1124.
- Wang, D.M., Dong, H., Lv, C., Fu, X., and Nie, J. 2009. Review of Practical Experience of Polymer Flooding at Daqing. *SPEERE* **12** (3): 470–476.
- Wu, W., Wang, D., and Jiang, H. 2007. Effect of the Visco-Elasticity of Displacing Fluids on the Relationship of Capillary Number and Displacement Efficiency in Weak Oil-Wet Cores. Paper SPE 109228 presented at the SPE Asia Pacific Oil and Gas Conference and Exhibition, Jakarta, Indonesia, 30 October–1 November.
- Zaitoun, A. and Kohler, N. 1987. The Role of Adsorption in Polymer Propagation Through Reservoir Rocks. Paper SPE 16274 presented at the SPE International Symposium on Oilfield Chemistry, San Antonio, Texas, 4–6 October.
- Zapata, V.J. and Lake, L.W. 1981. A Theoretical Analysis of Viscous Crossflow. Paper SPE 10111 presented at the SPE Annual Technical Conference and Exhibition, San Antonio, Texas, 5–7 October.

Zhang, G. and Seright, R.S. 2007. Conformance and Mobility Control: Foams versus Polymers. Paper SPE 105907 presented at the SPE International Symposium on Oilfield Chemistry, Houston, Texas, 28 February–2 March.

APPENDIX A—C1205 Resistance Factors versus Core Section, Flux, and Concentration

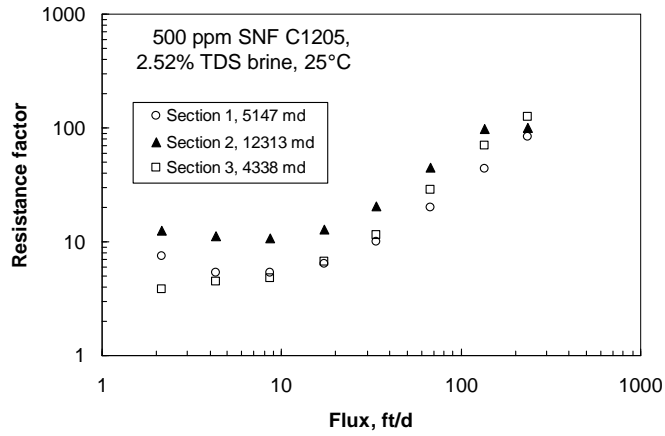


Fig. A-1—Resistance factor versus flux for 500-ppm C1205 in polyethylene.

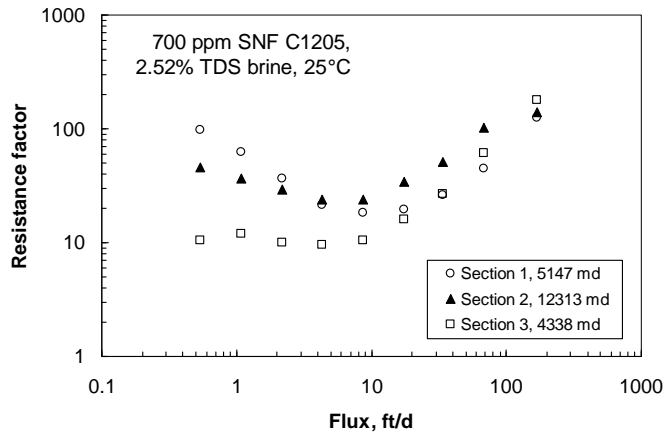


Fig. A-2—Resistance factor versus flux for 700-ppm C1205 in polyethylene.

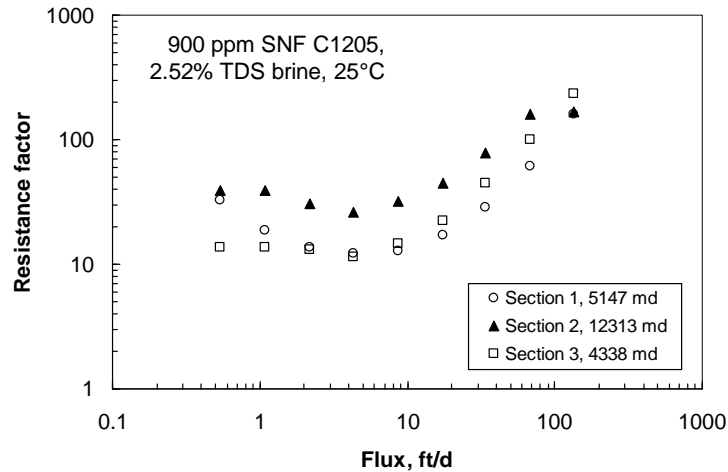


Fig. A-3—Resistance factor versus flux for 900-ppm C1205 in polyethylene.

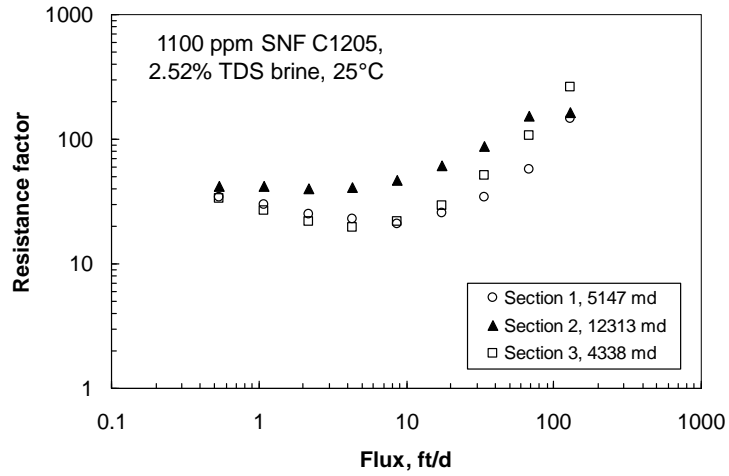


Fig. A-4—Resistance factor versus flux for 1,100-ppm C1205 in polyethylene.

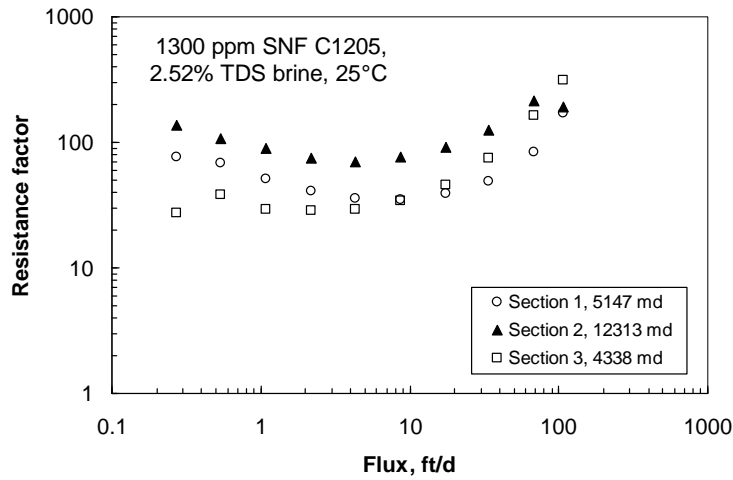


Fig. A-5—Resistance factor versus flux for 1,300-ppm C1205 in polyethylene.

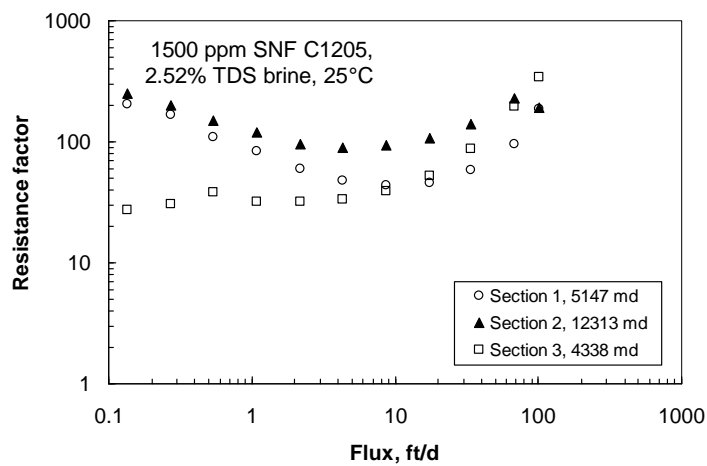


Fig. A-6—Resistance factor versus flux for 1,500-ppm C1205 in polyethylene.

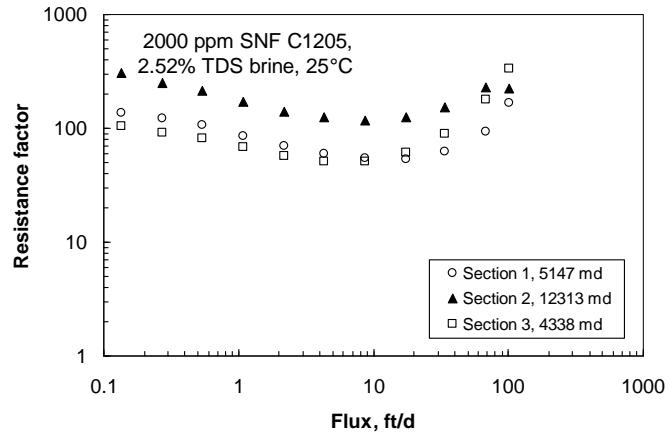


Fig. A-7—Resistance factor versus flux for 2,000-ppm C1205 in polyethylene.

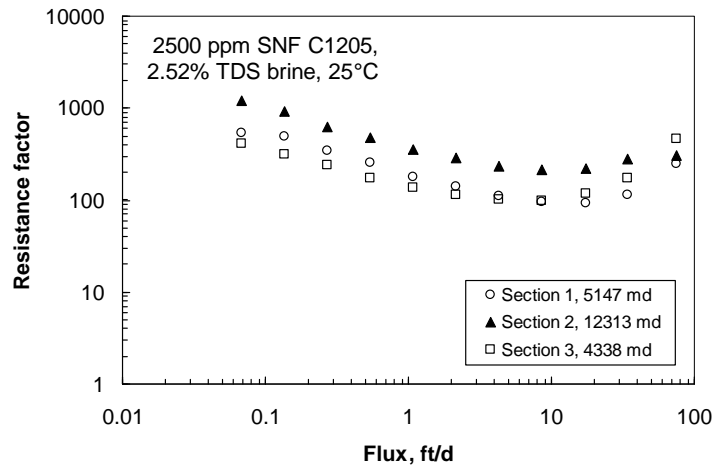


Fig. A-8—Resistance factor versus flux for 2,500-ppm C1205 in polyethylene.

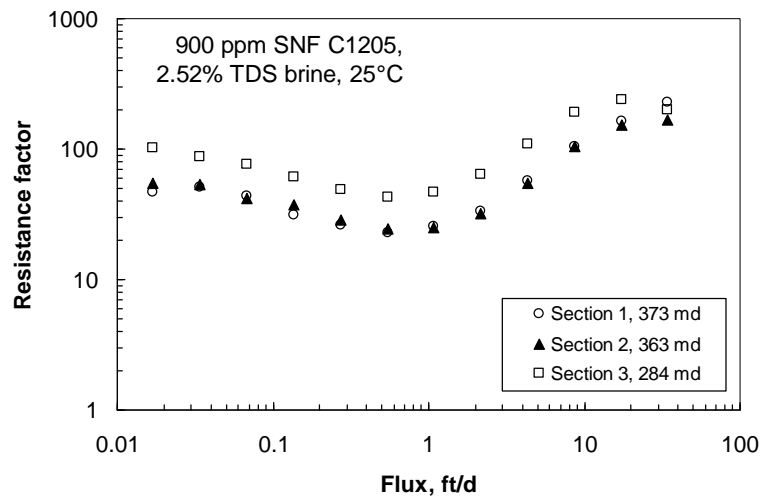


Fig. A-9—Resistance factor versus flux for 900-ppm C1205 in Berea.

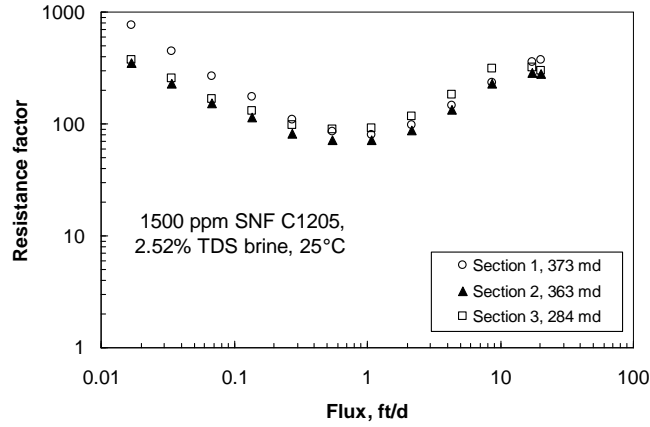


Fig. A-10—Resistance factor versus flux for 1,500-ppm C1205 in Berea.

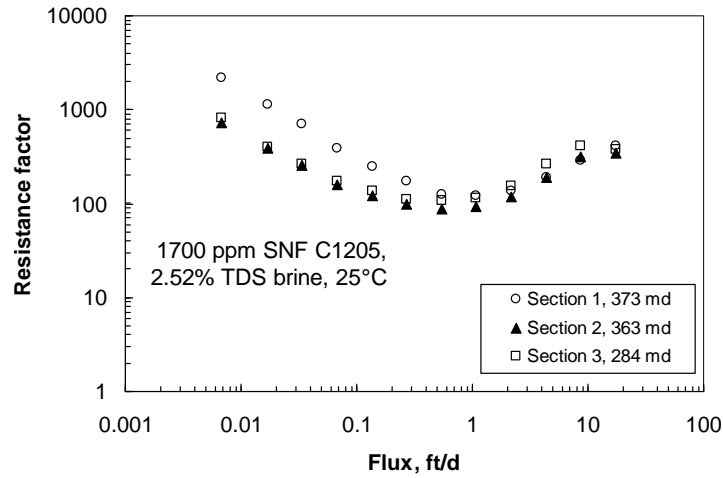


Fig. A-11—Resistance factor versus flux for 1,700-ppm C1205 in Berea.

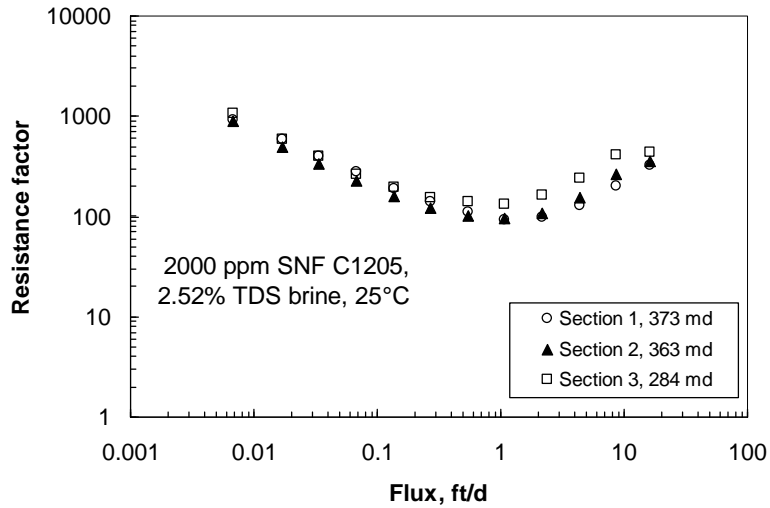


Fig. A-12—Resistance factor versus flux for 2,000-ppm C1205 in Berea.

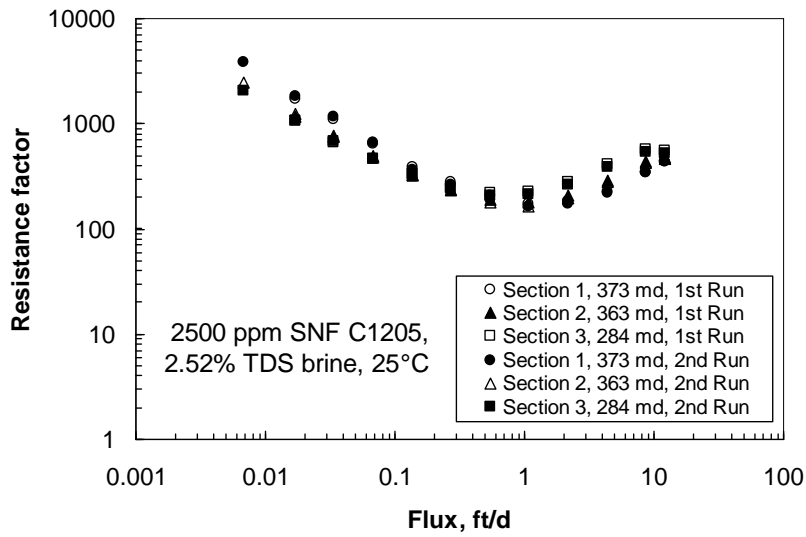


Fig. A-13—Resistance factor versus flux for 2,500-ppm C1205 in Berea.

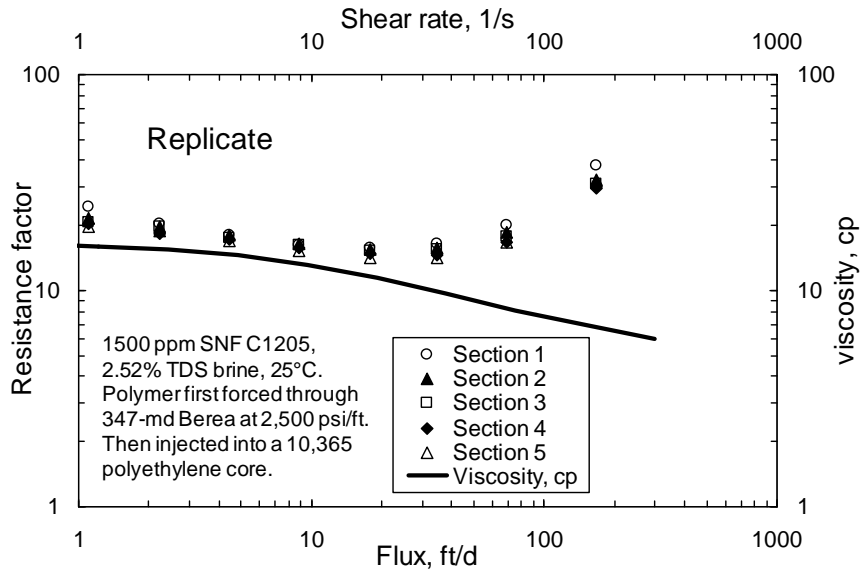


Fig. A-14—Resistance factor versus flux for 1,500-ppm C1205 in Berea. First forced through 347-md Berea at 2,500 psi/ft. Replicate run.

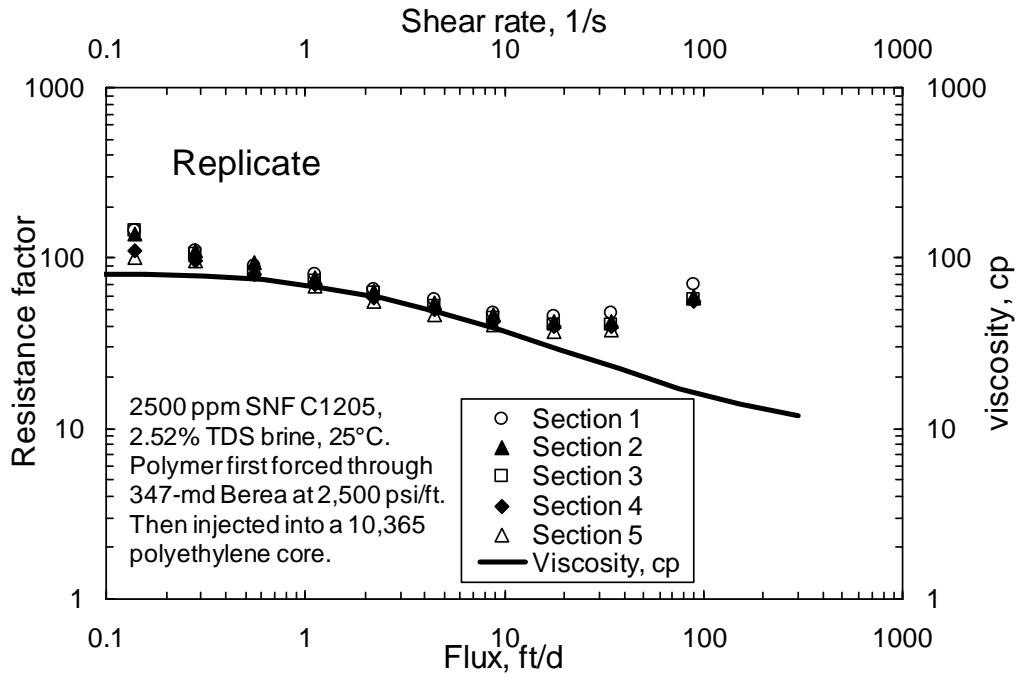


Fig. A-15—Resistance factor versus flux for 2,500-ppm C1205 in Berea. First forced through 347-md Berea at 2,500 psi/ft. Replicate run.